A GENETIC ALGORITHM GABOR FILTERED OPTIMIZATION FOR BLOOD VESSELS DETECTION OF DIGITAL RETINAL IMAGES

By
Heyam Bader

Supervisor
Dr.Abdullatif Abu-Dalhoum

Co-Supervisor
Dr.Mousa Al-Akhras

This Thesis was Submitted in Partial Fulfillment of the Requirements for the Master degree of Science in Computer Science

Faculty of Graduate Studies

The University of Jordan

August, 2009

Committee Decision

This Thesis (A Genetic Algorithm Gabor Filtered Optimization for Blood Vessels Detection of Digital Retinal Images) was Successfully Defended and Approved on 3/8/2009.

Examination Committee   Signature

Dr. Abdel Latif Abu-Dalhoum , (Supervisor)

Assoc. Prof. of Genetic Algorithms

Dr. Mousa Al-Akhras, (Co.Supervisor)

Assist. Prof. of Artificial Neural Networks and Comunication

Dr. Azzam Sleit, (Member)

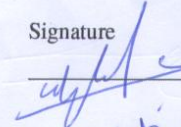Assoc. Prof. of Information Retrieval

Dr. Moh'd Belal Al-Zoubi, (Member)
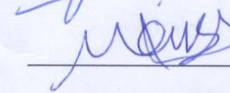
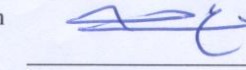Assoc. Prof. of Data Mining and Computer Graphics

Prof. Yahia Al Halabi (Member)

Prof. of Computer Studies

(Princess Sumaya University for Technology)

تعتمد كلية الدراسات العليا
هذه النسخة من الرسالة
التوقيع.......... التاريخ ١٦/٨/٢٠٠

DEDICATION

To my mother and my father..

To my brothers...

To my sisters..

Without their prayers, support, encouragement and love I would not be

who I am today.

ACKNOWLEDGMENT

I would like to thank Dr. Abdullatif Abu-Dalhoum for his scientific advices and support

throughout this research. Also I would like the thank Dr. Mousa Al-Akhras for his precious

time in scientific and non- scientific advices , and his comments about every step of

this work.

I would like to thank them deeply for the every comment, advice, and criticism that

helped me to complete my thesis.

Table of Contents

LIST OF TABLES

LIST OF FIGURES

LIST OF ABBREVIATIONS

2-D	Two Dimensional.
ANN	Artificial Neural Networks.
DRIVE	Digital Retinal Images for Vessel Detection.
FOV	Field Of View.
FPF	False Positive Fraction.
GA	Genetic Algorithms.
LoG	Laplacian of Gaussians.
MA	Maximum Accuracy.
MAA	Average Maximum Accuracy.
MFR	Matched Filter Response.
ROC	Receiver Operator Characteristics.
TPF	True Positive Fraction.

A GENETIC ALGORITHM GABOR FILTERED OPTIMIZATION FOR BLOOD VESSELS DETECTION OF DIGITAL RETINAL IMAGES

By
Heyam Bader

Supervisor
Dr.Abdullatif Abu-Dalhoum

Co-Supervisor
Dr.Mousa Al-Akhras

ABSTRACT

Detection of retinal blood vessels is important to diagnose many diseases. Many techniques are used for vessel detection, the first main type is the traditional edge detection techniques which are general techniques that consider vessels as edges, these techniques include Sobel and Prewitt. Because of the inaccuracy of traditional edge detection techniques in vessel detection, researchers investigate specialized vessel detection techniques. Vessel detection techniques include three detection types, namely: model-based, classifier based and vessel tracking approaches. One of the main model-based techniques is Gabor filter, which is a Gaussian shaped filter, that has optimal localization in both spatial and frequency domains.

This thesis introduces new methods for optimizing Gabor filter's performance in vessel detection using Genetic Algorithms (GA).

GAs will be used to get the best Gabor filter's parameters to maximize the Gabor filter response in vessel detection, by using the average area under Receiver Operator Characteristics (ROC) and Maximum Accuracy (MA) as measuring factors.

Five experiments are used for the purpose of optimization, these experiments are: optimizing the area under ROC for the first image in Digital Retinal Images for Vessel Extraction (DRIVE) database. The second experiment is the optimizing MA for the first image in DRIVE database. The third method is optimizing the average area under ROC for the 20 images of DRIVE. The fourth experiment is optimizing the average MA of the 20 images of DRIVE. The fifth experiment is dividing the first image of DRIVE into 4 regions, each region will have a different pair of Gabor filter parameters to gain more optimization of vessel detection.

Comparing the results of the first four experiments with the results of Rangayyan's Gabor filter (Rangayyan, et al., 2007), it was found that the average area under ROC improves Rangayan's area under ROC by nearly 1%, and the average MA by approximately 0.14%.

On the other hand, the average area under ROC obtained by this work improves Chaudhuri's matched filter (Chaudhuri,et al.,1989) by approximately 13% and the average MA is better than Chaudhuri's by nearly 6%.

The fifth method improves the average area under ROC by 2% in comparison with Rangayyan's Gabor filter, and improves Chaudhuri's average area under ROC by 7%.

CHAPTER 1
INTRODUCTION

1.1 Problem Definition

Retinal blood vessels are key to diagnose many human diseases. Diseases like diabetes, hypertension, and arteriosclerosis affect blood vessels' features and lead to restricted blood supply which may damage the retina and if deteriorates may cause blindness. Therefore, extracting and measuring retinal vessels can help ophthalmologists to study vessels' features in order to diagnose and treat such diseases. The usual approach is to study retinal images and detect blood vessels by ophthalmologists. However, automating detection of retinal blood vessels offers many advantages over manual detection. It gives the chance to examine large number of images within a short period of time and reduces the cost and the workload required from manually-trained graders (Patton, et al., 2006). Additionally, it gives more accurate resolution than manual detection which may allow for better characterization and detection of the features of blood vessels.

Figure 1.1 shows a test image of a retina and a corresponding image of blood vessels that are detected manually, this figure is taken from Digital Retinal Images for Vessel Detection (DRIVE) database which can be downloaded from http://www.isi.uu.nl/Research/Databases/DRIVE/.

(a) Retina Test Image.   (b) Retinal Vessels Detected Manually.
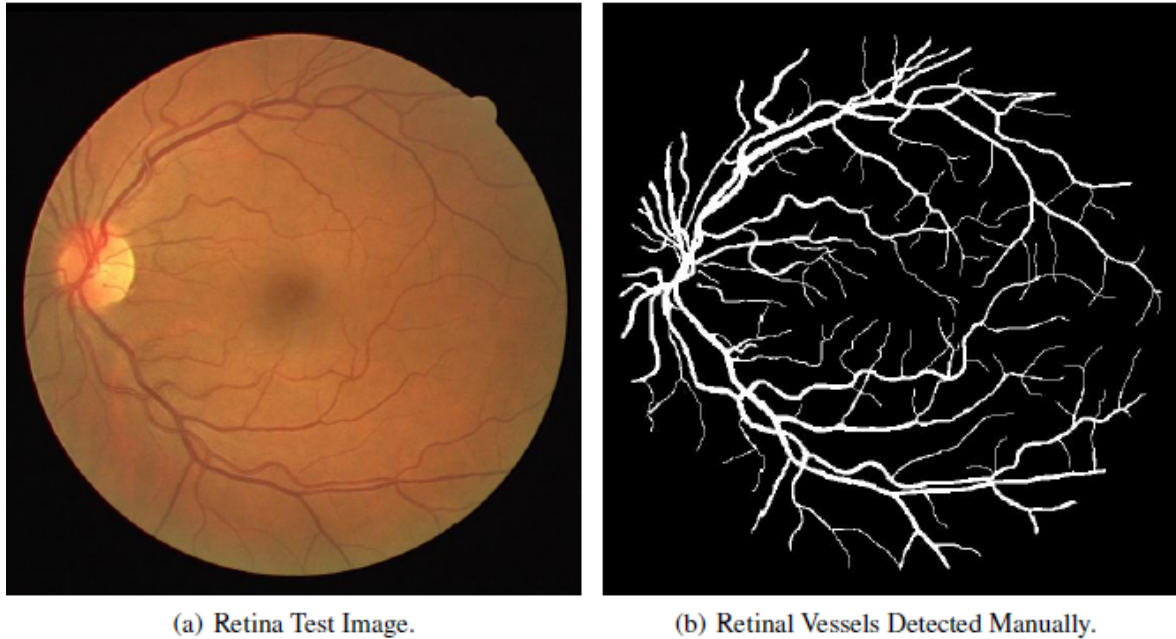
Figure 1.1: Retina test image and vessel detected manually.

DRIVE database is a set of 40 benchmark images that are divided into a training set and a test set, both containing 20 images, with their manual segmentations of the vasculature, that are segmented by ophthalmologists.

Specialized vessel detection techniques such as model-based, classification-based, and vessel tracking are more accurate in vessels segmentation of the retinal image than traditional edge detection techniques such as Sobel, Roberts, and Laplacian (Chaudhuri, et al., 1989).

1.2 Research Objectives

To detect blood vessels of retina, Gabor filter is used in this search. It is a sinusoidally modulated Gaussian function that has optimal localization in both the frequency and the

space domains and it can be used as lines' detector (Rangayyan, et al., 2007).

In this thesis the problem of vessels' detection will be investigated and new methods will be proposed to improve the performance of Gabor filter in vessel detection and maximizes the filter's response in blood vessels' detection using Genetic Algorithms (GA) as an optimization technique.

1.3 Research Methodology

In order to optimize the performance of Gabor filter in vessels' detection, GAs will be used to select the best combination of parameters' values of Gabor filter that give the best filtering results and maximize the filter's response in vessel detection. After the optimization process the obtained results will be compared with the results obtained by previous methods. To optimize the performance of Gabor filter, five methods will be used:

- Optimizing the area under Receiver Operator Characteristics curve (ROC) for the first image of DRIVE database.

- Optimizing the Maximum Accuracy MA for the first image of DRIVE database.

- Optimizing the average area under ROC for all DRIVE database images.

- Optimizing the average MA for the all DRIVE database images.

- Dividing the first DRIVE image into four regions, and calculate different Gabor parameters for each region.

1.4 Contribution

In this thesis a new idea has been proposed which is optimizing Gabor filter using GAs. The aim of optimization is to maximize the filter's response in detecting blood vessels

in retinal images that are used for medical diagnose purposes. Five methods have been proposed and implemented in this thesis for the purpose of Gabor's filter optimization, these methods are mentioned in section 1.3. The comparison of the performance of these methods with the previous work is based on two measuring factors which are:

- The average area under ROC for the 20 images of DRIVE.
- The average MA for the 20 images of DRIVE.

After the implementation of the proposed methods, comparisons are made with Rangayyan's et al. Gabor filter (Rangayyan, et al., 2007) and with Chaudhuri's et al. matched filter (Chaudhuri, et al., 1989). This work improved the average area under ROC by 2% than matched filter and by 15% than Gabor filter. In terms of average MA, this work improved the average MA by .02% than matched filter and by 6% than Gabor filter.

There are many aspects in which this research differs than other studies, these aspects are :

- Using genetic algorithm to improve Gabor filter in blood vessels' detection.
- Using a multi-scale thresholding of gray-levels to find all the possible blood vessels.
- Using the ROC as the fitness function for GA.
- Using the MA as the fitness function for GA.
- Dividing the image of DRIVE into four regions and filter each region using different filter parameters.

1.5 Thesis Outline

The rest of this thesis is structured as follows:

Chapter 2 reviews the literature and the methods that were used for vessel detection, from traditional edge detection to specialized vessel detection techniques including: model based, classifier-based and vessel tracking techniques. This chapter also gives some background information about GA as it is going to be used as optimization method.

Chapter 3 presents the main idea of this thesis which is optimizing the Gabor filter for blood vessels' detections. Different variations of the proposed techniques will be discussed.

Chapter 4 presents details about the methods used in the thesis and the obtained results. The results are also compared with the results obtained by previous detection methods.

In Chapter 5, conclusions are given and avenues for future work are explained.

Chapter 2

Literature Work

Retinal vessel detection has been investigated by many researchers due to its medical importance in diagnosing many diseases such as diabetes, hypertension, and arteriosclerosis. Usually, a specialized edge detection technique is used to detect blood vessels. Specialized vessel detection techniques are more accurate in vessels segmentation from the retinal image than traditional edge detection techniques (Chaudhuri, et al., 1989).

This chapter reviews several techniques that are used for retinal vessels' detection. Section 2.1 introduces the traditional edge detection techniques, section 2.2 introduces specialized vessel detection techniques, and section 2.3 gives theoretical background about Genetic Algorithms.

2.1 Traditional Edge Detection

In image processing, an edge is defined as a set of connected pixels between two regions of different intensities. An ideal step edge is the orthogonal transition in pixel's gray level. Unfortunately image acquisition tools such as cameras, yield blurred edges and therefore produce non-ideal edges. The degree of blurring depends on many factors such as the quality of the image acquisition system, and the illumination condition when the image was captured(Gonzalez & Woods 2002).

Figure 2.1: Ideal Step Edge Vs. Ramp Edge (Gonzalez and Woods, 2002).

Figure 2.1 shows an ideal step edge where the intensity changes orthogonally from black to white. The same figure also shows a non-ideal step edge where the change occurs in a ramp line (Gonzalez and Woods, 2002).
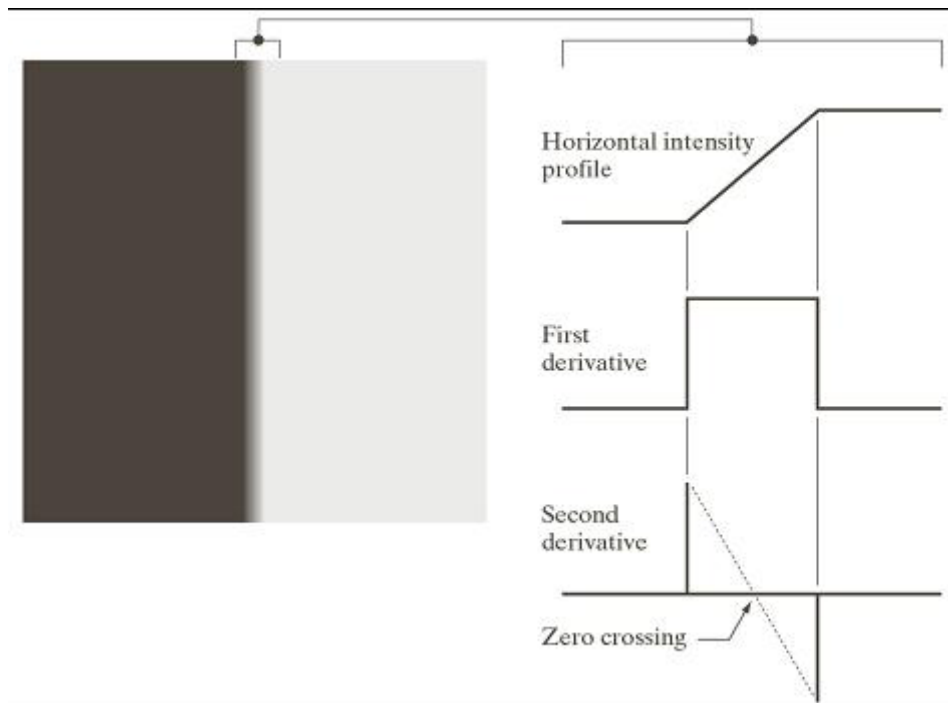
Figure 2.2: Ramp Edge, its First and Second Derivatives (Gonzalez and Woods,2002).

Figure 2.2 shows the first and the second derivatives for a non-ideal (ramp) edge. As can be noticed from the figure, in first derivative, the intensity of the edge is constant and greater than zero while the intensity of non-edge pixels is zero. On the other hand, the intensity of the second derivative of the image has positive value for the dark side of the edge, and has a negative value for the bright side. The point at which an imaginary straight line joining the positive and negative values crosses zero near the center of the edge is called zero crossing point, and it is used to determine the center of thick edges.

There are two main approaches for edge detection:

- The gradient method, in which the edge is detected using the first derivative of the image's intensity.

- The laplacian method, in which the zero crossing of the second derivative of image's intensity is used for edge detection.

- The Laplacian of Gaussian

2.1.1 Gradient Method

In the gradient method, the edge is detected using neighborhood differential operator, it detects edges by looking for the maximum and the minimum value in the first derivative of the Two Dimensional (2-D) image.

The gradient of an image f(x,y) at location (x,y) contains two components G_x and G_y:

$$G_x = \frac{\partial f}{\partial x} \tag{2.1}$$

$$G_y = \frac{\partial f}{\partial y} \tag{2.2}$$

The magnitude of gradient ($\tilde{N} f$) determines the maximum rate of change of f(x,y) per

unit distance and can be defined as:

$$\nabla f = \sqrt{G_x^2 + G_y^2}$$ (2.3)

The direction of gradient is perpendicular to the edge direction and is given in the

following equation (2.4)

$$\alpha(x, y) = \tan^{-1}(\frac{G_y}{G_x})$$ (2.4)

where a is measured with respect to the x- axis.

The simplest operator to implement the gradient method is by using Roberts method

(Ziou and Tabbone, 1997), in which a 2X2 mask similar to the one shown in Figure 2.3 is

used

$z1$	$z2$	$z3$
$z4$	$z5$	$z6$
$z7$	$z8$	$z9$

Figure 2.3: A 3X3 region of an Image

The gradients at point z5 which is illustrated in Figure 2.3 are:

$G_x = z_9 - z_5$ (2.5)

$G_y = z_8 - z_6$ (2.6)

Because Roberts method does not have a clear center, a 3x3 Prewitt mask operator

described by Ziou and Tabbone (Ziou and Tabbone, 1997) is proposed and the gradients

are defined as follows:

$G_x = (z_7+z_8+z_9) -- (z_1+z_2+z_3)$ (2.7)

Gy = (z3+z6+z9) - (z1+z4+z7) (2.8)

Another 3X3 operator that emphasizes the center point by multiplying it by 2 is Sobel methods described by Gonzalez (Gonzalez & Woods 2002) as given by

Gx = (z7+2z8+z9) - (z1+2z2+z3) (2.9)

Gy = (z3+2z6+z9) - (z1+2z4+z7) (2.10)

The drawbacks of gradient methods are that they are sensitive to noise, and they give inaccurate results with non-ideal edges, because the size of the kernel filter and coefficients are fixed and are not adaptable to distinguish valid edge from edge caused by noise. (Gonzalez and Woods, 2002)

2.1.2 Laplacian Method

The Laplacian method searches for zero crossings reading in the second derivative of the image in order to find edges

$$\nabla^2 f = \frac{\partial^2 f}{\partial x^2} + \frac{\partial^2 f}{\partial y^2}$$ (2.11)

An approximation of laplacian method is given by one of the following two forms

$$\nabla^2 f = 4z5 - (z2+z4+z6+z8)$$ (2.12)

$$\nabla^2 f = 8z5 - (z1+z2+z3+z4+z6+z7+z8+z9)$$ (2.13)

The laplacian drawbacks are that it is unacceptably sensitive to noise, its magnitude produces double edges, and the edge direction is not detected. (Gonzalez &Woods 2002)

2.1.3 The Laplacian of Gaussian (LoG)

Because the laplacian technique is sensitive to noise, it may be desirable to smooth the image first by convolution with a Gaussian kernel (Jin and Gao, 2002), which is given as follows:

$$G_\sigma(x,y) = \frac{1}{\sqrt{2\pi\sigma^2}} exp[-\frac{x^2+y^2}{2\sigma^2}] \qquad (2.14)$$

where s is the kernel's width.

The convolution formula is shown as follows :

$$\Delta[G_\sigma(x,y) * f(x,y)] = \Delta[G_\sigma(x,y)] * f(x,y) = LoG * f(x,y) \qquad (2.15)$$

Using LoG for edge detection includes the following steps:

- Applying LoG to the image

- Detection of zero-crossings in the image.

- Thresholding the zero-crossings in order to keep only zero-crossings which have large difference between positive maximum and negative minimum, and remove zero-crossings that are caused by noise.

2.2 Vessel Detection Techniques

There are three main types of vessel detection techniques:

1. Model based approaches, in which a two - dimensional Gaussian shaped filter is used to detect vessels.

2. Classifier based approaches, in which segmented regions are classified to vessel or non vessel according to some observed features.

3. Vessel tracking, in this approach the vessel is tracked according to previous knowledge of first location of the center of vessel cross-section, the vessel width and direction.

2.2.1 Model-Based Approaches

Model-based is the most widely used approach. It uses a 2-D Gaussian shaped filter that is rotated in all directions in order to detect vessels. The intensity of the cross section profile of retinal vessels is illustrated in Figure 2.4.
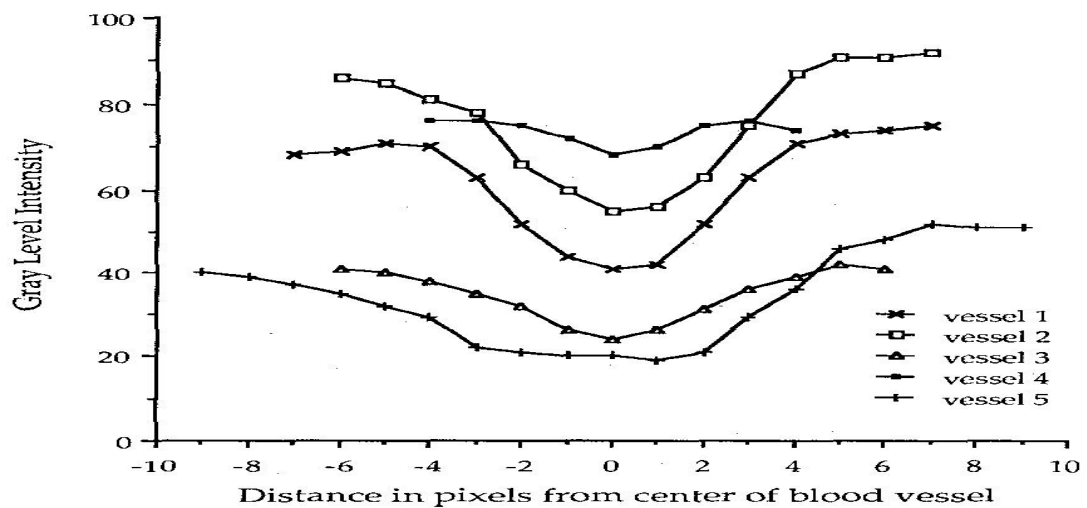
Figure 2.4: Vessels Intensity Profile (Chaudhuri, et al., 1989).

The x-axis represents the distance in pixels from the center of the vessel in both directions, the negative values represent the opposite direction, and the y-axis represents the intensity of each pixel. The intensity of blood vessels can be approximated to an inverted Gaussian shape, so it is appropriate to use a Gaussian shaped filter to model retinal vessels.

Two types of filters belong to this approach: matched filter and Gabor filter.

Matched Filter

The matched filter approach was firstly proposed by Chaudhuri et al. (Chaudhuri, et al., 1989). Chaudhuri et al. proposed the use of a 2-D matched filter that is based on the following assumptions:

1. Vessels have small curvature so they can be approximated by piece-wise linear segments.

2. Vessels are darker than background and their intensity profile can be approximated by Gaussian curve.

3. Vessels have constant width.

Each coefficient in the matched filter method is calculated as follows:

$$k_\theta(x,y) = -exp(\frac{-u^2}{2\sigma^2}), \forall p_\theta \in N \tag{2.16}$$

where k is the kernel of the matched filter, θ determines the orientation of the filter's kernel and it may have values between 0 and 180, and σ defines the spread of the intensity profile, u can be calculated by equation 2.17.

$$p_\theta = [\begin{array}{cc} u & v \end{array}] = [\begin{array}{cc} x & y \end{array}][\begin{array}{cc} cos\theta & sin\theta \\ -sin\theta & cos\theta \end{array}] \tag{2.17}$$

p is a point in the neighborhood N that is given by equation 2.18

$$N = (u,v) : |u| \leq T, |v| \leq L/2. \tag{2.18}$$

Where the width of profile segment = 2T+1, and L is the length of the vessel segment. Chaudhuri et al. (Chaudhuri, et al., 1989) used a matched filter for detecting vessels by rotating it in all directions, and recording the maximum response for each pixel. The resulted filter is illustrated in Figure 2.5.

(a) The Original Image   (b) The Result of Chaudhuri Filter
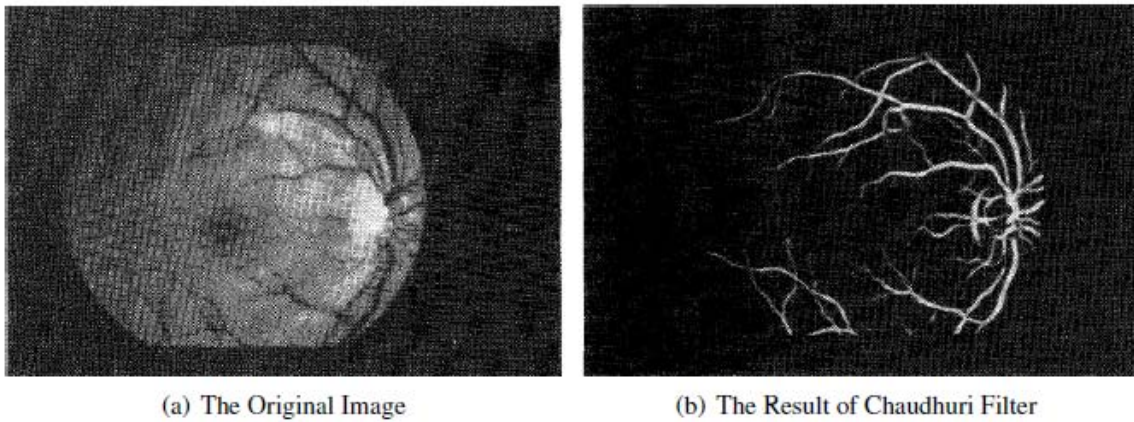
Figure 2.5: Chaudhuri Filtered Image (Chaudhuri, et al., 1989).

The matched filter method was then improved by Hoover et al. (Hoover, et al., 2000) by probing different pieces (regions) in the Matched Filter Response (MFR) image according to global image's attributes as illustrated in Figure 2.6.
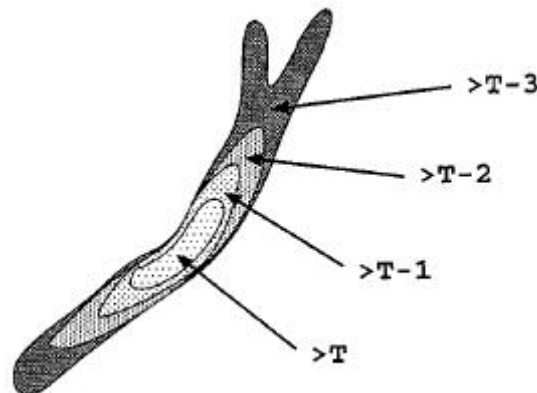
Figure 2.6: Threshold Probing (Hoover, et al., 2000).

During each probe the threshold is determined according to a set of criteria, then the area is classified to be either a blood vessel or not, in this way different probed areas are thresholded with different thresholds through the image. The result of Hoover thresholding is shown in Figure 2.7.

(a) The Original Image

(b) The Result of applying Hoover Filter (Hoover et al. 2000).
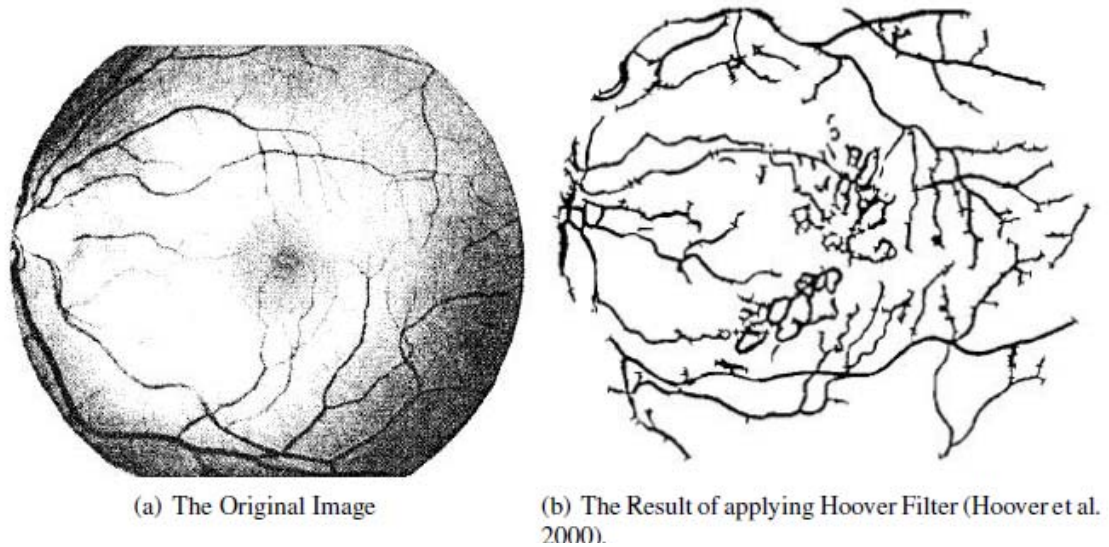
Figure 2.7: Hoover's Filtered Image (Hoover et al. 2000).

Image thresholding is a subclass of image segmentations. The objective of thresholding is to divide an image into two segments only. Depending on a prescribed threshold value, pixels with values less than the threshold are assigned zeros, and the remaining pixels are assigned ones (Sezgin and Sankur, 2004).

Al-Rawi et al. (Al-Rawi, et al., 2007) proposed an improved matched filter by searching for the matched filter's parameters (L, T, q) from a limited space that gives better results. After applying the matched filter to the image, the resulted image is thresholded.

Afterward the resulted image is compared to a retinal vessels' image that is labeled manually.

In another research Al-Rawi et al. (Al-Rawi & Karajeh 2007) also proposed a method for improving matched filter by using Genetic Algorithms (GA) to search for the matched filter's parameters (L, T, q) that give the best result. The filtered image is thresholded with different threshold values between 0 and 1. Each threshold produces a different binary image. For each binary image, the true positive fraction (TPF), and the false positive fraction (FPF) are calculated as follows:

TPF= True Vessel Pixels / Vessel pixels in hand labeled image   (2.19)

FPF = False Vessel Pixels / None Vessel pixels in hand labeled image   (2.20)

The true pixels are the pixels that are detected as vessel pixels in the resulted image and these pixels are actually vessel pixels in the hand-labeled image. The false pixels are pixels that are detected vessel pixels in the resulted image, but they are non-vessel in the hand-labeled image.

The Receiver Operating characteristic (ROC) curve, is a graphical plot of FPF versus TPF, and the larger the area under the curve, the better the performance of the filter. The area under the curve of ROC is the fitness function used in the GA to optimize parameters.

AL-Rawi's et al. matched filters are illustrated in Figure 2.8

(a) The Original Image

(b) The Result of Al-Rawi et al. Filter (Al-Rawi et al. 2007)
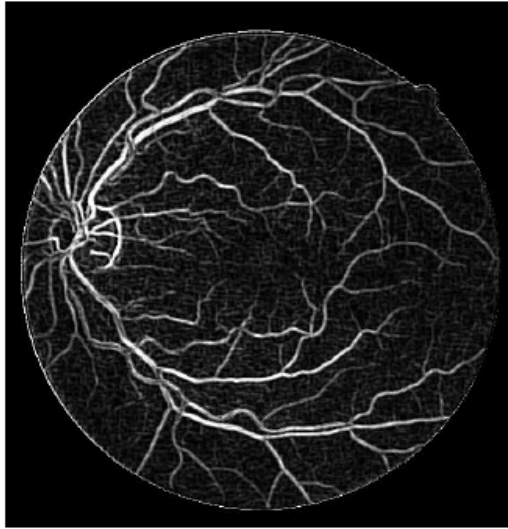
(c) The Result of Al-Rawi & Karajeh Filter (Al-Rawi & Karajeh 2007)

Figure 2.8: Al-Rawi Filtered Image.

Gabor Filter

Gabor filter is a Gaussian-shaped filter that can be used to detect linear features of positive contrast, that is, linear elements that are brighter than their immediate background. The real

Gabor filter kernel (or mother wavelet) oriented at the angle   = -π/2 can be written as

$$G(x,y) = \frac{1}{2\pi\sigma_x\sigma_y} \exp(-\frac{1}{2}(\frac{x^2}{\sigma_x^2} + \frac{y^2}{\sigma_y^2}))\cos(2\pi f_0 x)$$

(2.21)

Where σx and σy are the standard deviation values in the x- and y-directions for the vessel

intensity profile, and f0 is the frequency of the modulating sinusoid.

To be able to detect vessels in all possible orientations, the mother wavelet must be

rotated in all possible vessel orientations and the maximum response from the filter bank

is registered. The parameters in equation 2.21 which are : σx ,σy and f0 need to be derived

from the structure of the detected vessels . The amplitude of the exponential (Gaussian)

term in equation 2.21 is reduced to one-half of its maximum at x = t/2 and y = 0 where t is

the thickness of the line detector. Therefore:

$$\sigma_x = \tau/2\sqrt{2\ln 2}$$

(2.22)

The cosine term has a period of t; hence,

$$f_0 = 1/\tau.$$

(2.23)

The value of σy could be defined as

$$\sigma_y = \ell\sigma_x$$

(2.24)

Where ℓ determines the elongation of the Gabor filter in the orientation direction, with

respect to its thickness. The value of t is varied to prepare a bank of filters at different

scales for multi-resolution filtering and analysis.

Rangayyan et al. (Rangayyan, et al., 2007) used Gabor filter to detect retinal blood vessels, in this method each pixel is converted to a vector of color components and then each component is normalized by dividing its value by 255, the result was converted to the luminance component Y, computed as follows:

Y = 0.299R+0.587G+0.114B   (2.25)

Each image is extended beyond the effective region to avoid edge artifact in Gabor filter. For each set of Gabor parameters (L, t) the highest response of applying Gabor filter is obtained over 180 angles and then the filtered image is thresholded using sliding threshold, and compared to a ground-truth image to obtain TPF and FPF. Then TPF is plotted against FPF for the 20 Digital Retinal Images for Vessel Detection (DRIVE) images that are described by (Staal, et al., 2004) obtaining ROC and the area under the curve is measured. Rangayyan et al. resulted image is show in Figure 2.9.

(a) The Original Image

(b) The Result of Rangayyan et al. Filter (Rangayyan et al. 2007)
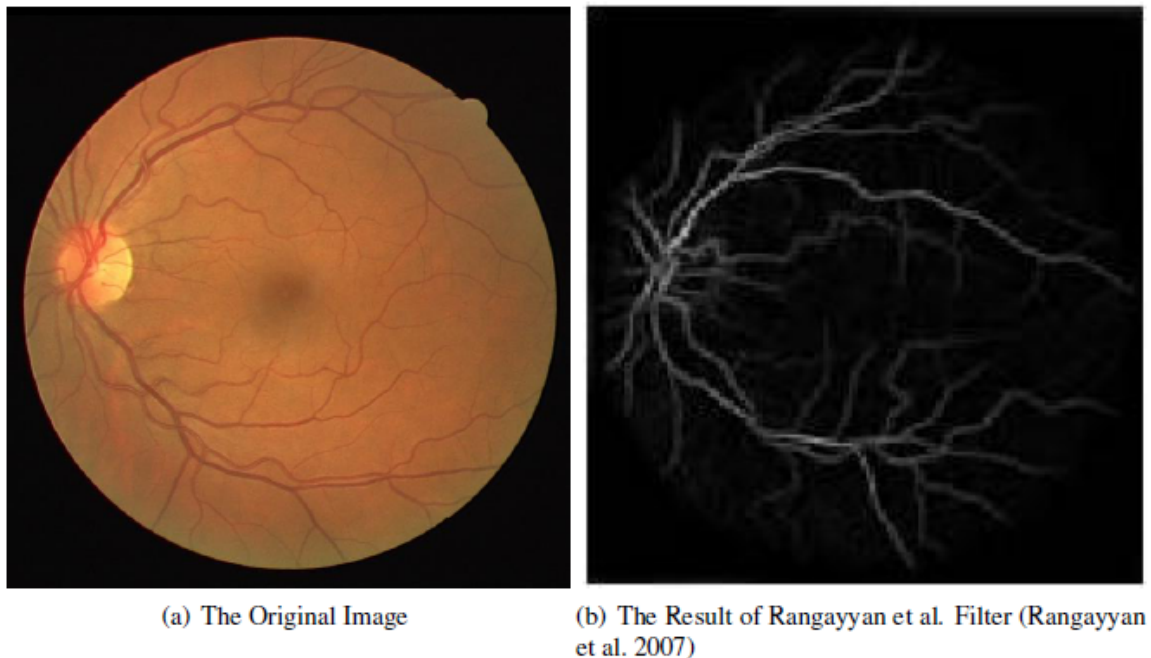
Figure 2.9: Rangayyan's et al. Filtered Image (Rangayyan, et al., 2007).

2.2.2 Classifier-Based Approaches

Classifier-based vessel detection includes two steps: segmenting the image into connected regions, then each region is classified into either vessel or non-vessel according to many features.

This approach incorporates large scale properties, but it has a drawback that no classification is applied until the first step is completely finished.

Staal et al. (Staal, et al., 2004) introduced the ridge-based method that extracts the image ridges (points coincide with vessel centers), then ridges are grouped into sets, a feature vector is computed for every pixel depending on patches and ridges.

Adaptive local thresholding is introduced by Jiang and Mojon (Jiang and Mojon, 2003), in this approach a binary image is obtained after applying a threshold, then this image is used in a classification procedure to accept or reject any region in the image as a certain

object. A series of different thresholds are applied and the final detection result is a combination of the results provided by individual thresholds.

Other researchers include Soares et al. (Soares, et al., 2006) who proposed an algorithm that used Gabor filters for feature vector pixel classification. David et al. (David, et al., 2008) used Artificial Neural Networks (ANN) classifiers to detect retinal vessels.

2.2.3 Vessel Tracking

Vessel tracking approach works by first locating the center of vessel cross-section, the vessel width and direction then exploit local image properties to trace the vessels recursively. This approach is based on region growing.

The drawbacks of this approach is that it requires intervention from the user and its performance is affected by vessel's bifurcations (Jung and Hong, 2006)

2.3 Genetic Algorithms

Genetic Algorithms (GA) is a search technique used in computing to find exact or approximate solutions to optimization and search problems (Thede, 2004). The algorithm starts with a set of solutions called population. Each population is used to generate another population to find better solutions. When a new population is generated, new solutions (individuals) are born while other solutions die.

The generated solutions (individuals) are selected according to their fitness, the fitness of an individual is the measure of how suitable is the solution (individual) to solve the problem, the fitness of the solution is evaluated using the fitness function (objective function). Each individual is represented by a binary string which is called a chromosome, the length of the string depends on the problem's encoding.

Roughly speaking, GA works according to the following steps:

1. Generate random population of n chromosomes.

2. Calculate the fitness of each chromosome in the current population.

3. Create a new population through the following operations.

- Selection: Select two parent chromosomes from a population according to their fitness.

- Cross-over: With cross-over probability, parents are crossed-over to form a new offspring (children). If no crossover was performed, offspring is an exact copy of parents.

- Mutation: With a mutation probability mutate new offspring at each locus (position in chromosome).

- Accepting: Place new offspring in a new population.

4. The new generated population becomes the current population.

5. If the termination condition is satisfied, then stop and return the best solution in the current population.

6. Go to step 2.

As can be noticed, the main parts of GA are: encoding, selection, cross-over, and mutation.

2.3.1 Encoding

Before applying the GA to solve your problem, the way of encoding the chromosomes must be taken into consideration. There are many types of chromosomes' encoding that will be discussed in this section.

Binary Encoding

In binary encoding every chromosome is a set of bits 0 or 1, this type of encoding gives many possible chromosomes, but it is not suitable for many types of problems.

Value Encoding

Value encoding can be used in problems, where some complicated values are used. In

value encoding, every chromosome is a string of some values. Values can be real numbers or characters or some complicated data types.

Permutation Encoding

Permutation encoding can be used in ordering problems, such as traveling salesman problem.

In permutation encoding, every chromosome is a string of numbers, which represents the order of these numbers.

2.3.2 Selection

There are many methods for selecting parents to produce new chromosomes (offspring).

Roulette Wheel Selection

In roulette wheel selection the chromosomes that have more fitness value have more chance to be selected, the same idea as in the roulette wheel.

Rank Selection

In rank selection the chromosomes are ranked according to their fitness. The worst chromosome will have rank 1, second worst 2 etc. and the best will have rank N (number of chromosomes in population), so the selection depends on the rank rather than the fitness.

This prevents the very fittest chromosomes from getting dominance of the selection early at the expense of less fit chromosomes.

Elitism

After the steps of cross-over and mutation, we may lose some of the best chromosomes from the old population. To solve this problem, elitism copies the best chromosomes in the old population to the new population directly without being cross-overed or mutated. By applying elitism, the new generation is guaranteed not to be worse than the old (current) generation.

2.3.3 Cross-Over

After selecting parents , cross-over works by changing genes (bits) in parent chromosomes to create children (offspring). There are many types of cross-over that are described as follows.

Single point cross-over

In single point cross-over, one crossover point is selected, the binary string from the beginning of the chromosome to the crossover point is copied from one parent, the remaining bits are then copied from the second parent. Example of single-point cross-over is the crossover of the following two chromosomes:

11001-011 and 11011-**111** to produce 2 new chromosomes **11001-111** and 11011-

011.

Two points cross-over

In two points cross-over two points are selected, binary string from the beginning of the chromosome to the first crossover point is copied from one parent, the part from the first

to the second crossover point is copied from the second parent and the rest is copied from the first parent. Example of two points cross-over:

11-**0010**-01 and **11**-0111-**11** to produce 11-0111-01 and **11-0010-11**

Uniform cross-over

In uniform cross-over bits are randomly copied from the first parent to the second and unmodified bits in the second parent are moved to the first parent. Example of uniform cross-over:

1**1**0010**11** + **11**011**1**01 = **11011111**

2.3.4 Mutation

After a crossover is performed, mutation takes place to make the distribution of chromosomes investigate all possible solutions. Therefore, each bit of each individual is given the chance to mutate, but the probability of mutation is typically low with percentage less than 1%.

2.3.5 Fitness Function

Fitness function (also called objective function) is the optimization function of the problem that is being solved or searched, fitness function is used to assign a fitness value of each chromosome, the fitness value determines how much the chromosome is close to the solution of the problem.

2.3.6 GA Parameters

To calculate the best value of the fitness function, some of the GA's parameters need to be determined. These parameters are problem dependent and they are:

Population size: Population size determines how many chromosomes are in population (in one generation), and that depends on the problem to be solved. The larger the population size, the faster the best solution can be found as fewer generations are needed

to reach the goal. On the other hand, if the population size is very large, it slows the execution of GA. The population size also depends on how complex the fitness function is.

Elite count: Elite count determines how many solutions (individuals) are chosen to survive to new generation without being cross-overed or mutated.

Cross-over rate (fraction): Cross over rate determines how often cross-over is performed, if there is no cross-over then the offspring is an exact copy of parents, if its 100% then all offspring is made by cross-over, the rate of cross-over is recommended to be high to give more chance to the new generation to be different from the old generation.

Mutation rate (fraction): Mutation rate determines how often will be some parts of the chromosome be mutated. If there is no mutation, offspring is taken after crossover without any change. If mutation is performed, part of the chromosome is changed. If mutation probability is 100%, whole population is mutated.

CHAPTER 3

OPTIMIZING GABOR FILTER USING GENETIC ALGORITHMS

As Gabor filter is one of the major and best techniques used in vessel detection, it was chosen in this thesis for further improvement. The aim of this thesis is to optimize the Gabor filter's parameters which are τ, ℓ and to improve filter's performance for blood vessels' detection using Genetic Algorithms (GA). The optimized Gabor filter is obtained by taking into account the variation of blood vessels over several images. Therefore, a standard database such as Digital Retinal Images for Vessel Extraction (DRIVE), that is described by Staal et al. (Staal, et al., 2004) will be used.

DRIVE database contains 40 digital retinal images and their corresponding masks and labels, they are divided into a training set and a test set. The optimization fitness functions is obtained by comparing each vessel-detected image to a reference hand-labeled image to judge the effectiveness of the filter parameters.

This chapter presents a detailed description of the methods that are used in this thesis.

Next chapter will detail the results of the proposed methods and make comparisons with the related methods that previously used for vessel detection.

To optimize Gabor filter's parameters, five experiments are conducted as following:

- Optimizing the area under Receiver Operating Characteristic curve (ROC) for the first image of DRIVE database.

- Optimizing the average area under ROC for all DRIVE database images.

- Optimizing the Maximum Accuracy (MA) for the first image of DRIVE database

- Optimizing the average MA for the all DRIVE database images

- Dividing the first DRIVE image into four regions so that the derived parameters are specific to each region as it is expected to perform better on that region..

Section 3.1 describes the procedure of preparing images before filtering, section 3.2 describes how the images are filtered, section 3.3 presents the methods that are used to measure the Gabor filter's performance, and section 3.4 describes the setting of GA to optimize Gabor filter's performance. Section 3.5 describes the 5 methods that are used in the thesis.

3.1 Image Preparation

All the experiments are implemented using DRIVE database that is described by Staal et al. (Staal, et al., 2004); a set of 40 images that were divided into a training set and a test set, both containing 20 images, with their manual segmentations of the vasculature, that are segmented by ophthalmologists who marked all the pixels that were at least 70% certain that they are vessels. All of the images contained in the database were actually used for making clinical diagnoses. The green band of each red, green and blue model (RGB) retinal image is extracted for filtering. The green band is chosen rather than the red or the blue band for two reasons:

1. The green band determines image features, its dominant of the other bands.

2. To compare our results with other methods as most of them used the green band.

After extracting the green band, the image's intensity is inverted, so the vessels become of positive contrast than the background, so it can be filtered by Gabor filter. After that the

image is masked using the corresponding mask image in DRIVE database to identify the boundaries of the effective region, or the Field of View (FOV).

3.2 Image Filtering

The real Gabor filter kernel (or mother wavelet) oriented at the angle   = -π/2 may be formulated as

$$G(x,y) = \frac{1}{2\pi\sigma_x\sigma_y}\exp(-\frac{1}{2}(\frac{x^2}{\sigma_x^2} + \frac{y^2}{\sigma_y^2}))\cos(2\pi f_0 x) \tag{3.1}$$

A bank of 180 filters is used by rotating the kernel in the range of q = [-p/2,p/2], so the maximum response of these filters is recorded to be taken into account. The parameters of Gabor filter which are σx, σy and f0 are calculated from the vessel's structure as following:

The amplitude of the exponential (Gaussian) term in equation 3.1 is reduced to one half of its maximum at x = t/2 and y = 0 where t is the thickness of the line detector.

Therefore:

$$\sigma_x = \tau/2\sqrt{2\ln 2} \tag{3.2}$$

The cosine term has a period of t; hence,

$$\sigma_y = \ell\sigma_x \tag{3.3}$$

The value of σ_y could be defined as

$$f_0 = 1/\tau. \tag{3.4}$$

3.3 Filter's Performance

In order to measure the filter's performance, the filtered image should be compared to the corresponding hand-labeled image, in this work the filtered image is compared to a corresponding hand-labeled vessel image from the DRIVE database. A method is needed to determine whether the detected vessel pixel is true vessel pixels or not. Two methods of comparison are used in this work, these methods are:

- The Area Under ROC curve
- MA

These Methods will be discussed in details in the following two sections.

3.3.1 The Area Under The Receiver Operating Curve (ROC)

After applying Gabor filter on the image, the resulted image is thresholded. A sliding threshold between the values 0 and 1 in step of 0.001 is used, then a 1000 binary images is obtained after threshodling.

For each binary image, the True Positive Fraction (TPF), and the False Positive Fraction (FPF) are calculated as following:

TPF = True Vessel Pixels / Vessel pixels in hand labeled image   (3.5)

FPF = False Vessel Pixels / None Vessel pixels in hand labeled image   (3.6)

The true vessel pixels are the pixels that are detected as vessel pixels in the resulted image and these pixels are actually vessel pixels in the hand-labeled image, and the false pixels

are pixels that are detected vessel pixels in the resulted image, but they are non vessels in the hand-labeled image.

ROC curve, is a graphical plot of FPF versus TPF, and the larger the area under the curve the better the performance of the filter. An example of ROC is shown in figure 3.1
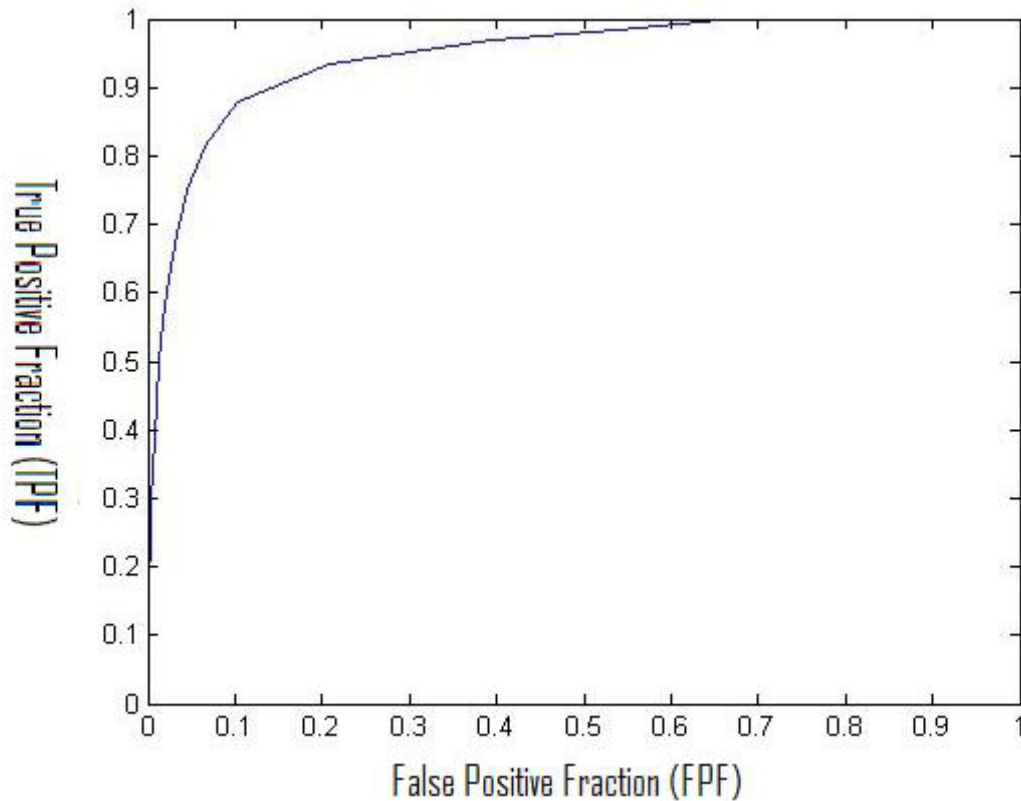
Figure 3.1: Example of ROC Curve.

3.3.2 Maximum Accuracy(MA)

Another measurement criterion is the MA, which is calculated as following: After thresholding the resulted image as mentioned in the previous section, the accuracy is calculated for each binary image by calculating the sum of true vessel pixels and true non-vessel pixels and divide the sum by the number of FOV pixels, which is the circular area in

the retinal image. Then the MA between the 1000 thresholds is taken into account. The average maximum accuracy (MAA) is the average MA over all the 20 images of DRIVE database.

3.4 Settings of Genetic Algorithm (GA)

As mentioned earlier, there are two parameters of Gabor filter that must be optimized in order to improve the performance of Gabor filter, these parameters are τ and ℓ.

The GA is used to calculate the values of these parameters that give the best Gabor filter response, the main procedures for GA setting is to determine the encoding criteria, the fitness function and the GA's parameters (Al-Akhras, 2007).

Encoding

The value encoding is used in this work, since the parameters t, ℓ are real numbers, so each chromosome is a string of two variables t, ℓ.

Fitness Function

The fitness function of the GA depends on the problem that is to be optimized, the optimization depends on the two comparison measurements for Gabor filter performance which were explained in the previous sections, these measurements are:

- The Area Under ROC.
- MA.

GA calculates the best values for Gabor filter's parameters that are used to achieve the best fitness value, i.e. the highest output of the fitness function.

GA **Parameters**

To calculate the best value of the fitness function some of of GA's parameters that are problem dependent need to be determined, these parameters are:

1. Population size: This parameter depends on how complicated the computation of the problem is, and so affects the speed of GA, so due to the intensive computations in this work, a moderate population size of 30 is chosen.

2. Crossover rate: Generally crossover rate should be high to produce new chromosomes, so it is chosen to be 0.80.

3. Elite count: Elite number should be low, to give chance to the new population to be different from old one, so it is chosen to be 2.

4. Mutation rate: The mutation rate should be low, it is chosen to be 0.1.

3.5 The Proposed Methods

This section presents a detailed description of the methods that are used in this thesis and their block diagrams.

3.5.1 Optimizing The Area Under ROC for the First Image of DRIVE Database

In this method the fitness function of the GA is the area under ROC for the first image of DRIVE database, the block diagram of this method is shown in Figure 3.2.
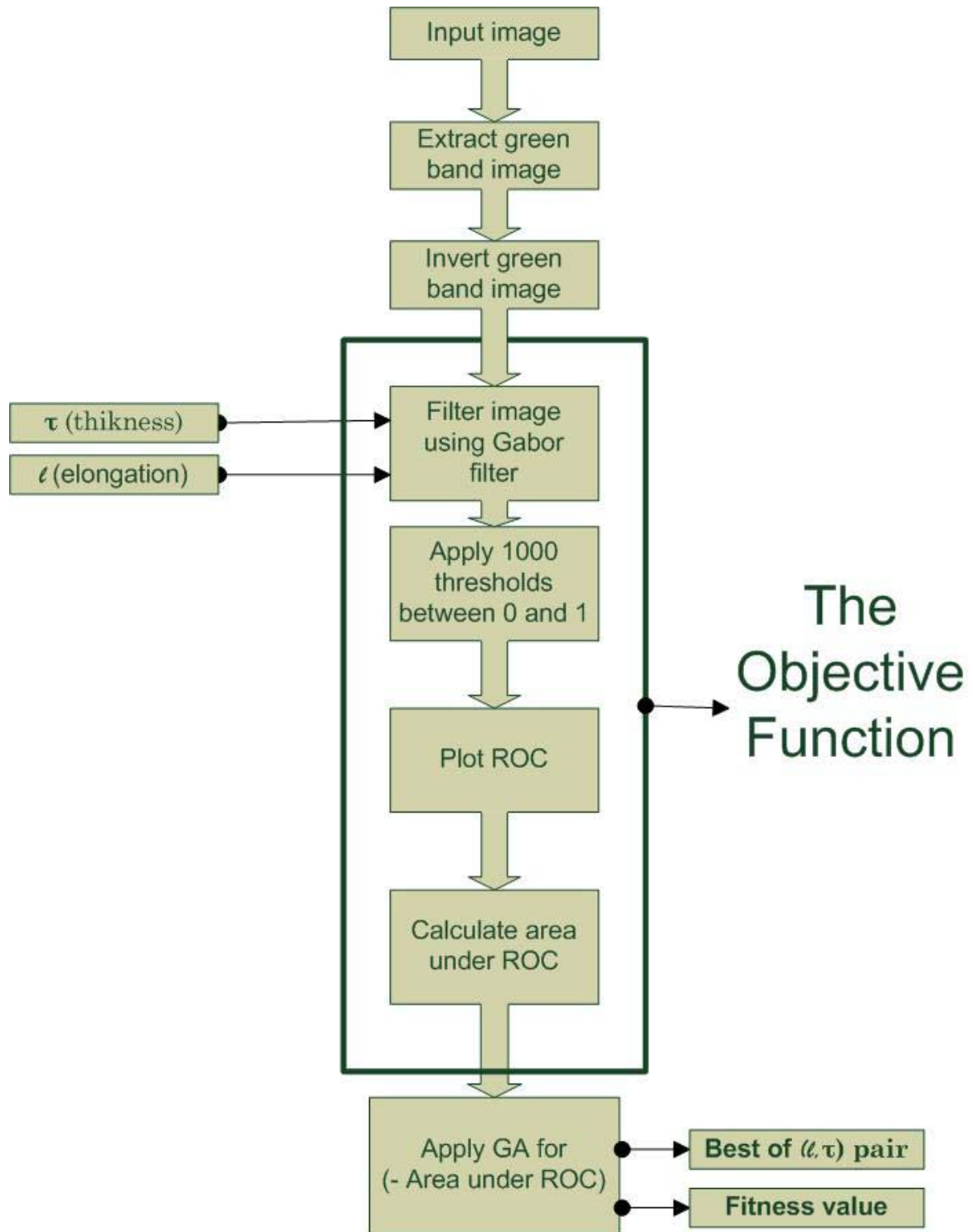
Figure 3.2: Optimizing The Area Under ROC For The First Image of DRIVE

database.

The first stage of this method is image preparation as described in the previous sections; the first image of DRIVE database that is shown in Figure 3.3 with its manually hand-labeled image, was used as an input for the optimization method.

(a) Retinal Test Image

(b) Retinal Vessels Image that Detected Manually
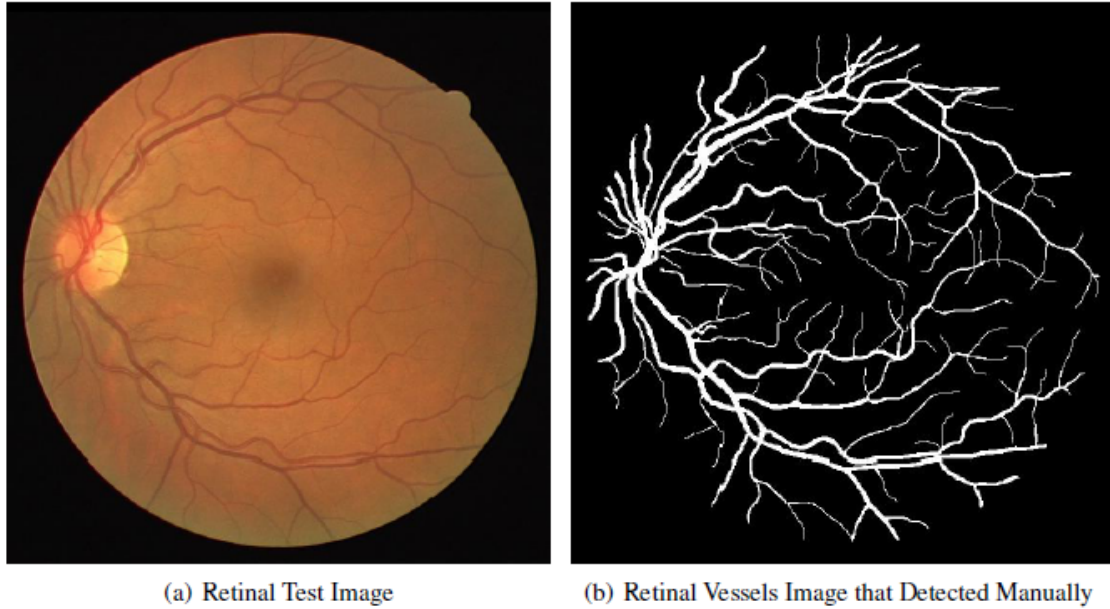
Figure 3.3: Retina Test Image and Vessels Detected Manually.

The green band is extracted from the image, after that the green band image is inverted so that we can implement Gabor filter on it as shown in Figure 3.4.

After the image has been prepared the second stage is image filtering, the image is filtered using Gabor filter, then the filtered image is thresholded 1000 times using threshold values between 0 and 1, for each thresholded image the TPF and FPF are calculated and the ROC curve is plotted, therefore the area under ROC curve is the fitness function of the

GA. The larger the area under the curve, the fitter the solution.

(a) Green Band Image.   (b) The Inverse of Green Band.
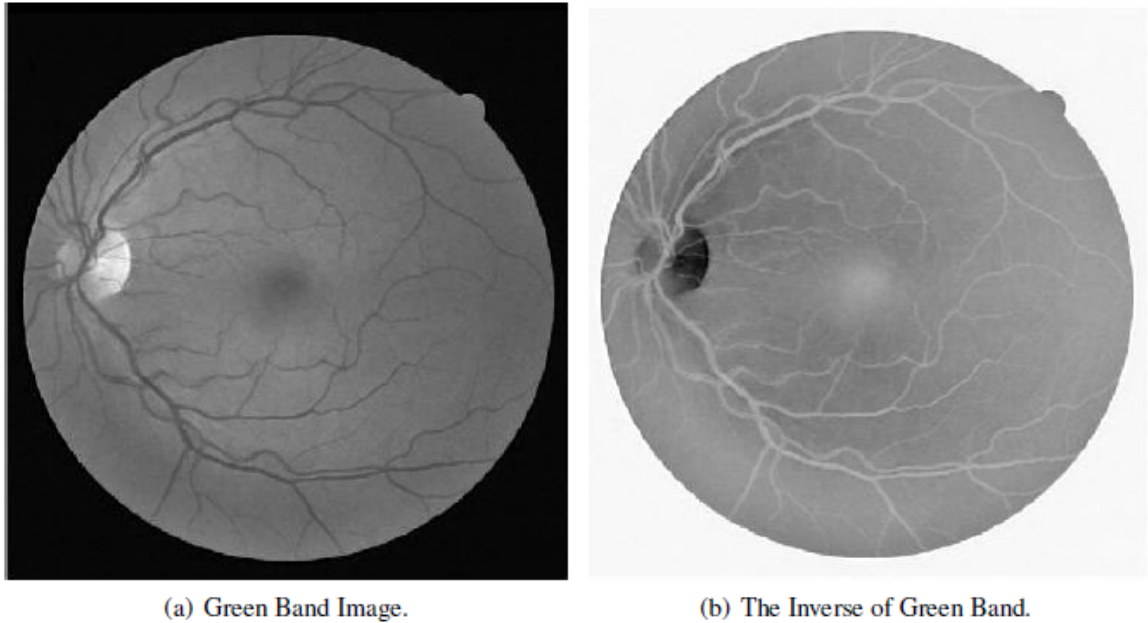
Figure 3.4: Green Band Image and its Inverse.

3.5.2 Optimizing the MA for the First Image of DRIVE Database

In this method the fitness function of the GA is the MA for the first image of DRIVE database, the block diagram of this method is shown in Figure 3.5.
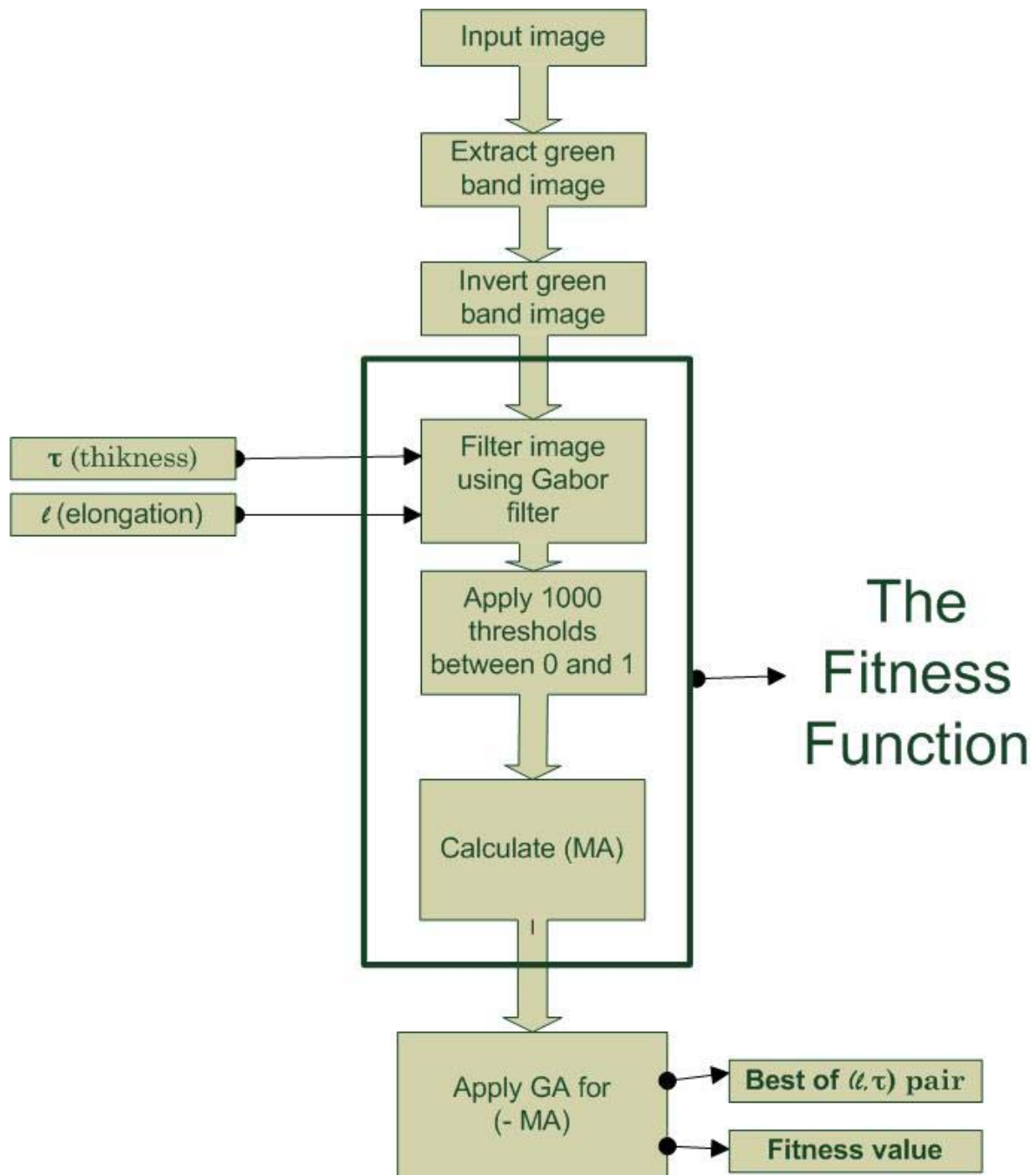
Figure 3.5: Optimizing the MA For The First Image of DRIVE Database Block Diagram

The first stage of this method is image preparing as described in the previous sections; the

first image of DRIVE database that is shown in Figure 3.3 with its manually hand-labeled

image, was used as an input for the optimization method. The green band is extracted from the image, after that the green band image is inverted so that we can implement Gabor filter on it as shown in Figure 3.4. After the image has been prepared the second stage is image filtering, the image is filtered using Gabor filter, then the filtered image is thresholded 1000 times using threshold values between 0 and 1, for each thresholded image the accuracy is calculated for each threshold, the maximum accuracy among the 1000 is taken into account and the MA is the fitness function of the GA.

3.5.3 Optimizing the Average Area Under ROC for All DRIVE Database Images

In this method the fitness function of GA is the average area under ROC for the 20 DRIVE images, the block diagram of this method is shown in Figure 3.6.
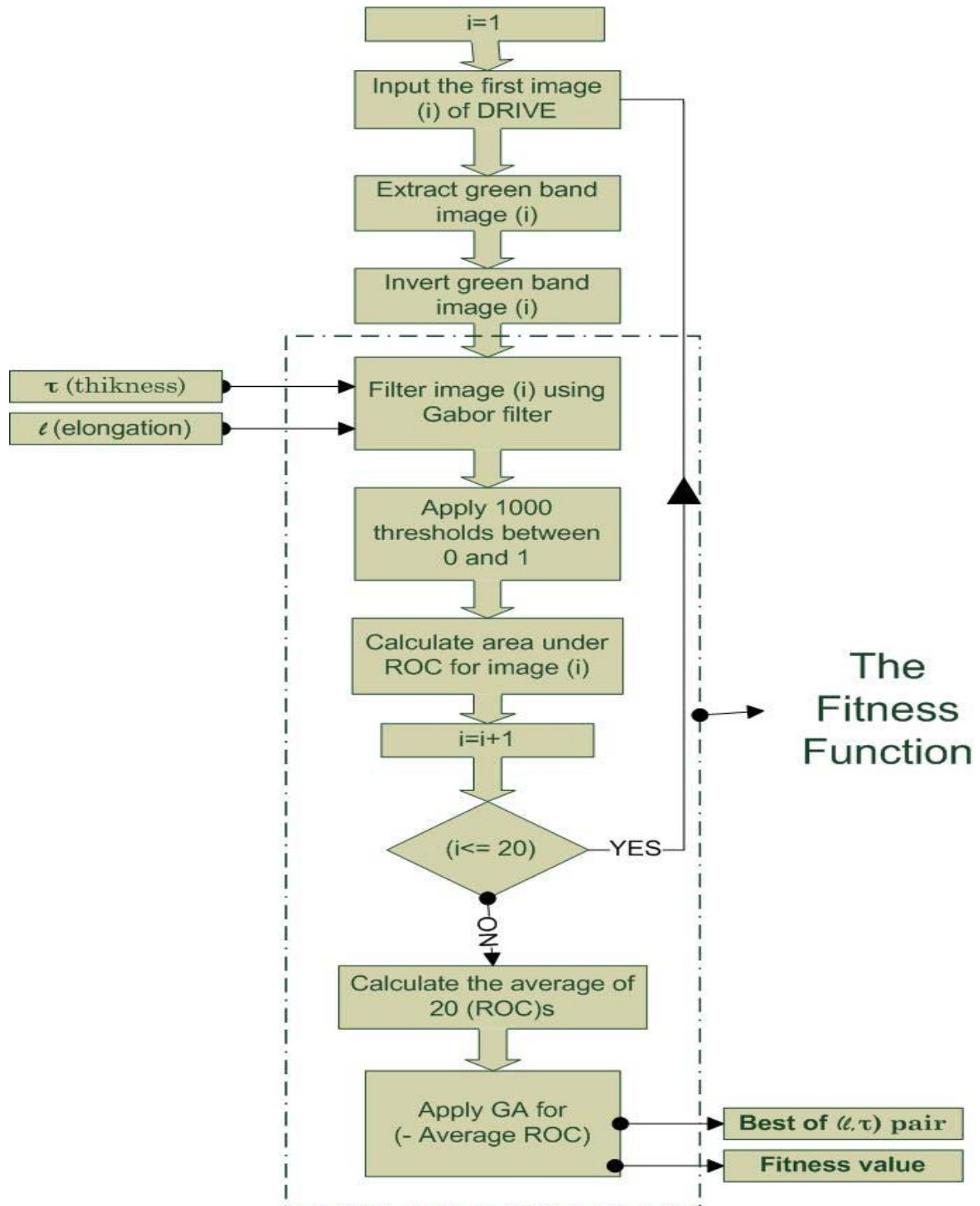
Figure 3.6: Optimizing The Average Area Under ROC For All DRIVE Database Images Block Diagram.

As shown in the block diagram in Figure 3.6 the first stage is image preparation in which the green band image is extracted for each of the 20 images of the training set of the DRIVE database. Then each green band image is filtered using Gabor filter, then the filtered image is thresholded in step of 0.001 of threshold values between 0 and 1. For each thresholded image the TPF and FPF are calculated and the ROC curve is plotted, and the area under ROC is calculated for each image, and the average area under ROC for the 20 images is the fitness function of GA.

3.5.4 Optimizing the average MA for the all DRIVE database

In this method the fitness function of GA is the average MA for the 20 images of DRIVE database, the block diagram of this method is shown in Figure 3.7.
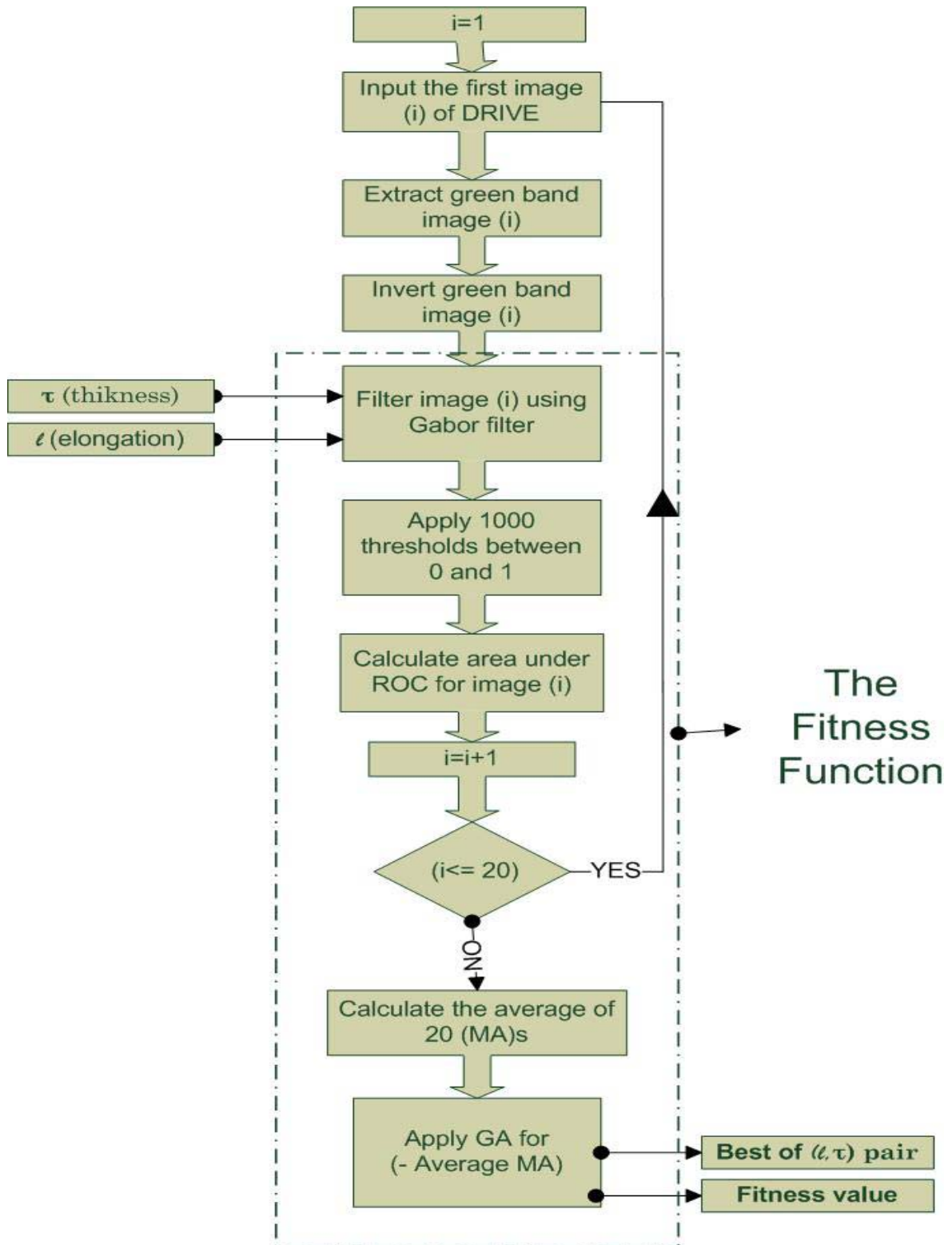
Figure 3.7: Optimizing The Average MA For All DRIVE Database.

As shown in the block diagram in Figure 3.7 the first stage is image preparation in which the green band image is extracted from each of the 20 images of the training set of the DRIVE database. Then each green band image is filtered using Gabor filter, then the filtered image is thresholded in step of 0.001 of threshold values between 0 and 1. For each thresholded image the accuracy is calculated and the MA is taken into account for each image then the average MA of the all 20 images MAA is the fitness function of GA.

3.5.5 Dividing The First DRIVE Image Into Four Regions

In this method after extracting the green-band from the first image of DRIVE database, it is divided into four equal regions as show in Figure 3.8, then the area under ROC for each region is calculated using different Gabor filter parameters than the other regions, and the average of the area under ROC is calculated and so the fitness function of the GA is the average area under ROC of the areas under ROC of the for regions.
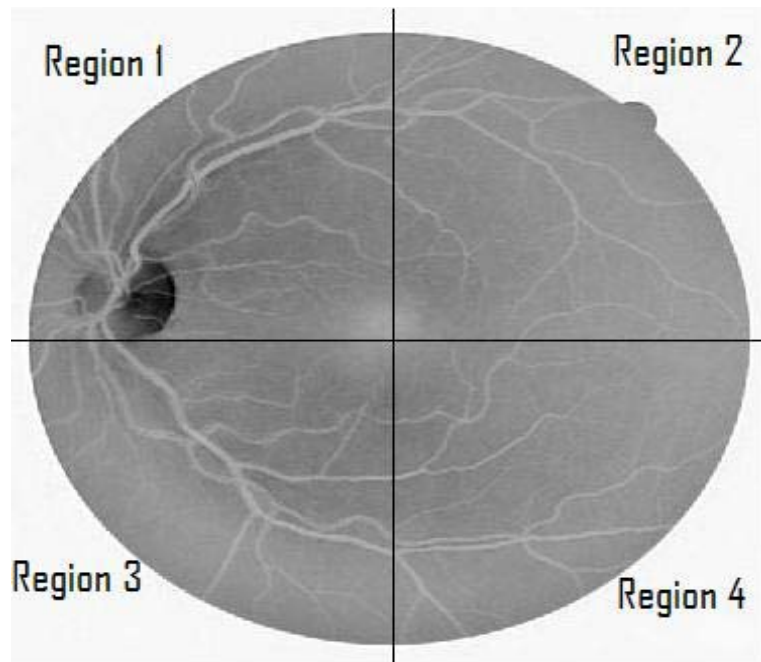
Figure 3.8: Dividing The Green Band of The First DRIVE Image.

The rationale behind this method is to find the best parameters for each region, when different set of parameters are used for each region, they are going to be optimized for that area and better accuracy is expected. The block diagram that describes this method is shown in Figure 3.9.
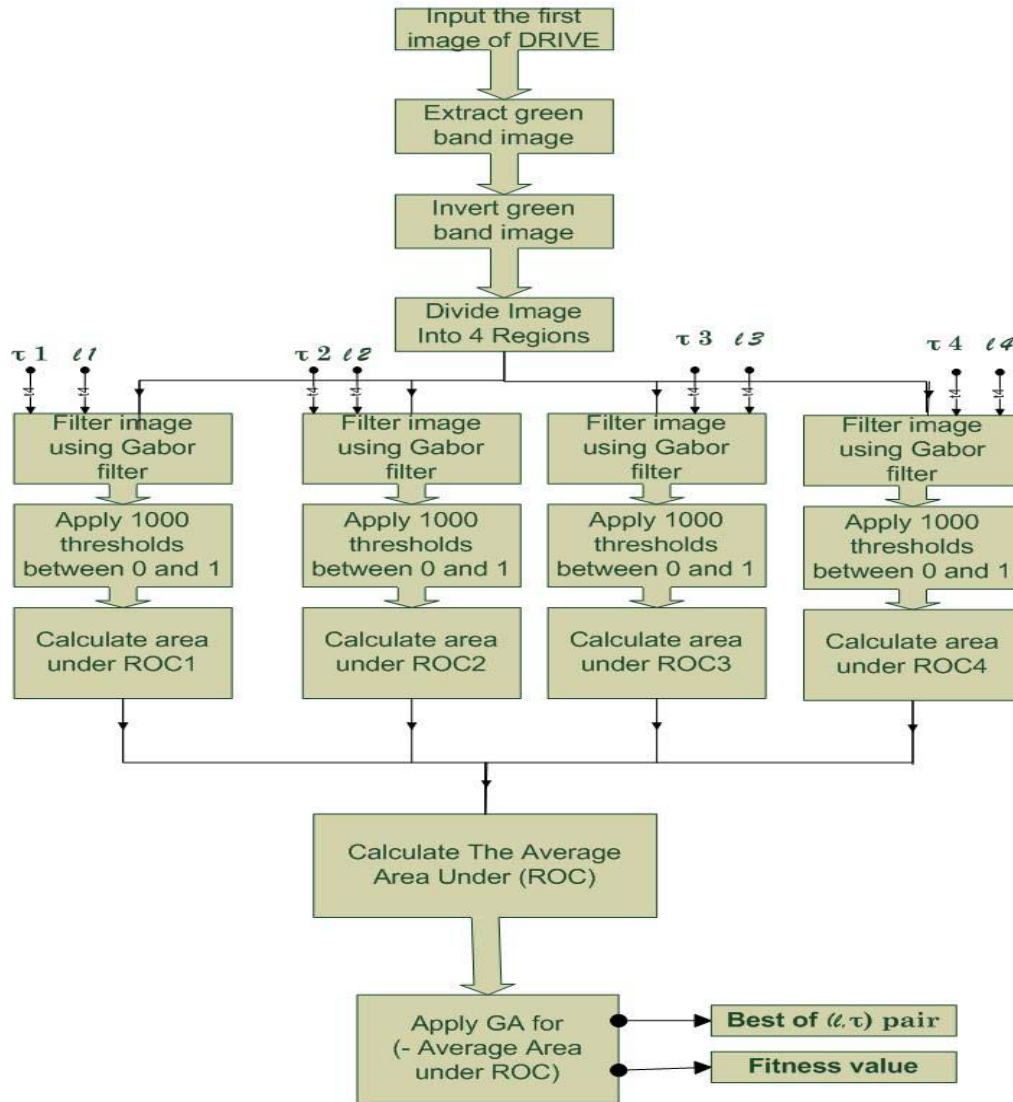
Figure 3.9: Dividing The First DRIVE Image Into Four Regions.

CHAPTER 4
SIMULATION AND RESULTS

This chapter presents a detailed description of the methods that are used in this thesis and their results, then the results are compared with the related methods that previously used for vessel detection. To optimize Gabor filter five experiments were conducted as following:

- Optimizing the area under Receiver Operating characteristic (ROC) curve for the first image of Digital Retinal Images for Vessel Extraction (DRIVE) database.

- Optimizing the Maximum Accuracy (MA) for the first image of DRIVE database.

- Optimizing the average area under ROC for all DRIVE database images.

- Optimizing the average MA for all DRIVE database images.

- Dividing the first DRIVE image into four regions.

The above experiments and their results are explained in the following sections. The last section of the chapter summarizes the findings.

4.1 Optimizing the area under ROC for the first image of DRIVE database

This section describes optimizing the area under ROC for the first image of DRIVE, the

following subsections includes the pseudo code, the results of the experiments including

tables and graphs and comparisons between this method and matched filter, Gabor filter,

Prewitt and Sobel (Chaudhuri et al. 1989), (Rangayyan et al. 2007).

Pseudo Code

The pseudo code for the fitness function of the Genetic Algorithm (GA) is described in

Figure 4.1.

Function ROC(image, ℓ, τ)

1. Extract green-band form image.

2. Invert green-band.

3. Filter invert-green-band using Gabor filter with ℓ and τ.

4. t=0.

5. while(t < =1).

6. Threshold(filter-image ,t).

7. Find TPF and FPF.

8. t=t+.001

9. end while.

10. Plot FPF vs. TPF to have ROC curve.

11. Return the area under ROC.

Figure 4.1: Pseudo Code of area under ROC.

The fitness function of the GA is -(area under ROC), since the GA gives the smallest result

and we want the maximum result for area under ROC. After applying GA to the area under

ROC for the first image of DRIVE database, the parameters that gave the best result of the

area under ROC are τ =10.188 and ℓ=1.26 and the best area under ROC = 0.9486, the

resulted image is shown in Figure 4.2.
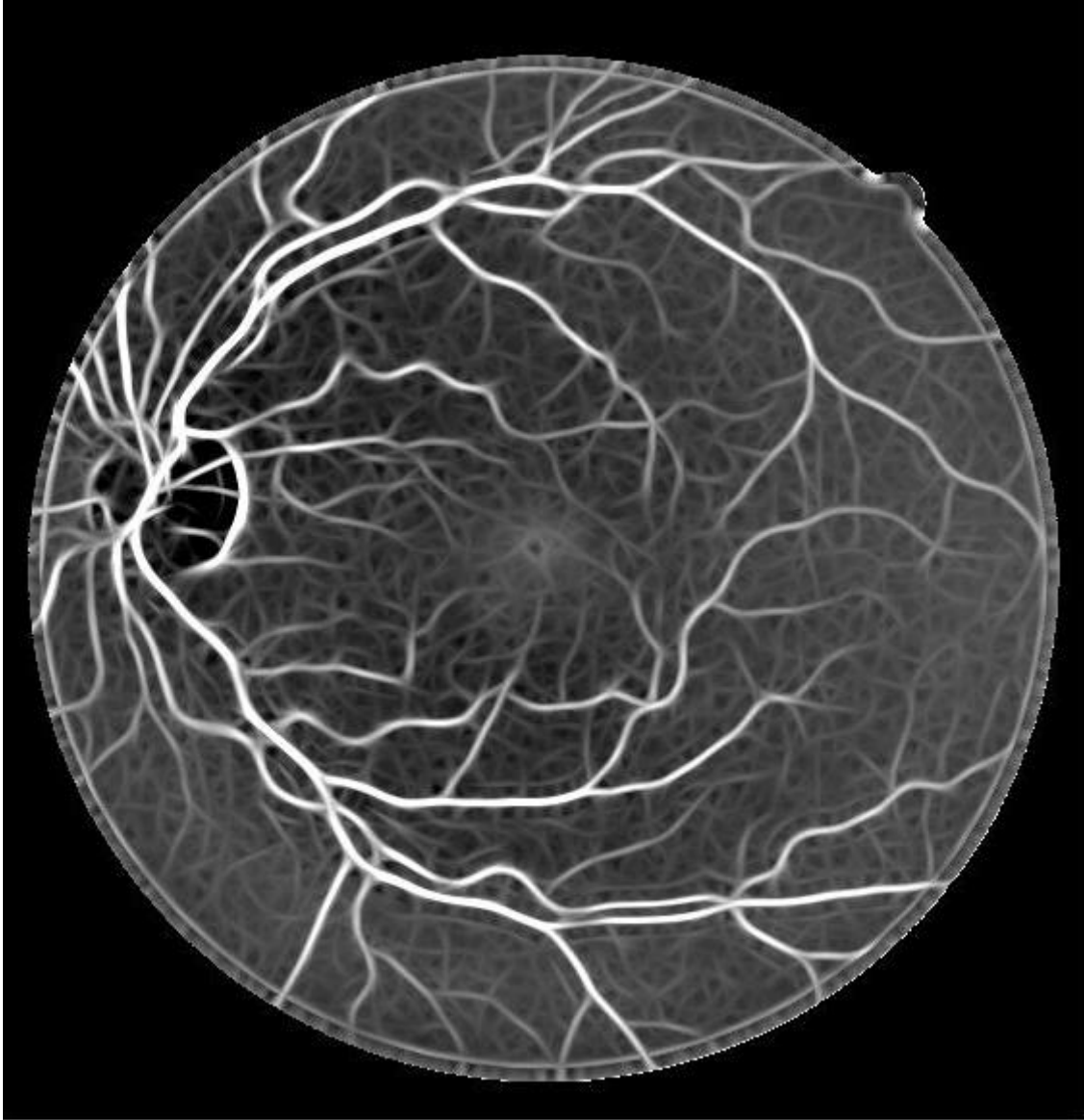
Figure 4.2: First Image of DRIVE Filtered By Filter1.

Results of Area Under ROC For Experiment 1

Table 4.1 shows the area under ROC for the 20 images of DRIVE that were filtered using

the Gabor filter parameters that were obtained using this experiment τ =10.188 and

ℓ=1.26. Figure 4.3 illustrates the ROC graph of this experiment.
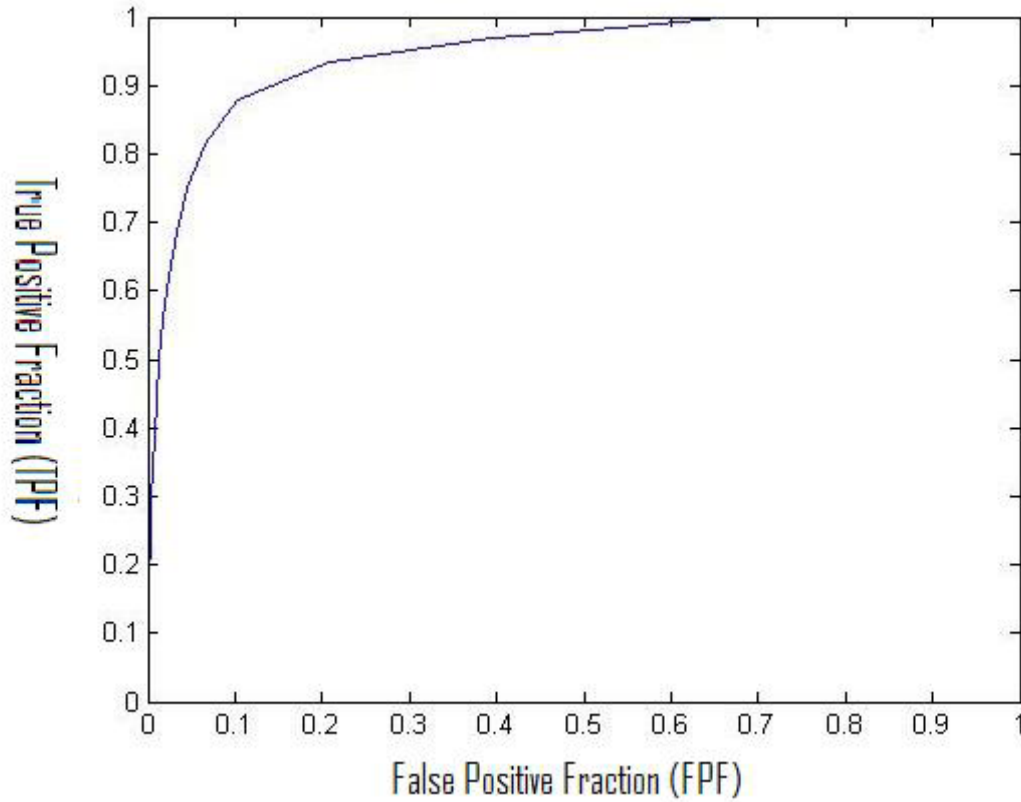
Figure 4.3: Experiment 1 ROC Graph.

Results of MA For Experiment 1

Table 4.2 shows the MA for the 20 images of DRIVE that were filtered using Gabor filter

parameters that obtained using this experiment τ =10.188 and ℓ=1.26.

Filter1 Vs. Gabor Filter (Rangayyan, et al., 2007)

Table 4.3 shows the area under ROC for DRIVE images compared with the results

obtained by applying Gabor filter (Rangayyan, et al., 2007).

Table 4.1: Results of Area Under ROC For Experiment 1.

Image	Filter1 t=10.188, l=1.26
Image1	0.9486
Image2	0.9455
Image3	0.9338
Image4	0.9204
Image5	0.9385
Image6	0.9208
Image7	0.9127
Image8	0.9255
Image9	0.9204
Image10	0.9244
Image11	0.9175
Image12	0.9366
Image13	0.9113
Image14	0.9405
Image15	0.9382
Image16	0.9463
Image17	0.9339
Image18	0.9438
Image19	0.9489
Image20	0.9558
Average	**0.93317**

Table 4.2: Results of MA For Experiment

Image	Filter1 t=10.188, l=1.26
Image1	0.945
Image2	0.9438
Image3	0.9371
Image4	0.9409
Image5	0.9378
Image6	0.9318
Image7	0.9339
Image8	0.9373
Image9	0.9322
Image10	0.9423
Image11	0.9355
Image12	0.9383
Image13	0.9278
Image14	0.9471
Image15	0.953
Image16	0.9317
Image17	0.9362
Image18	0.9385
Image19	0.9451
Image20	0.9449
Average	**0.93901**

Table 4.3: Results of Area Under ROC Filter1 Vs. (Rangayyan et al. 2007).

Method	Filter1 t=10.188, l=1.26	Rangayyan
Image1	0.9486	0.9422
Image2	0.9455	0.9415
Image3	0.9338	0.933
Image4	0.9204	0.9182
Image5	0.9385	0.9273
Image6	0.9208	0.918
Image7	0.9127	0.9007
Image8	0.9255	0.9193
Image9	0.9204	0.9152
Image10	0.9244	0.9174
Image11	0.9175	0.9166
Image12	0.9366	0.9341
Image13	0.9113	0.9031
Image14	0.9405	0.9375
Image15	0.9382	0.936
Image16	0.9463	0.9343
Image17	0.9339	0.9289
Image18	0.9438	0.9415
Image19	0.9489	0.9452
Image20	0.9558	0.9496
Average	**0.93317**	**0.92798**

It can be seen from Table 4.3 that the average area under ROC for Filter1 = 0.93317

and for Gabor it is 0.92798 (Rangayyan, et al., 2007), it can be concluded that Filter1

improves Gabor's results (Rangayyan et al. 2007).

Figure 4.4 shows the results of area under ROC for the 20 DRIVE images using Filter1 vs.

Gabor filter (Rangayyan et al. 2007).
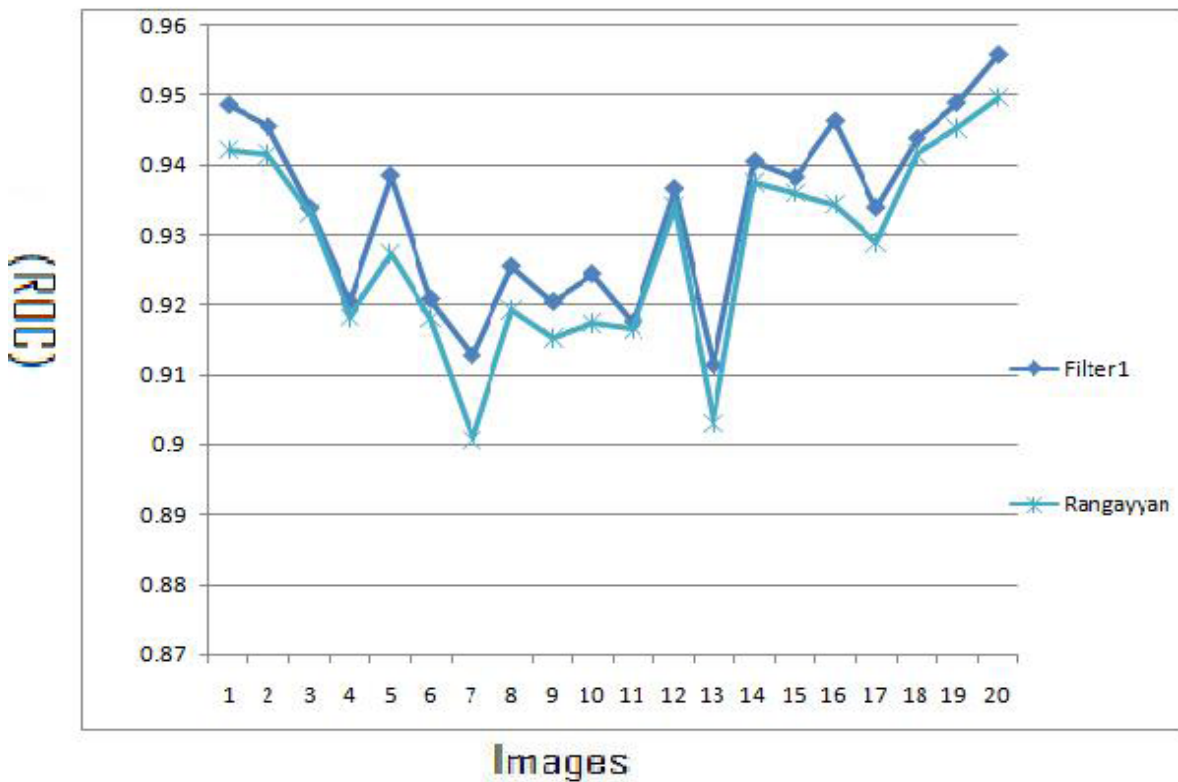
Figure 4.4: ROC Results of Filter1 Vs. Rangayyan's Gabor (Rangayyan, et al., 2007)

Figure 4.5 shows the ROC curve for the first image of DRIVE using Filter1 vs. Gabor

filter (Rangayyan et al. 2007).
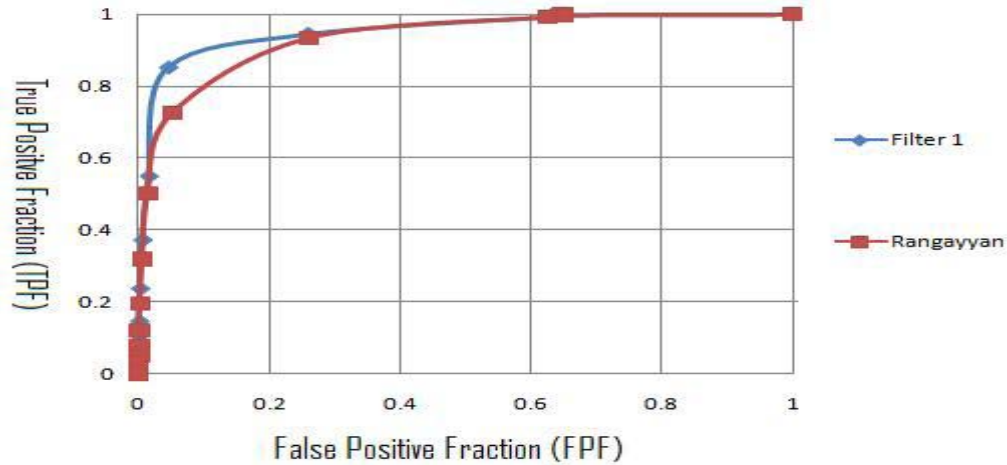
Figure 4.5: ROC Graph of Filter1 Vs. Rangayyan's Gabor (Rangayyan et al. 2007).

Table 4.4 shows the MA of DRIVE images compared with the results obtained by applying Gabor filter (Rangayyan et al. 2007). It can be seen from Table 4.4 that the average MA for Filter1 = 0.93901 and for Gabor = 0.93862, therefore it can be concluded that Filter1 improves Gabor's results (Rangayyan, et al., 2007).

Figure 4.6 shows the results of MA of the 20 DRIVE images using Filter1 vs. (Rangayyan et al. 2007) filter.
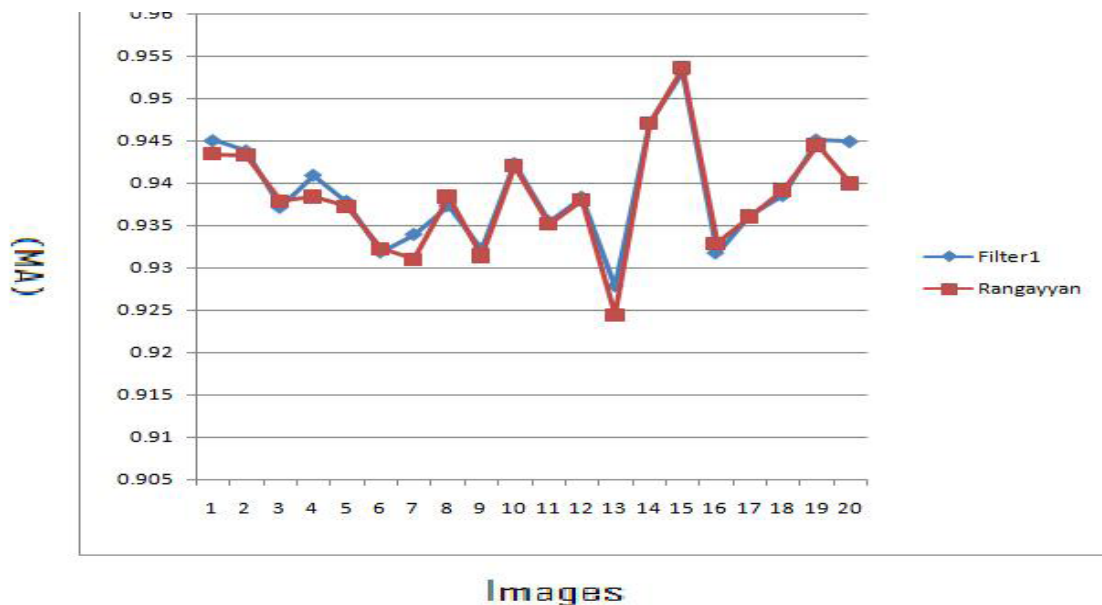
Figure 4.6: MA Results of Filter1 Vs.(Rangayyan, et al., 2007).

Table 4.4: Results of MA Filter1 Vs. (Rangayyan et al. 2007).

Method	Filter1 t=10.188, l=1.26	Rangayyan
Image1	0.945	0.9435
Image2	0.9438	0.9433
Image3	0.9371	0.9379
Image4	0.9409	0.9384
Image5	0.9378	0.9373
Image6	0.9318	0.9323
Image7	0.9339	0.931
Image8	0.9373	0.9384
Image9	0.9322	0.9314
Image10	0.9423	0.9421
Image11	0.9355	0.9352
Image12	0.9383	0.938
Image13	0.9278	0.9245
Image14	0.9471	0.9471
Image15	0.953	0.9536
Image16	0.9317	0.9329
Image17	0.9362	0.9361
Image18	0.9385	0.9392
Image19	0.9451	0.9445
Image20	0.9449	0.94
Average	**0.93901**	**0.93862**

Filter1 Vs. Matched Filter (Chaudhuri et al. 1989)

Table 4.5 shows the area under ROC of DRIVE images compared with the results

obtained by applying Chaudhuri's et al. matched filter (Chaudhuri, et al., 1989).

Table 4.5: Results of Area Under ROC Filter1 Vs. (Chaudhuri, et al., 1989).

Method	Filter1 t=10.188, l=1.26	Chaudhuri
Image1	0.9486	0.8357
Image2	0.9455	0.822
Image3	0.9338	0.8145
Image4	0.9204	0.8025
Image5	0.9385	0.8299
Image6	0.9208	0.7692
Image7	0.9127	0.758
Image8	0.9255	0.7643
Image9	0.9204	0.8199
Image10	0.9244	0.8209
Image11	0.9175	0.7436
Image12	0.9366	0.822
Image13	0.9113	0.7835
Image14	0.9405	0.8281
Image15	0.9382	0.8084
Image16	0.9463	0.8204
Image17	0.9339	0.7797
Image18	0.9438	0.8295
Image19	0.9489	0.8522
Image20	0.9558	0.8409
Average	**0.93317**	**0.8073**

From Table 4.5 it can be seen that the average area under ROC for Filter1 = 0.93317 and for matched filter it is 0.8073 (Chaudhuri, et al., 1989), therefore it can be concluded that Filter1 improves Chaudhuri's results.

Figure 4.7 shows the results of area under ROC for the 20 DRIVE images using Filter1 vs. matched filter.
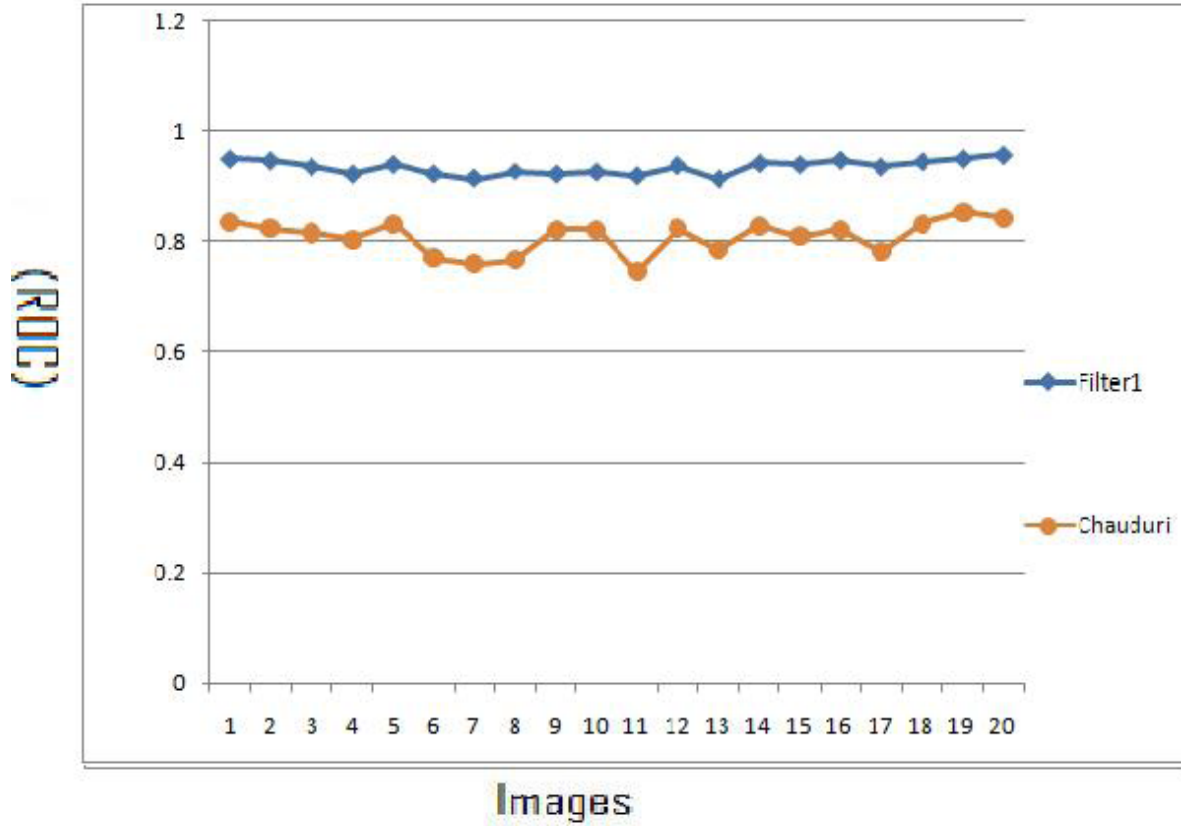
Figure 4.7: ROC Results of Filter1 Vs. (Chaudhuri, et al., 1989).

Figure 4.8 shows the ROC curve for the first image of DRIVE using Filter1 vs. matched filter (Chaudhuri, et al., 1989).
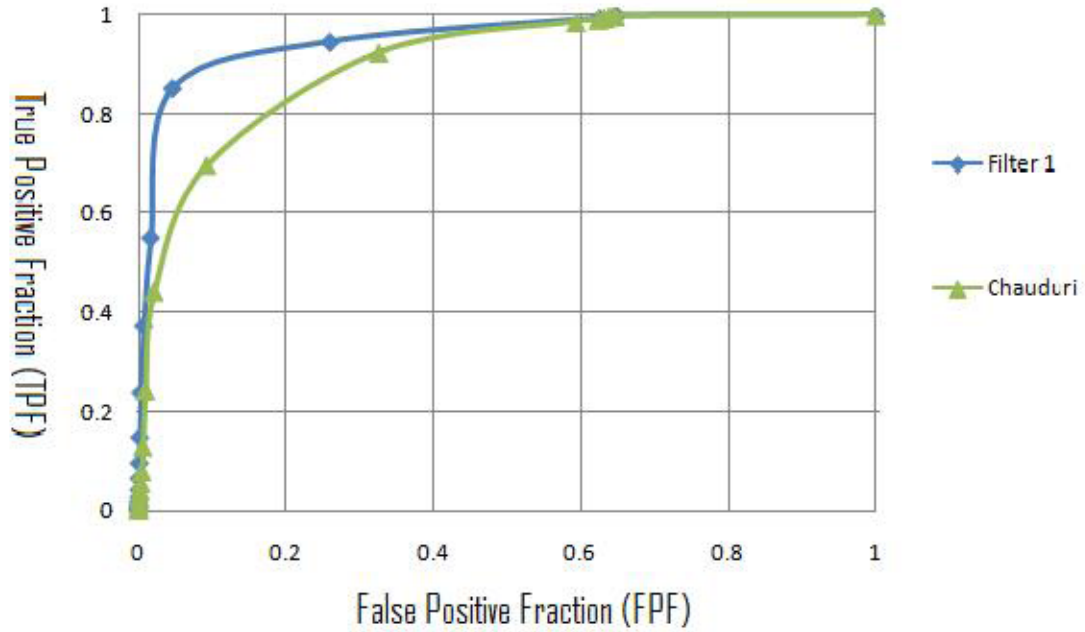
Figure 4.8: ROC Graph of Filter1 Vs. Chaudhuri's et al. Matched Filter (Chaudhuri et al., 1989).

Table 4.6 shows the MA of DRIVE images compared with the results obtained by

applying matched filter (Chaudhuri et al. 1989).

Table 4.6: Results of MA Filter1 Vs. Chaudhuri's matched filter(Chaudhuri et al. 1989).

Method	Filter1 t=10.188, l=1.26	Chaudhuri
Image1	0.945	0.9012
Image2	0.9438	0.8917
Image3	0.9371	0.8946
Image4	0.9409	0.8788
Image5	0.9378	0.8898
Image6	0.9318	0.8598
Image7	0.9339	0.878
Image8	0.9373	0.878
Image9	0.9322	0.8906
Image10	0.9423	0.8982
Image11	0.9355	0.8786
Image12	0.9383	0.8898
Image13	0.9278	0.8892
Image14	0.9471	0.897
Image15	0.953	0.9003
Image16	0.9317	0.8936
Image17	0.9362	0.8795
Image18	0.9385	0.8996
Image19	0.9451	0.9015
Image20	0.9449	0.9053
Average	**0.93901**	**0.8897**

From Table 4.6 it can be seen that the average MA for Filter1 = 0.93901 and for

(Chaudhuri, et al., 1989) it is 0.8897, therefore it can be concluded that Filter1

improves the matched filter results (Chaudhuri, et al., 1989).

Figure 4.9 shows the results of MA of the 20 DRIVE images using Filter1 vs.

Chaudhuri's matched filter (Chaudhuri, et al., 1989).
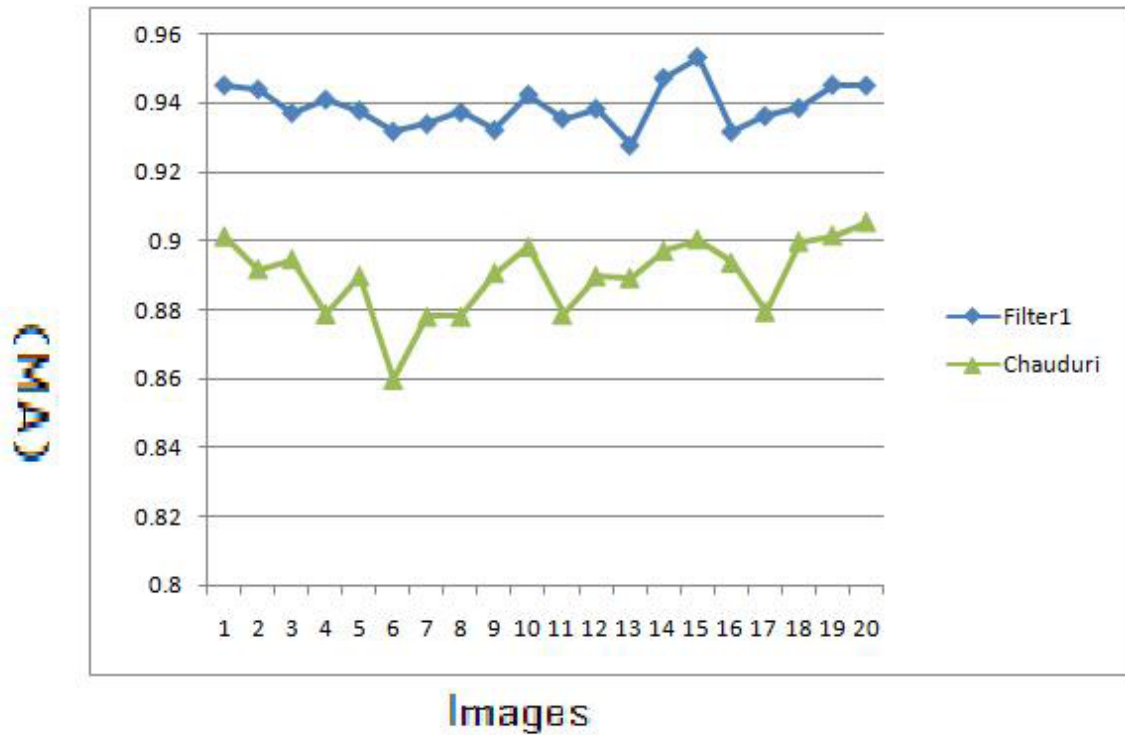
 Figure 4.9: MA Results of Filter1 Vs. Chaudhuri's matched filter (Chaudhuri, et al.,

1989).

Filter1 Vs. Traditional Edge Detection Techniques

Table 4.7 shows the area under ROC of DRIVE images compared with the results obtained

by applying Sobel and Prewitt filters described by Gonzalez &Woods (2002).

Table 4.7: Results of Area Under ROC for Filter1 Vs. Sobel and Prewitt.

Method	Filter1 t=10.188, l=1.26	Sobel	Prewitt
Image1	0.9486	0.7325	0.7322
Image2	0.9455	0.7611	0.7591
Image3	0.9338	0.7088	0.7088
Image4	0.9204	0.767	0.7646
Image5	0.9385	0.7369	0.7362
Image6	0.9208	0.7232	0.7219
Image7	0.9127	0.7484	0.7478
Image8	0.9255	0.7169	0.7167
Image9	0.9204	0.7397	0.7383
Image10	0.9244	0.7306	0.7308
Image11	0.9175	0.7538	0.7531
Image12	0.9366	0.706	0.7045
Image13	0.9113	0.7428	0.7414
Image14	0.9405	0.7274	0.7251
Image15	0.9382	0.7476	0.7474
Image16	0.9463	0.7202	0.718
Image17	0.9339	0.6974	0.6956
Image18	0.9438	0.6797	0.6788
Image19	0.9489	0.7136	0.7129
Image20	0.9558	0.6962	0.6939
Average	**0.93317**	**0.7275**	**0.72636**

From Table 4.7 it can be seen that the average area under ROC for Filter1 = 0.93317 and for Sobel it is 0.7275, and for Prewitt it is 0.72636, significant improvement is achieved using Filter1 than traditional edge techniques.

Table 4.8 shows the MA of DRIVE images obtained using filter1 compared with the results obtained by applying Sobel and Prewitt filters described by (Gonzalez and Woods, 2002).

Table 4.8 shows that the average MA for Filter1 = 0.93901 and for Sobel it is 0.8714, and for Prewitt it is 0.8749, therefore Filter1's results are better than traditional edge detection techniques.

Table 4.8: Results of Maximum Accuracy MA for Filter1 Vs. Sobel and Prewitt.

Method	Filter1 t=10.188,l=1.26	Sobel	Prewitt
Image1	0.945	0.8699	0.8715
Image2	0.9438	0.8612	0.861
Image3	0.9371	0.8572	0.8572
Image4	0.9409	0.8728	0.8733
Image5	0.9378	0.867	0.8672
Image6	0.9318	0.8587	0.8598
Image7	0.9339	0.8694	0.8696
Image8	0.9373	0.87	0.876
Image9	0.9322	0.8776	0.8832
Image10	0.9423	0.8777	0.8814
Image11	0.9355	0.873	0.8732
Image12	0.9383	0.8681	0.8756
Image13	0.9278	0.8608	0.861
Image14	0.9471	0.8786	0.8835
Image15	0.953	0.897	0.897
Image16	0.9317	0.861	0.8699
Image17	0.9362	0.8683	0.8784
Image18	0.9385	0.8764	0.8858
Image19	0.9451	0.8745	0.8805
Image20	0.9449	0.8871	0.894
Average	**0.93901**	**0.8714**	**0.8749**

4.2 Optimizing the MA for the first image of DRIVE database

This section describes optimizing the MA for the first image of DRIVE, the following

subsections includes the pseudo code, the results of the experiments including tables and

graphs and comparisons between this method and matched filter, Gabor filter, Prewitt and

Sobel.

Pseudo Code

The pseudo code of the fitness function of the GA is described in Figure 4.10

```
Function MA(image,l,tau)
1.Extract green-band form image.
2.Invert green-band.
3.Filter invert-green-band using Gabor filter with l and tau.
4.t=0, temp=0
5.while(t< =1).
6.IMG=Threshold(filter-image,t).
7.Find Accuracy(IMG).
8.If Accuracy(IMG) >temp then temp =Accuracy(IMG).
9.t=t+.001
10.end while.
11.MA=temp.
```

Figure 4.10: Pseudo Code of MA.

The fitness function of the GA is -(MA), since GA gives the smallest result and we want

the maximum result for MA. The GA is applied to the Gabor-filtered image more than

once, the fitness function for the GA is the MA, the parameters that gave the best result of

MA are τ =9.519 and ℓ=.403, and the MA = 0.9476 the resulted image is shown in Figure

4.11.
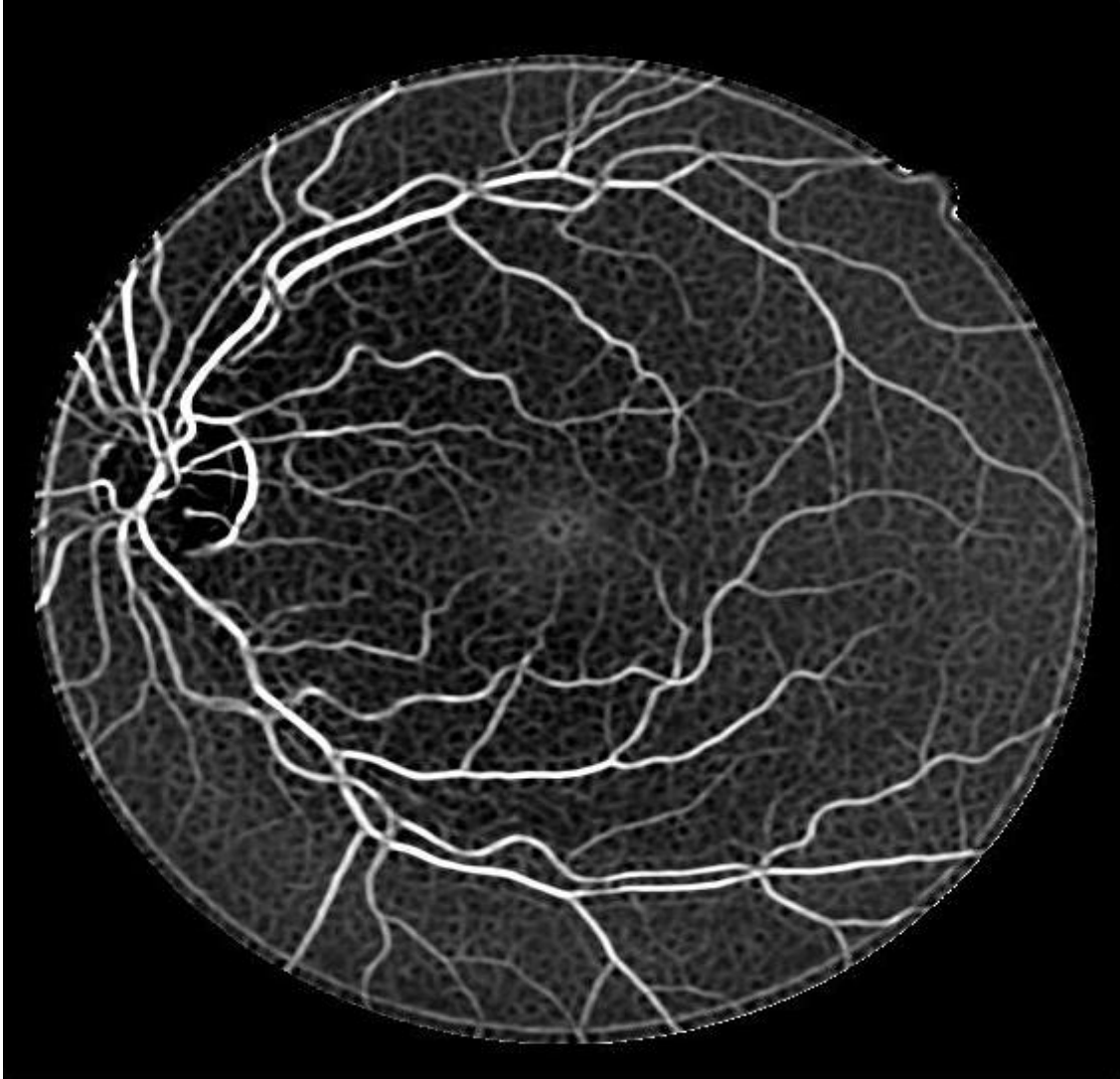
Figure 4.11: DRIVE First Image Filtered By Filter2.

Results of Area Under ROC For Experiment 2

Table 4.9 shows the area under ROC for the 20 images of DRIVE that are filtered

using the Gabor filter parameters that obtained using this experiment τ =9.519 and

ℓ=.403.

Table 4.9: Results of Area Under ROC For Experiment 2.

Image	Filter2 t=9.519, l=.403
Image1	0.9368
Image2	0.926
Image3	0.9069
Image4	0.8982
Image5	0.9109
Image6	0.9041
Image7	0.8896
Image8	0.8989
Image9	0.9028
Image10	0.9055
Image11	0.9049
Image12	0.9172
Image13	0.8934
Image14	0.9224
Image15	0.9223
Image16	0.932
Image17	0.9235
Image18	0.934
Image19	0.9401
Image20	0.9392
Average	**0.915435**

Figure 4.12 illustrates the ROC graph of this experiment.
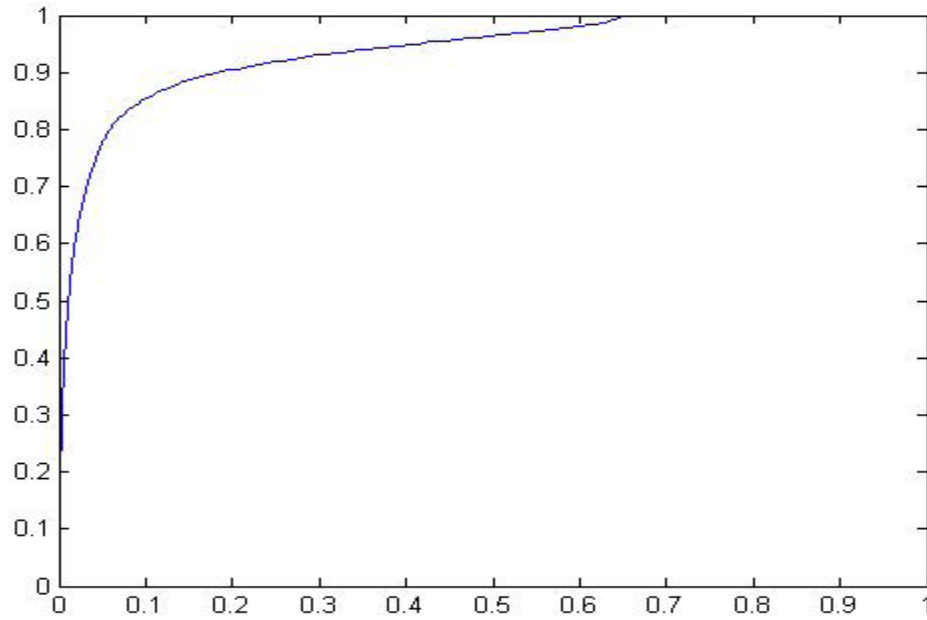
Figure 4.12: Experiment 2 ROC Graph.

Results of MA for Experiment 2

Table 4.10 shows the MA for the 20 images of DRIVE that are filtered using the Gabor

filter parameters that obtained using this experiment τ =9.519 and ℓ=.403.

Filter2 Vs. Gabor Filter (Rangayyan et al. 2007)

Table 4.11 shows the area under ROC of DRIVE images compared with the results

obtained by applying Gabor filter (Rangayyan et al. 2007).

Table 4.10: Results of MA For Experiment

Image	Filter2 t=9.519, l=.403
Image1	0.9476
Image2	0.943
Image3	0.9347
Image4	0.9388
Image5	0.9378
Image6	0.9317
Image7	0.9332
Image8	0.9354
Image9	0.9333
Image10	0.9424
Image11	0.9362
Image12	0.9382
Image13	0.9269
Image14	0.9469
Image15	0.9523
Image16	0.9338
Image17	0.9366
Image18	0.941
Image19	0.9463
Image20	0.9456
Average	**0.939085**

Table 4.11: Results of Area Under ROC Filter2 Vs. Rangayyan's Gabor Filter (Rangayyan, et al., 2007).

Method	Filter2 t=9.519, l=.403	Rangayyan
Image1	0.9368	0.9422
Image2	0.926	0.9415
Image3	0.9069	0.933
Image4	0.8982	0.9182
Image5	0.9109	0.9273
Image6	0.9041	0.918
Image7	0.8896	0.9007
Image8	0.8989	0.9193
Image9	0.9028	0.9152
Image10	0.9055	0.9174
Image11	0.9049	0.9166
Image12	0.9172	0.9341
Image13	0.8934	0.9031
Image14	0.9224	0.9375
Image15	0.9223	0.936
Image16	0.932	0.9343
Image17	0.9235	0.9289
Image18	0.934	0.9415
Image19	0.9401	0.9452
Image20	0.9392	0.9496
Average	**0.915435**	**0.92798**

From Table 4.11 it can be seen that the average area under ROC for Filter2 = 0.915435 and

for Gabor it is 0.92798. Figure 4.13 shows the results of area under ROC of the 20 DRIVE

images using Filter2 vs. Gabor filter (Rangayyan, et al., 2007)
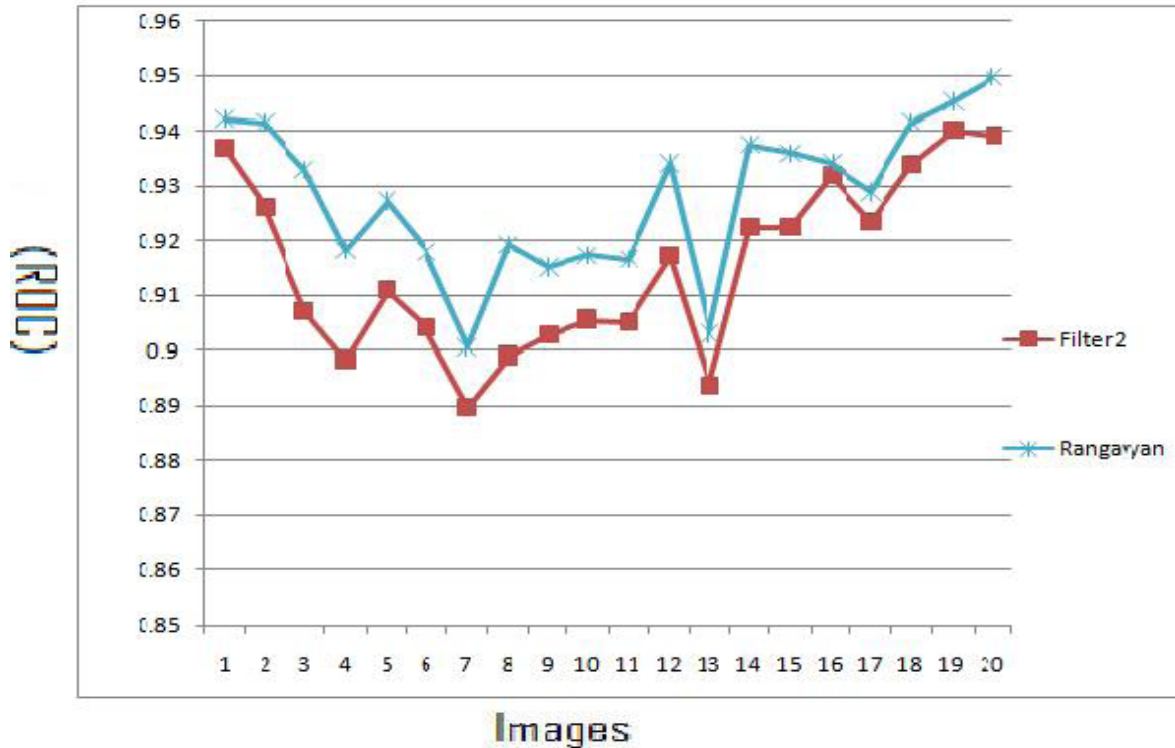
Figure 4.13: ROC Results of Filter2 Vs. Rangayyan's Gabor Filter (Rangayyan, et al., 2007).
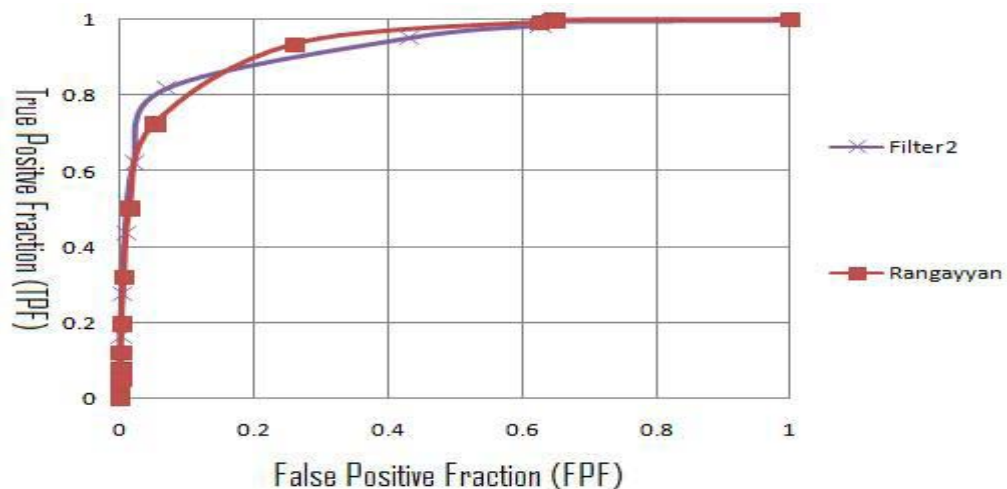
Figure 4.14: ROC Graph of Filter2 Vs. Rangayyan's Gabor Filter (Rangayyan et al.)

Table 4.12 shows the MA of DRIVE images compared with the results obtained by applying Gabor filter (Rangayyan, et al., 2007).

Table 4.12: Results of MA Filter2 Vs. (Rangayyan, et al., 2007).

Method	Filter2 t=9.519,l=.403	Rangayyan
Image1	0.9476	0.9435
Image2	0.943	0.9433
Image3	0.9347	0.9379
Image4	0.9388	0.9384
Image5	0.9378	0.9373
Image6	0.9317	0.9323
Image7	0.9332	0.931
Image8	0.9354	0.9384
Image9	0.9333	0.9314
Image10	0.9424	0.9421
Image11	0.9362	0.9352
Image12	0.9382	0.938
Image13	0.9269	0.9245
Image14	0.9469	0.9471
Image15	0.9523	0.9536
Image16	0.9338	0.9329
Image17	0.9366	0.9361
Image18	0.941	0.9392
Image19	0.9463	0.9445
Image20	0.9456	0.94
Average	**0.939085**	**0.93862**

It can be noticed from Table 4.12 that the average MA for Filter2 = 0.939085 and for Gabor (Rangayyan et al. 2007) is 0.93862, therefore it can be concluded that Filter2 improves Gabor filter (Rangayyan, et al., 2007).

Figure 4.15 shows the results of MA for the 20 DRIVE images using Filter2 vs. Gabor filter (Rangayyan, et al., 2007).
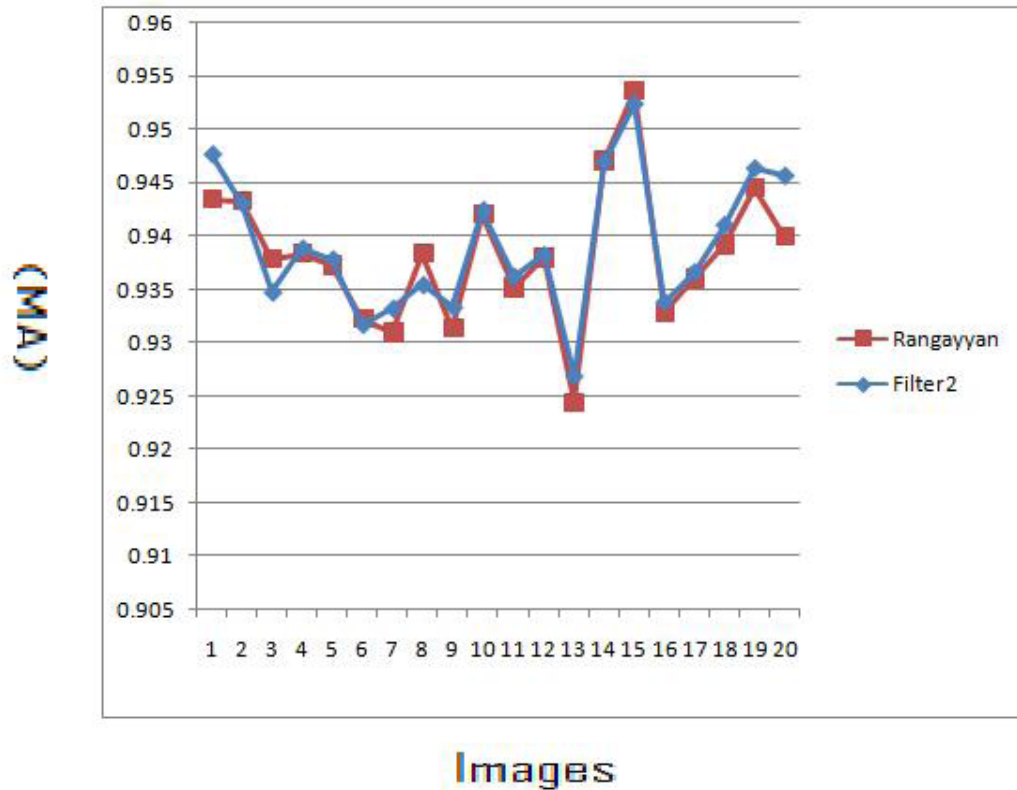
Figure 4.15: MA Results of Filter2 Vs.(Rangayyan et al. 2007).

Filter2 Vs. Matched Filter (Chaudhuri et al. 1989)

Table 4.13 shows the area under ROC of DRIVE images compared with the results

obtained by applying Chaudhuri's matched filter (Chaudhuri et al. 1989).

Table 4.13: Results of Area Under ROC Filter2 Vs. Chaudhuri's matched filter (Chaudhuri, et al., 1989).

Method	Filter2 t=9.519,l=.403	Chaudhuri
Image1	0.9368	0.8357
Image2	0.926	0.822
Image3	0.9069	0.8145
Image4	0.8982	0.8025
Image5	0.9109	0.8299
Image6	0.9041	0.7692
Image7	0.8896	0.758
Image8	0.8989	0.7643
Image9	0.9028	0.8199
Image10	0.9055	0.8209
Image11	0.9049	0.7436
Image12	0.9172	0.822
Image13	0.8934	0.7835
Image14	0.9224	0.8281
Image15	0.9223	0.8084
Image16	0.932	0.8204
Image17	0.9235	0.7797
Image18	0.934	0.8295
Image19	0.9401	0.8522
Image20	0.9392	0.8409
Average	**0.915435**	**0.8073**

From the Table 4.13 it can be seen that the average area under ROC for Filter2 = 0.915435 and for the matched filter it is 0.8073 (Chaudhuri, et al., 1989), it can concluded that Filter2 improves the matched filter's results (Chaudhuri, et al., 1989).

Figure 4.16 shows the results of area under ROC of the 20 DRIVE images using Filter2 vs. matched filter (Chaudhuri, et al., 1989).
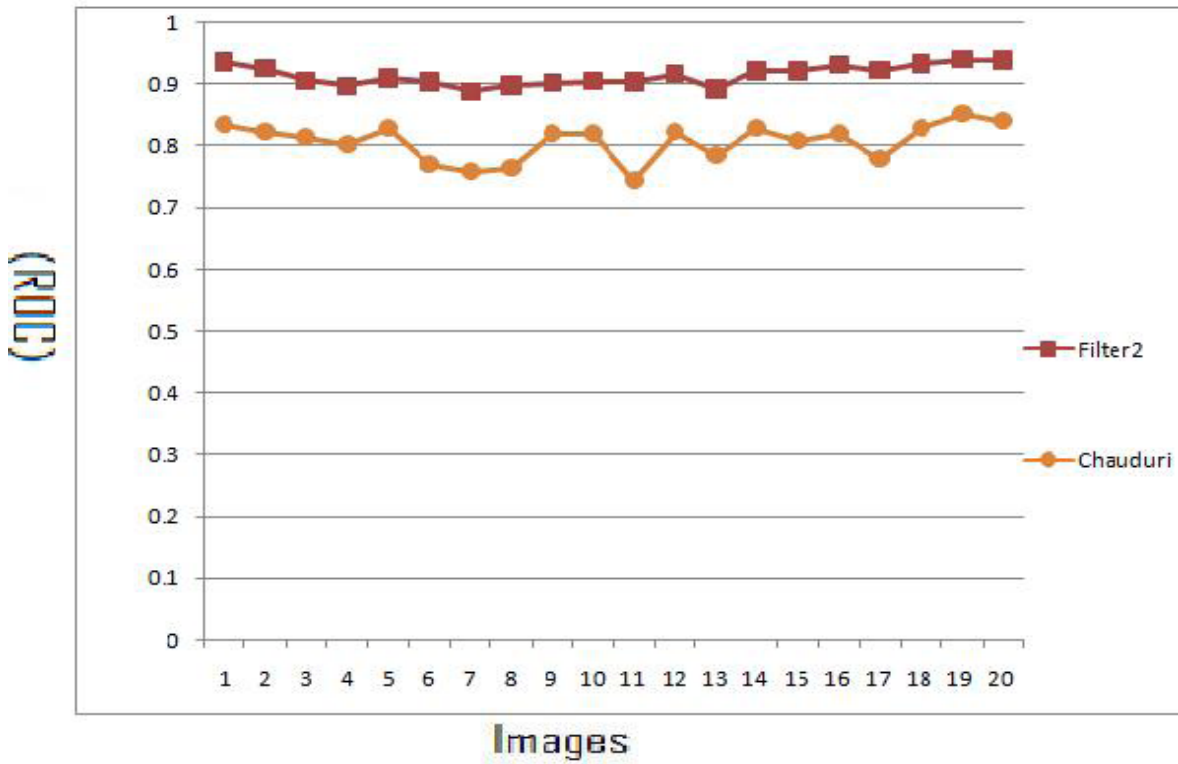
Figure 4.16: ROC Results of Filter2 Vs. (Chaudhuri et al. 1989).

Figure 4.17 show the ROC curve for the first image of DRIVE using Filter2 vs. matched filter (Chaudhuri, et al., 1989).
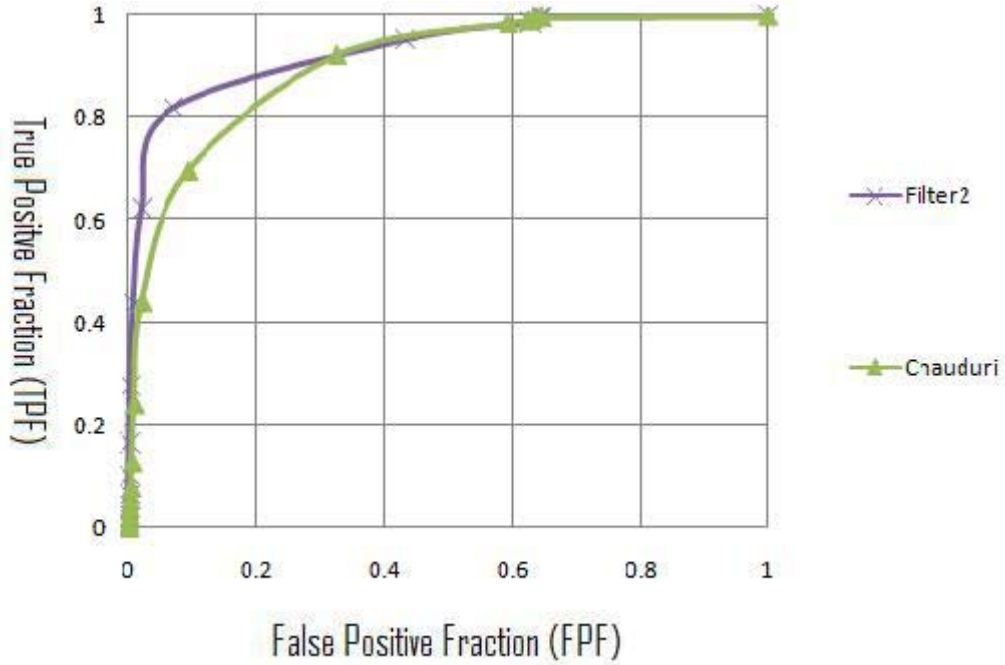
Figure 4.17: ROC Graph of Filter2 Vs. (Chaudhuri, et al., 1989).

Table 4.14 shows the MA of DRIVE images compared with the results obtained by applying matched filter (Chaudhuri, et al., 1989).

It can be noticed that the average MA for Filter2 = 0.939085 and for (Chaudhuri, et al., 1989) it is 0.8897, it can be concluded that Filter2 improves matched filter results (Chaudhuri, et al., 1989).

Table 4.14: Results of MA Filter2 Vs. Chaudhuri's matched filter(Chaudhuri et al. 1989).

Method	Filter2 t=9.519,l=.403	Chaudhuri
Image1	0.9476	0.9012
Image2	0.943	0.8917
Image3	0.9347	0.8946
Image4	0.9388	0.8788
Image5	0.9378	0.8898
Image6	0.9317	0.8598
Image7	0.9332	0.878
Image8	0.9354	0.87
Image9	0.9333	0.8906
Image10	0.9424	0.8982
Image11	0.9362	0.8786
Image12	0.9382	0.8898
Image13	0.9269	0.8892
Image14	0.9469	0.897
Image15	0.9523	0.9003
Image16	0.9338	0.8936
Image17	0.9366	0.8795
Image18	0.941	0.8996
Image19	0.9463	0.9015
Image20	0.9456	0.9053
Average	**0.939085**	**0.8897**

Figure 4.18 shows the results of MA of the 20 DRIVE images using Filter2 vs.

matched filter (Chaudhuri, et al., 1989).
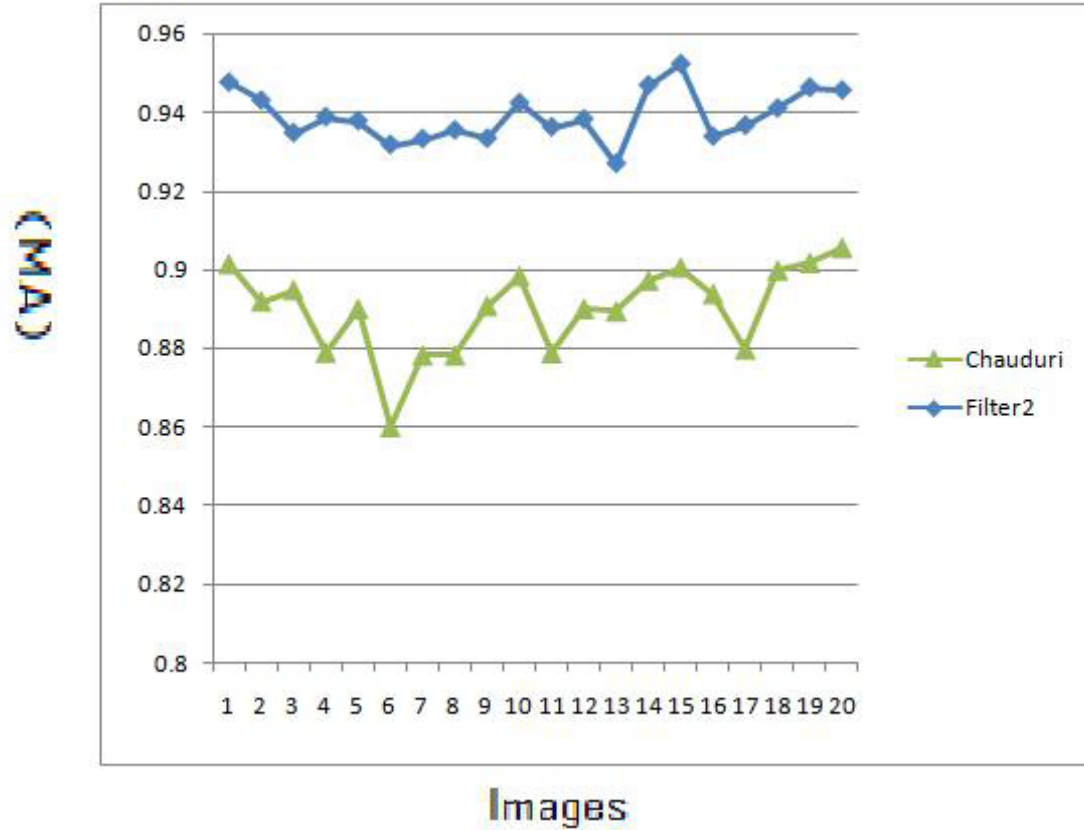
Figure 4.18: MA Results of Filter2 Vs.(Chaudhuri, et al., 1989).

Filter2 Vs. Traditional Edge Detection Techniques

Table 4.15 shows the area under ROC of DRIVE images compared with the results

obtained by applying Sobel and Prewitt filters described by Gonzalez & Woods (2002).

Table 4.15: Results of Area Under ROC for Filter2 Vs. Sobel and Prewitt.

Method	Filter2 t=9.519,l=.403	Sobel	Prewitt
Image1	0.9368	0.7325	0.7322
Image2	0.926	0.7611	0.7591
Image3	0.9069	0.7088	0.7088
Image4	0.8982	0.767	0.7646
Image5	0.9109	0.7369	0.7362
Image6	0.9041	0.7232	0.7219
Image7	0.8896	0.7484	0.7478
Image8	0.8989	0.7169	0.7167
Image9	0.9028	0.7397	0.7383
Image10	0.9055	0.7306	0.7308
Image11	0.9049	0.7538	0.7531
Image12	0.9172	0.706	0.7045
Image13	0.8934	0.7428	0.7414
Image14	0.9224	0.7274	0.7251
Image15	0.9223	0.7476	0.7474
Image16	0.932	0.7202	0.718
Image17	0.9235	0.6974	0.6956
Image18	0.934	0.6797	0.6788
Image19	0.9401	0.7136	0.7129
Image20	0.9392	0.6962	0.6939
Average	**0.915435**	**0.7275**	**0.72636**

From the Table 4.15 it can be seen that the average area under ROC for Filter2 = 0.915435 and for Sobel it is 0.7275, and for Prewitt it is 0.72636, therefore it can be concluded that Filter1's results are better than traditional edge techniques.

Table 4.16 shows the MA of DRIVE images compared with the results obtained by applying Sobel and Prewitt filters described by (Gonzalez & Woods, 2002). From the table, it can be seen that the average MA for Filter1 = 0.939085 and for Sobel it is 0.8714, and for Prewitt it is 0.8749, therefore it can be concluded that Filter1's results are better than traditional edge techniques.

Table4.16. Results of MA for Filter2 Vs. Sobel and Prewitt.

Method	Filter2 t=9.519,l=.403	Sobel	Prewitt
Image1	0.9476	0.8699	0.8715
Image2	0.943	0.8612	0.861
Image3	0.9347	0.8572	0.8572
Image4	0.9388	0.8728	0.8733
Image5	0.9378	0.867	0.8672
Image6	0.9317	0.8587	0.8598
Image7	0.9332	0.8694	0.8696
Image8	0.9354	0.87	0.876
Image9	0.9333	0.8776	0.8832
Image10	0.9424	0.8777	0.8814
Image11	0.9362	0.873	0.8732
Image12	0.9382	0.8681	0.8756
Image13	0.9269	0.8608	0.861
Image14	0.9469	0.8786	0.8835
Image15	0.9523	0.897	0.897
Image16	0.9338	0.861	0.8699
Image17	0.9366	0.8683	0.8784
Image18	0.941	0.8764	0.8858
Image19	0.9463	0.8745	0.8805
Image20	0.9456	0.8871	0.894
Average	**0.939085**	**0.8714**	**0.8749**

4.3 Optimizing the average area under ROC for all DRIVE database images

This section describes optimizing the area under ROC for all images of DRIVE, the following subsections includes the pseudo code, the results of the experiments including tables and graphs and comparisons between this method and matched filter, Gabor filter, Prewitt and Sobel.

Pseudo Code

The pseudo code of the fitness function of the GA is described in Figure 4.19

```
Function averageROC( image[20],l,tau)
1.i=1
2. while(i<21)
3.Extract green-band[i] form image[i].
4.Invert green-band[i].
5.Filter invert-green-band [i] using Gabor filter with l and tau.
6.t=0.
7.while(t<=1). 8.Threshold(filter-image[i],t).
9.Find TPF and FPF.
10.t=t+.001
11.end while.
12.Plot FPF vs. TPF to have ROC curve.
13.Calculate the area under ROC.
14.i=i+1
15.end while
16.return the average of the ROCs of the 20 images.
```

Figure 4.19: Pseudo Code of Average Area Under ROC.

In this method the 20 images of the DRIVE database were used as an input for the GA optimization, After calculating the ROC of each Gabor-filtered image, the - (average area under ROC for the 20 images) is the fitness function of the GA, since the GA gives the smallest result and we want the maximum result for average ROC. The parameters that

gave the best result after applying GA are τ =10.352 and ℓ=1.541, and the average area under ROC = 0.934035. The resulted image is shown in Figure 4.20 .
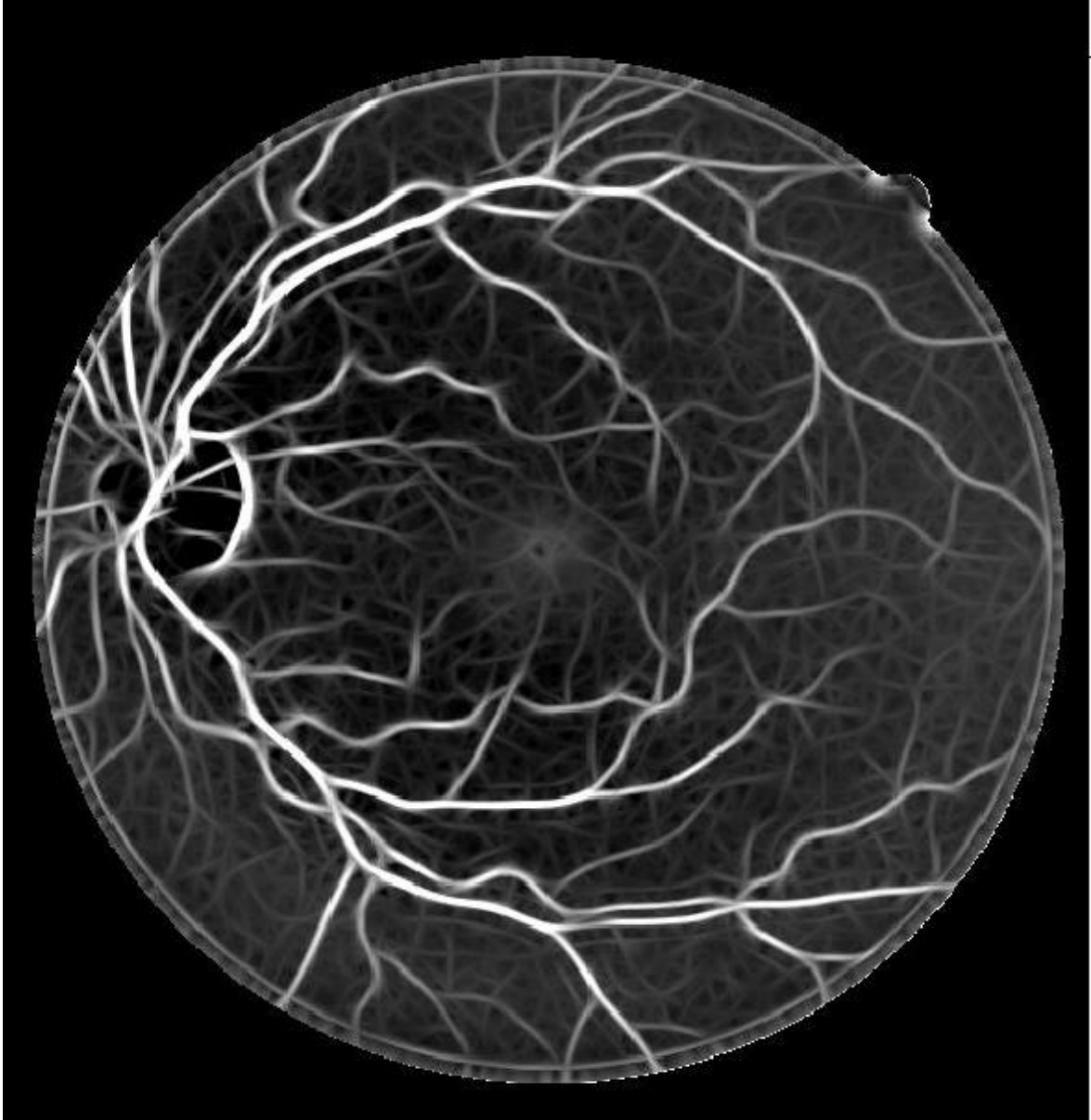
Figure 4.20: DRIVE First Image Filtered By Filter3.

Results of Area Under ROC For Experiment 3

Table 4.17 shows the area under ROC for the the 20 images of DRIVE) that are filtered

using the Gabor filter parameters the obtained using this experiment τ =10.352 and ℓ=1.541

Table 4.17: Results of Area Under ROC For Experiment 3.

Image	Filter3 t=10.352, l=1.541
Image1	0.9473
Image2	0.9456
Image3	0.9355
Image4	0.9224
Image5	0.9323
Image6	0.9213
Image7	0.9221
Image8	0.9209
Image9	0.9199
Image10	0.9241
Image11	0.9177
Image12	0.9397
Image13	0.9117
Image14	0.9474
Image15	0.9395
Image16	0.9482
Image17	0.9327
Image18	0.9434
Image19	0.9539
Image20	0.9551
Average	**0.934035**

Figure 4.21 illustrates the ROC graph of this experiment.
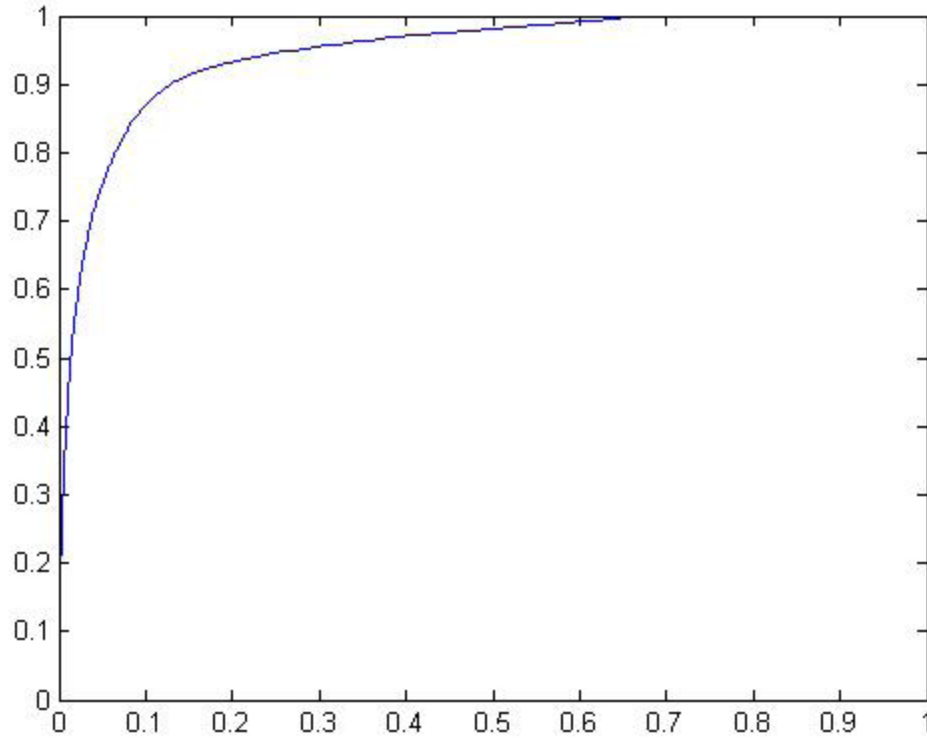
Figure 4.21: Experiment 3 ROC Graph.

Results of MA For Experiment 3

Table 4.18 shows the MA for the the 20 images of DRIVE that are filtered using the Gabor filter parameters that obtained using this experiment τ =10.352 and ℓ=1.541.

Filter3 Vs. Gabor filter (Rangayyan et al. 2007)

Table 4.19 shows the area under ROC of DRIVE images compared with the results obtained by applying Gabor filter (Rangayyan et al. 2007).

Table 4.19: Results of Area Under ROC Filter3 Vs. (Rangayyan, et al., 2007).

Method	Filter3 t=10.352, l=1.541	Rangayyan
Image1	0.9473	0.9422
Image2	0.9456	0.9415
Image3	0.9355	0.933
Image4	0.9224	0.9182
Image5	0.9323	0.9273
Image6	0.9213	0.918
Image7	0.9221	0.9007
Image8	0.9209	0.9193
Image9	0.9199	0.9152
Image10	0.9241	0.9174
Image11	0.9177	0.9166
Image12	0.9397	0.9341
Image13	0.9117	0.9031
Image14	0.9474	0.9375
Image15	0.9395	0.936
Image16	0.9482	0.9343
Image17	0.9327	0.9289
Image18	0.9434	0.9415
Image19	0.9539	0.9452
Image20	0.9551	0.9496
Average	**0.934035**	**0.92798**

From Table 4.19 it can be seen that the average area under ROC for Filter3 = 0.934035 and

for Gabor filter (Rangayyan, et al., 2007) it is 0.92798, it can be concluded that Filter3

improves Gabor's results (Rangayyan, et al., 2007).

Figure 4.22 shows the results of area under ROC of the 20 DRIVE images using Filter3 vs.

Gabor filter (Rangayyan, et al., 2007).
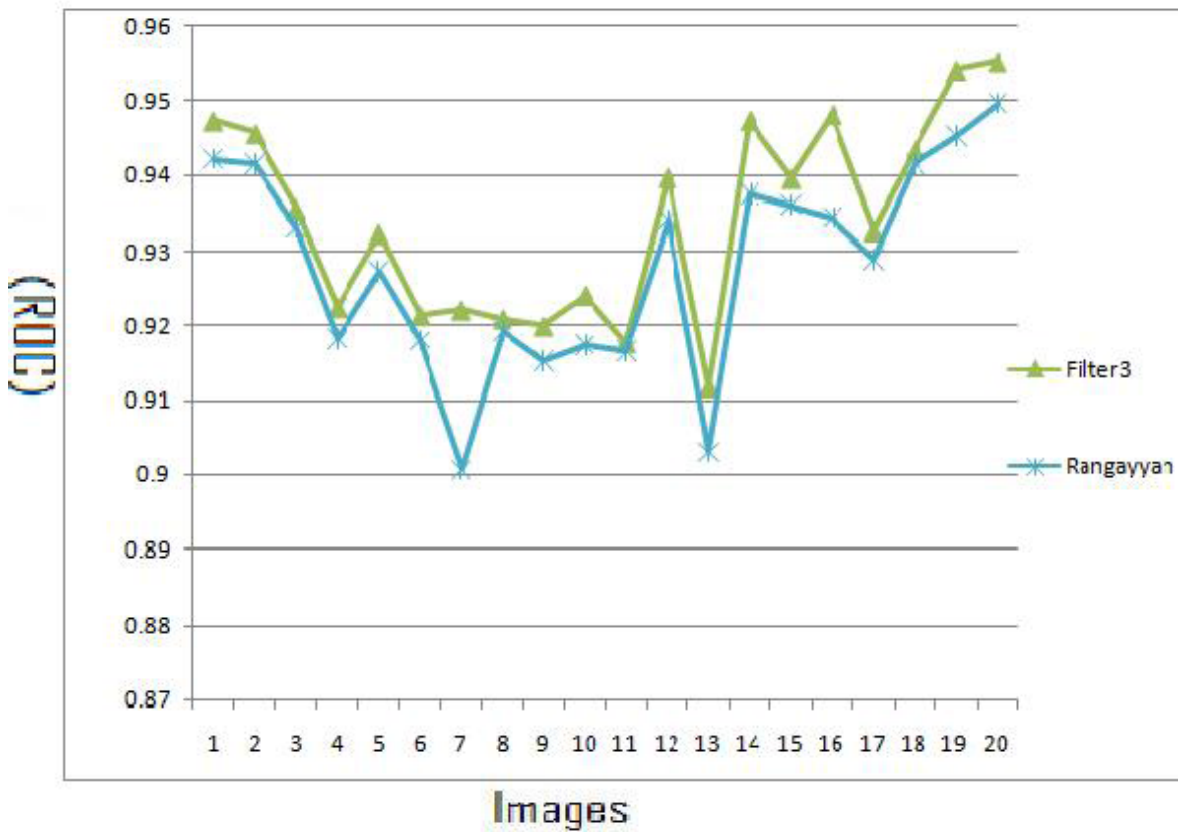
Figure 4.22: ROC Results of Filter3 Vs.(Rangayyan et al. 2007).

Figure 4.23 show the ROC curve for the first image of DRIVE using Filter3 vs. Gabor

filter (Rangayyan et al. 2007).
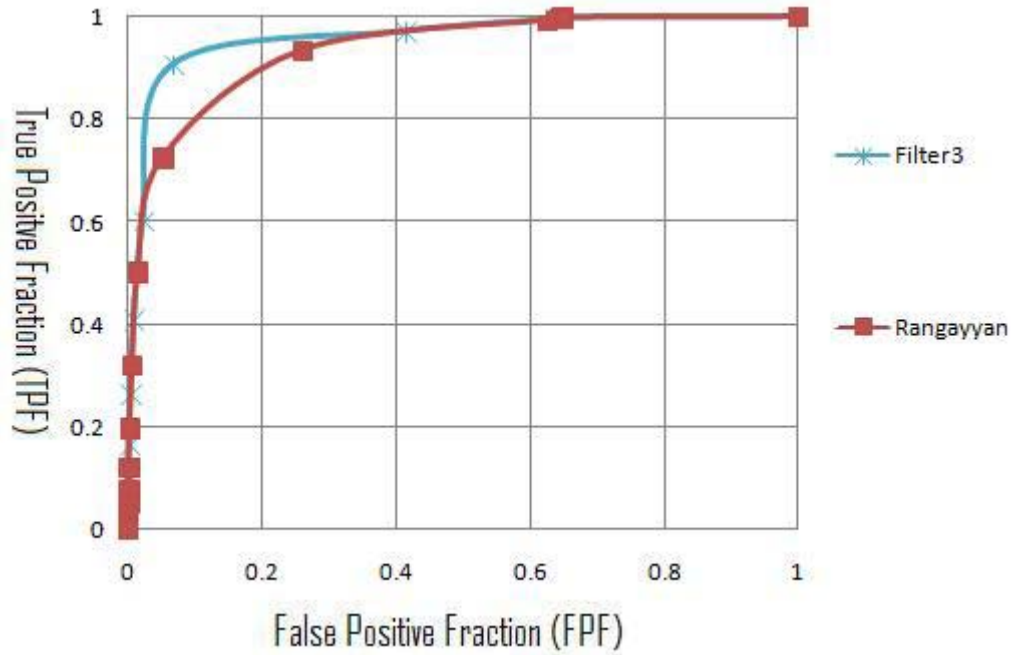
Figure 4.23: ROC Graph of Filter3 Vs. (Rangayyan, et al., 2007).

Table 4.20 shows the MA of DRIVE images compared with the results o applying Gabor filter (Rangayyan et al. 2007).

It can be noticed from Table 4.20 that the average MA for Filter3 = 0.93901 and for (Rangayyan et al. 2007) it is 0.93862, i.e.Filter3 improved Gabor filter results (Rangayyan et al. 2007).

Figure 4.24 shows the results of MA of the 20 DRIVE images using Filter3 vs. Gabor filter (Rangayyan et al. 2007).

Table 4.20: Results of MA Filter3 Vs. (Rangayyan et al. 2007).

Method	Filter3 t=10.352,l=1.541	Rangayyan
Image1	0.9442	0.9435
Image2	0.9439	0.9433
Image3	0.9381	0.9379
Image4	0.9408	0.9384
Image5	0.9381	0.9373
Image6	0.9321	0.9323
Image7	0.9334	0.931
Image8	0.9374	0.9384
Image9	0.9319	0.9314
Image10	0.9423	0.9421
Image11	0.9354	0.9352
Image12	0.9385	0.938
Image13	0.9278	0.9245
Image14	0.9475	0.9471
Image15	0.9532	0.9536
Image16	0.9318	0.9329
Image17	0.9361	0.9361
Image18	0.9381	0.9392
Image19	0.9448	0.9445
Image20	0.9448	0.94
Average	**0.93901**	**0.93862**
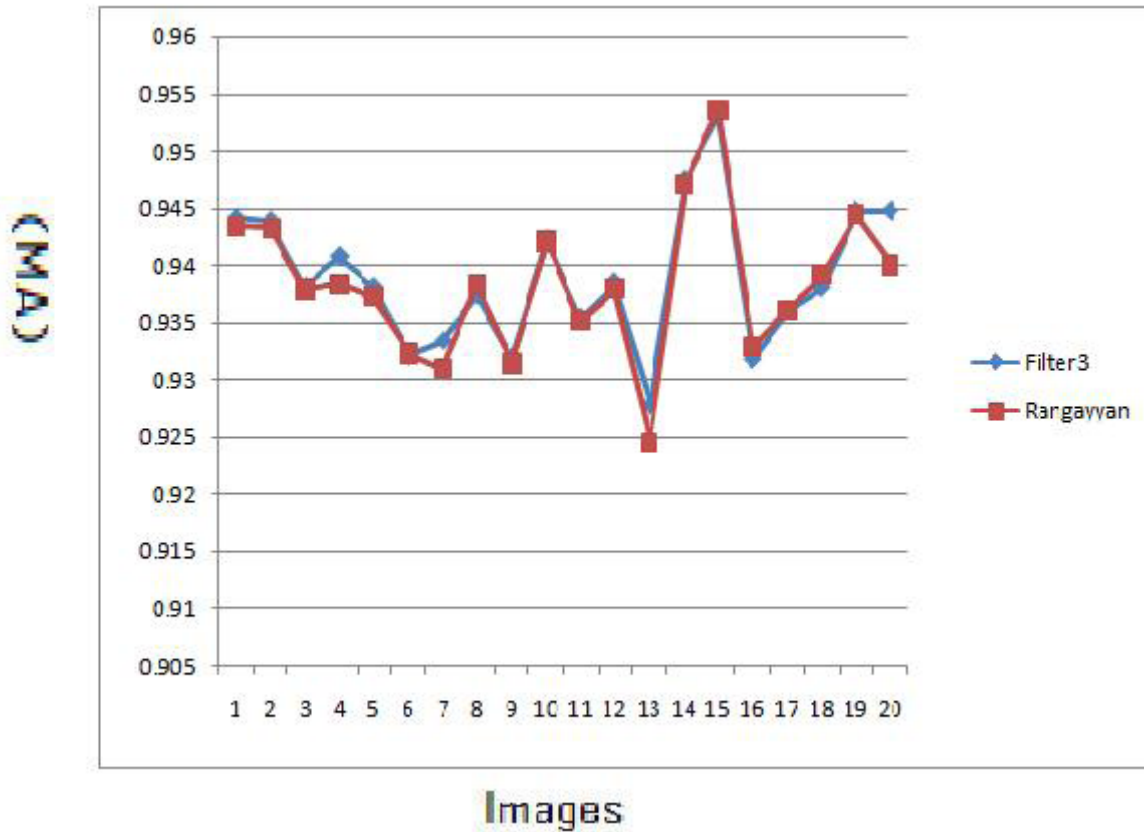
Figure 4.24: MA Results of Filter3 Vs.(Rangayyan et al. 2007).

Filter3 Vs. Matched filter (Chaudhuri, et al., 1989)

Table 4.21 shows the area under ROC of DRIVE images compared with the results

obtained by applying matched filter (Chaudhuri et al. 1989). From Table 4.21 it can be

seen that the average area under ROC for Filter3 = 0.934035 and for the matched filter is

0.8073 (Chaudhuri, et al., 1989), therefore it can be concluded that Filter3 improves

matched filter results.

Figure 4.25 shows the results of area under ROC of the 20 DRIVE images using Filter3 vs.

matched filter.

Table 4.21: Results of Area Under ROC Filter3 Vs. (Chaudhuri, et al., 1989).

Method	Filter3 t=10.352,l=1.541	Chaudhuri
Image1	0.9473	0.8357
Image2	0.9456	0.822
Image3	0.9355	0.8145
Image4	0.9224	0.8025
Image5	0.9323	0.8299
Image6	0.9213	0.7692
Image7	0.9221	0.758
Image8	0.9209	0.7643
Image9	0.9199	0.8199
Image10	0.9241	0.8209
Image11	0.9177	0.7436
Image12	0.9397	0.822
Image13	0.9117	0.7835
Image14	0.9474	0.8281
Image15	0.9395	0.8084
Image16	0.9482	0.8204
Image17	0.9327	0.7797
Image18	0.9434	0.8295
Image19	0.9539	0.8522
Image20	0.9551	0.8409
Average	**0.934035**	**0.8073**
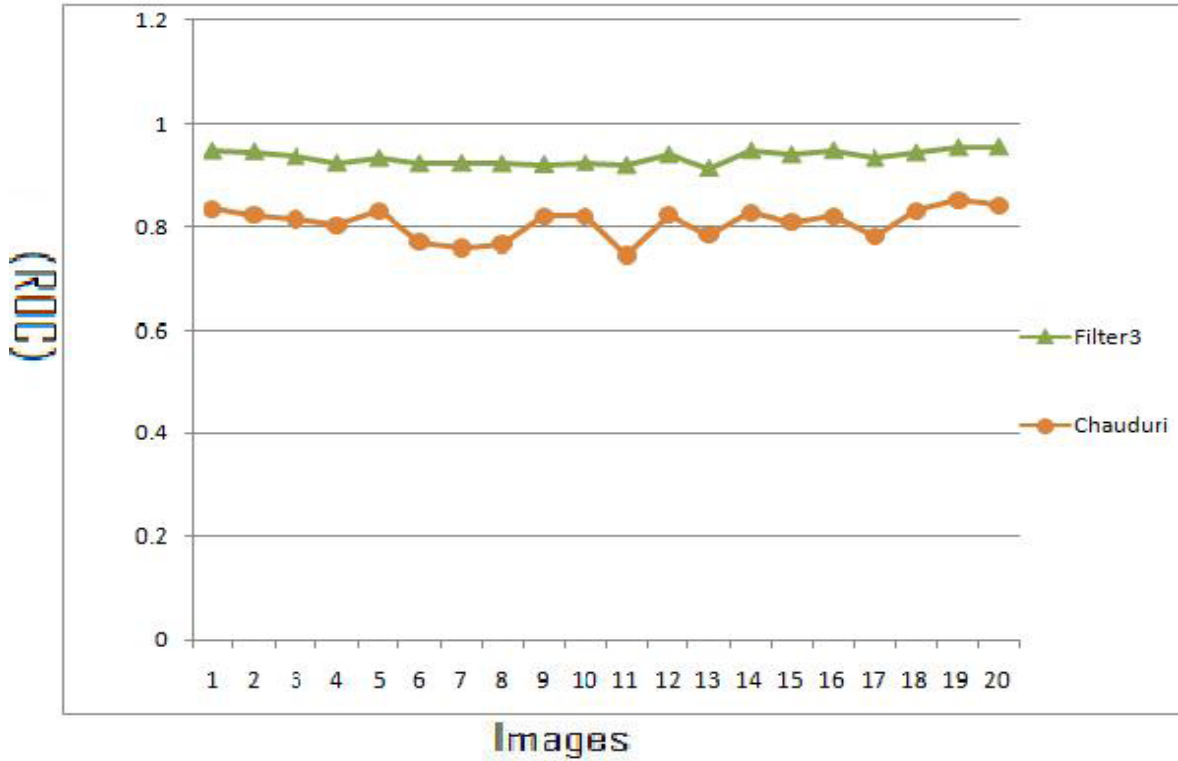
Figure 4.25: ROC Results of Filter3 Vs. (Chaudhuri, et al., 1989).

Figure 4.26 shows the ROC curve for the first image of DRIVE using Filter3 vs. matched filter filter (Chaudhuri et al. 1989).
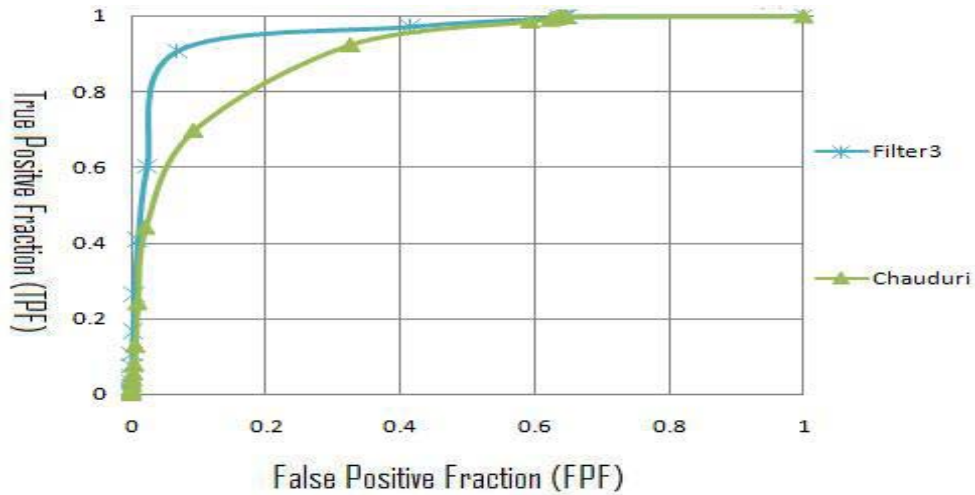
Figure 4.26: ROC Graph of Filter3 Vs. (Chaudhuri et al. 1989).

Table 4.22 shows the MA of DRIVE images compared with the results obtained bybtained

by applying matched filter (Chaudhuri et al. 1989).

Table 4.22: Results of MA Filter3 Vs.(Chaudhuri et al. 1989).

Method	Filter3 t=10.352, l=1.541	Chaudhuri
Image1	0.9442	0.9012
Image2	0.9439	0.8917
Image3	0.9381	0.8946
Image4	0.9408	0.8788
Image5	0.9381	0.8898
Image6	0.9321	0.8598
Image7	0.9334	0.878
Image8	0.9374	0.878
Image9	0.9319	0.8906
Image10	0.9423	0.8982
Image11	0.9354	0.8786
Image12	0.9385	0.8898
Image13	0.9278	0.8892
Image14	0.9475	0.897
Image15	0.9532	0.9003
Image16	0.9318	0.8936
Image17	0.9361	0.8795
Image18	0.9381	0.8996
Image19	0.9448	0.9015
Image20	0.9448	0.9053
Average	**0.93901**	**0.8897**

From Table 4.22 it can be noticed that the average MA for Filter3 = 0.93901 and for

matched filter (Chaudhuri, et al., 1989) it is 0.8897, therefore it can be concluded that

Filter3 improves matched filter results.

Figure 4.27 shows the results of MA of the 20 DRIVE images using Filter3 vs. matched

filter (Chaudhuri et al. 1989).
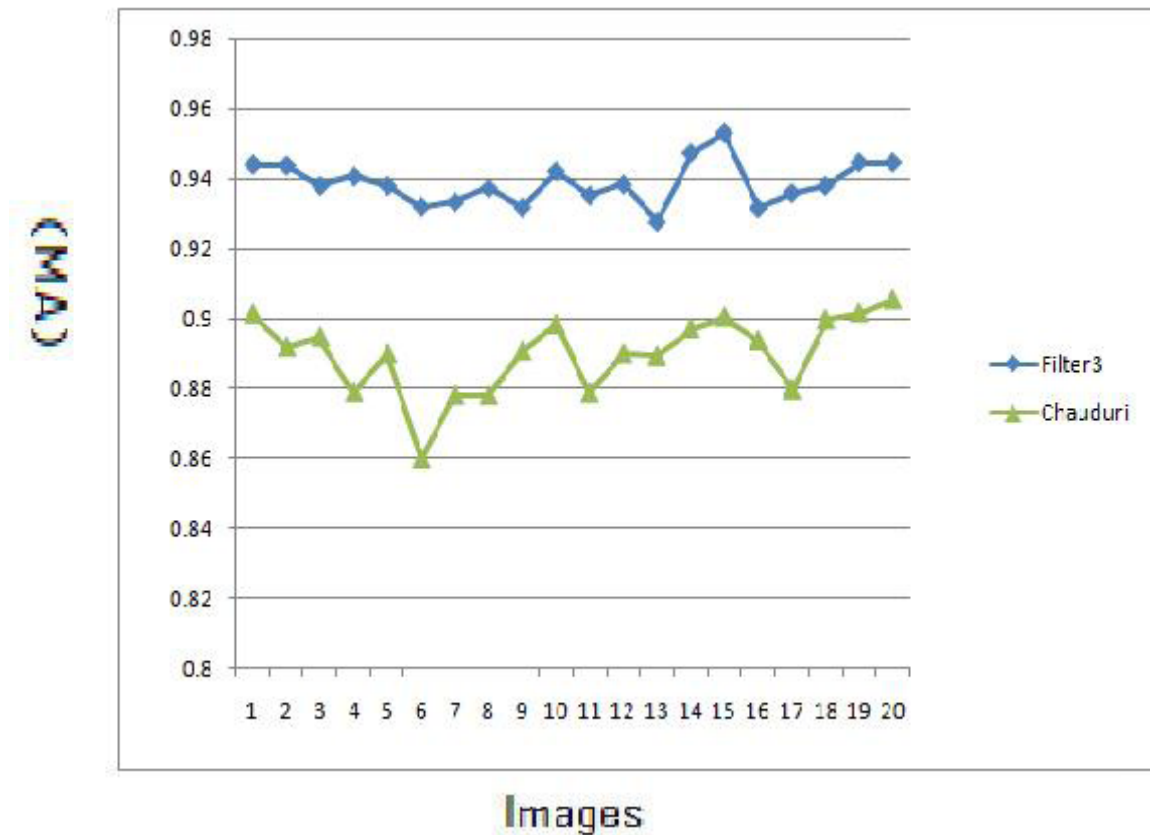
F

igure 4.27: MA Results of Filter3 Vs.(Chaudhuri et al. 1989).
edge techniques.

Filter3 Vs. Traditional Edge Detection Techniques

Table 4.23 shows the area under ROC of DRIVE images compared with the results

obtained by applying Sobel and Prewitt filters described by (Gonzalez and Woods, 2002).

Table 4.23: Results of Area Under ROC for Filter3 Vs. Sobel and Prewitt.

Method	Filter3 t=10.352,l=1.541	Sobel	Prewitt
Image1	0.9473	0.7325	0.7322
Image2	0.9456	0.7611	0.7591
Image3	0.9355	0.7088	0.7088
Image4	0.9224	0.767	0.7646
Image5	0.9323	0.7369	0.7362
Image6	0.9213	0.7232	0.7219
Image7	0.9221	0.7484	0.7478
Image8	0.9209	0.7169	0.7167
Image9	0.9199	0.7397	0.7383
Image10	0.9241	0.7306	0.7308
Image11	0.9177	0.7538	0.7531
Image12	0.9397	0.706	0.7045
Image13	0.9117	0.7428	0.7414
Image14	0.9474	0.7274	0.7251
Image15	0.9395	0.7476	0.7474
Image16	0.9482	0.7202	0.718
Image17	0.9327	0.6974	0.6956
Image18	0.9434	0.6797	0.6788
Image19	0.9539	0.7136	0.7129
Image20	0.9551	0.6962	0.6939
Average	**0.934035**	**0.7275**	**0.72636**

According to Table 4.23 the average area under ROC for Filter3 = 934035 and for Sobel it is 0.7275, and for Prewitt it is 0.72636, it can be concluded that Filter3 is better than traditional edge techniques.

Table 4.24 shows the MA of DRIVE images compared with the results obtained by applying Sobel and Prewitt filters described by (Gonzalez and Woods , 2002).

Table 4.24: Results of MA for Filter3 Vs. Sobel and Prewitt.

Method	Filter3 t=10.352, l=1.541	Sobel	Prewitt
Image1	0.9442	0.8699	0.8715
Image2	0.9439	0.8612	0.861
Image3	0.9381	0.8572	0.8572
Image4	0.9408	0.8728	0.8733
Image5	0.9381	0.867	0.8672
Image6	0.9321	0.8587	0.8598
Image7	0.9334	0.8694	0.8696
Image8	0.9374	0.87	0.876
Image9	0.9319	0.8776	0.8832
Image10	0.9423	0.8777	0.8814
Image11	0.9354	0.873	0.8732
Image12	0.9385	0.8681	0.8756
Image13	0.9278	0.8608	0.861
Image14	0.9475	0.8786	0.8835
Image15	0.9532	0.897	0.897
Image16	0.9318	0.861	0.8699
Image17	0.9361	0.8683	0.8784
Image18	0.9381	0.8764	0.8858
Image19	0.9448	0.8745	0.8805
Image20	0.9448	0.8871	0.894
Average	**0.93901**	**0.8714**	**0.8749**

Similarly, from Table 4.24 it can be seen that the average MA for Filter3 = 0.93901 and for

Sobel it is 0.8714, and for Prewitt it is 0.8749 and Filter3 performance is better than

traditional edge techniques.

4.4 Optimizing the averageMAfor the all DRIVE database

This section describes optimizing the MA for all images of DRIVE, the following

subsections includes the pseudo code, the results of the experiments including tables and

graphs and comparisons between this method and matched filter, Gabor filter, Prewitt and

Sobel.

Pseudo Code

The pseudo code of the fitness function of the GA is described in Figure 4.28

```
Function averageMA( image[20],l,tau)
1.i=1
2. while(i<21)
3.Extract green-band[i] form image[i].
4.Invert green-band[i].
5.Filter invert-green-band [i] using Gabor filter with l and tau.
6.t=0, temp=0
7.while(t<=1).
8.IMG=Threshold(filter-image[i],t).
9.Find Accuracy(IMG).
10.If Accuracy(IMG) > temp then temp =Accuracy(IMG).
11.t=t+.001
12.end while.
13.MA=temp.
14.i=i+1
15.end while
16.return the average of the MAs of the 20 images.
```

Figure 4.28: Pseudo Code of Average MA.

In this method all the 20 images of the DRIVE database were used as an input for the GA optimization. After calculating the MA for each Gabor-filtered image, the -(average MA for the 20 images) is the fitness function of the GA, since we want the maximum result of average MA and GA gives the smallest result. The parameters that gave the best result after applying GA are τ=9.902 and ℓ=0.556, and the average MA =0.94. The resulted image is shown in Figure 4.29 .
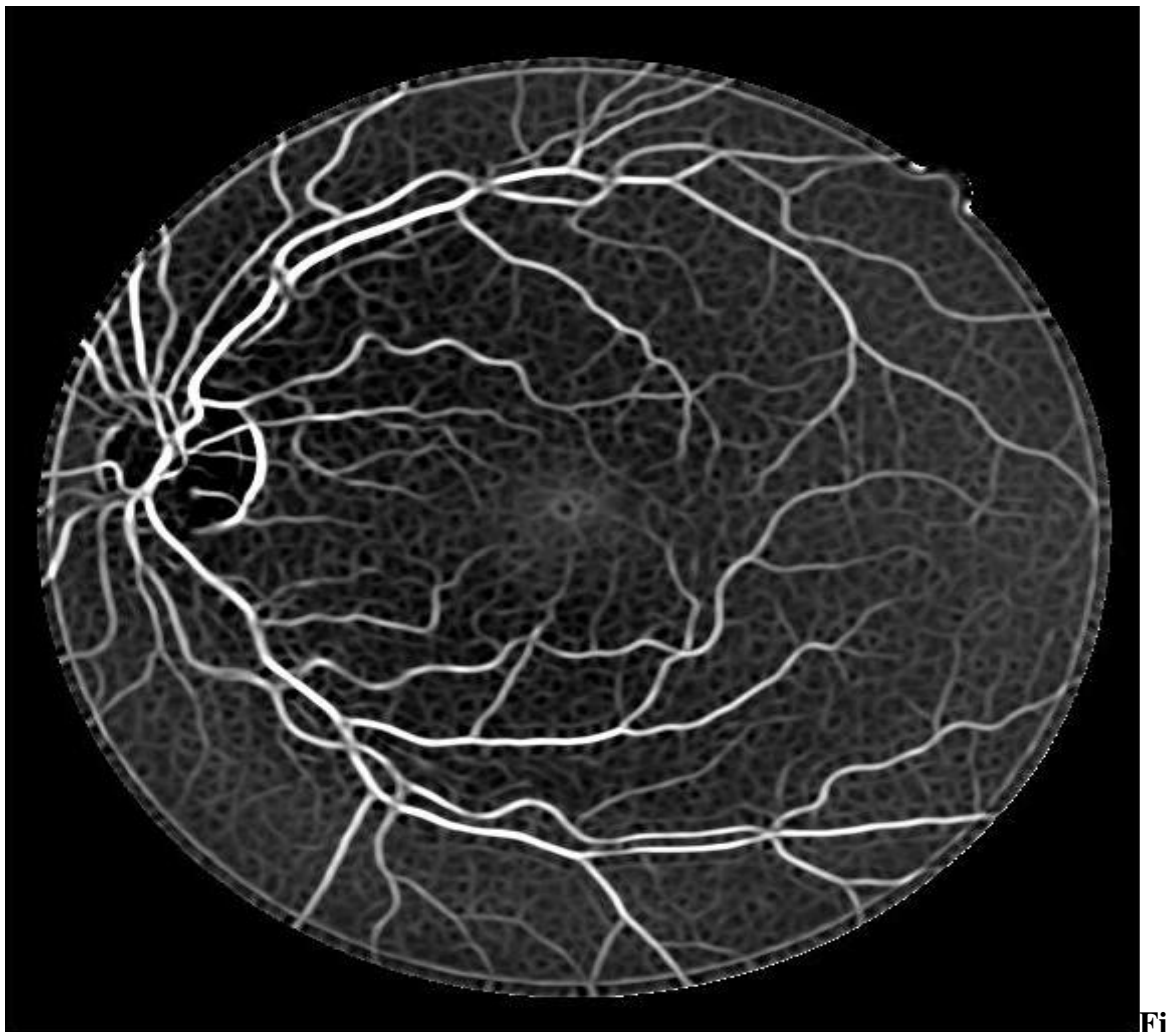
Figure 4.29: DRIVE First Image Filtered By Filter4.

Results of Area Under ROC For Experiment 4

Table 4.25 shows the area under ROC for the 20 images of DRIVE that were filtered using the Gabor filter parameters that obtained using this experiment $\tau =9.902$ and $\ell=0.556$.

Table 4.25: Results of Area Under ROC For Experiment 4.

Image	Filter4 t=9.902, l=.556
Image1	0.9408
Image2	0.9312
Image3	0.9146
Image4	0.9027
Image5	0.9187
Image6	0.9094
Image7	0.8942
Image8	0.9046
Image9	0.9096
Image10	0.9117
Image11	0.9074
Image12	0.9234
Image13	0.8996
Image14	0.9284
Image15	0.9265
Image16	0.937
Image17	0.9281
Image18	0.937
Image19	0.9429
Image20	0.9434
Average	**0.92056**

Figure 4.30 illustrates the ROC graph of this experiment.
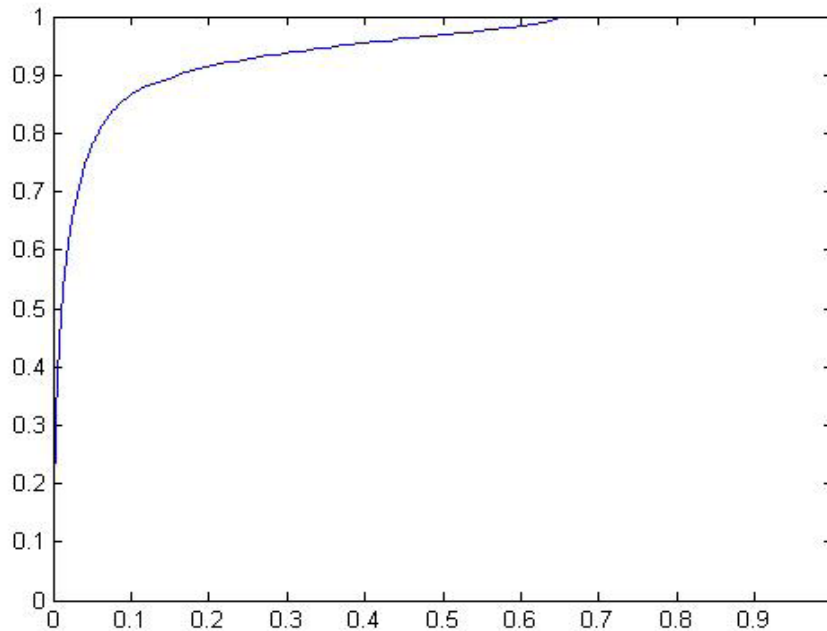
Figure 4.30: Experiment 4 ROC Graph.

Results of MA For Experiment 4

Table 4.26 shows the MA for the 20 images of DRIVE that were filtered using the Gabor filter parameters that obtained using this experiment τ =9.902 and ℓ=0.556.

Table 4.27 shows the area under ROC of DRIVE images compared with the results obtained by applying Gabor filter (Rangayyan et al. 2007). From Table 4.27 it can be noticed that the average area under ROC for Filter4 = 0.92056 and for Gabor filter it is 0.92798 which indicates that Filter4 outperformed Gabor filter in terms of MA.

Table 4.26: Results of MA For Experiment 4.

Image	Filter4 t=9.902, l=.556
Image1	0.9476
Image2	0.9443
Image3	0.9361
Image4	0.941
Image5	0.9388
Image6	0.9322
Image7	0.934
Image8	0.938
Image9	0.934
Image10	0.9428
Image11	0.937
Image12	0.9392
Image13	0.9279
Image14	0.948
Image15	0.953
Image16	0.9337
Image17	0.9377
Image18	0.942
Image19	0.9465
Image20	0.9463
Average	**0.94**

Table 4.27: Results of Area Under ROC Filter4 Vs. (Rangayyan, et al., 2007).

Method	Filter4 t=9.902, l=.556	Rangayyan
Image1	0.9408	0.9422
Image2	0.9312	0.9415
Image3	0.9146	0.933
Image4	0.9027	0.9182
Image5	0.9187	0.9273
Image6	0.9094	0.918
Image7	0.8942	0.9007
Image8	0.9046	0.9193
Image9	0.9096	0.9152
Image10	0.9117	0.9174
Image11	0.9074	0.9166
Image12	0.9234	0.9341
Image13	0.8996	0.9031
Image14	0.9284	0.9375
Image15	0.9265	0.936
Image16	0.937	0.9343
Image17	0.9281	0.9289
Image18	0.937	0.9415
Image19	0.9429	0.9452
Image20	0.9434	0.9496
Average	**0.92056**	**0.92798**

Figure 4.31 shows the results of area under ROC of the 20 DRIVE images using Filter4 vs. Gabor filter.
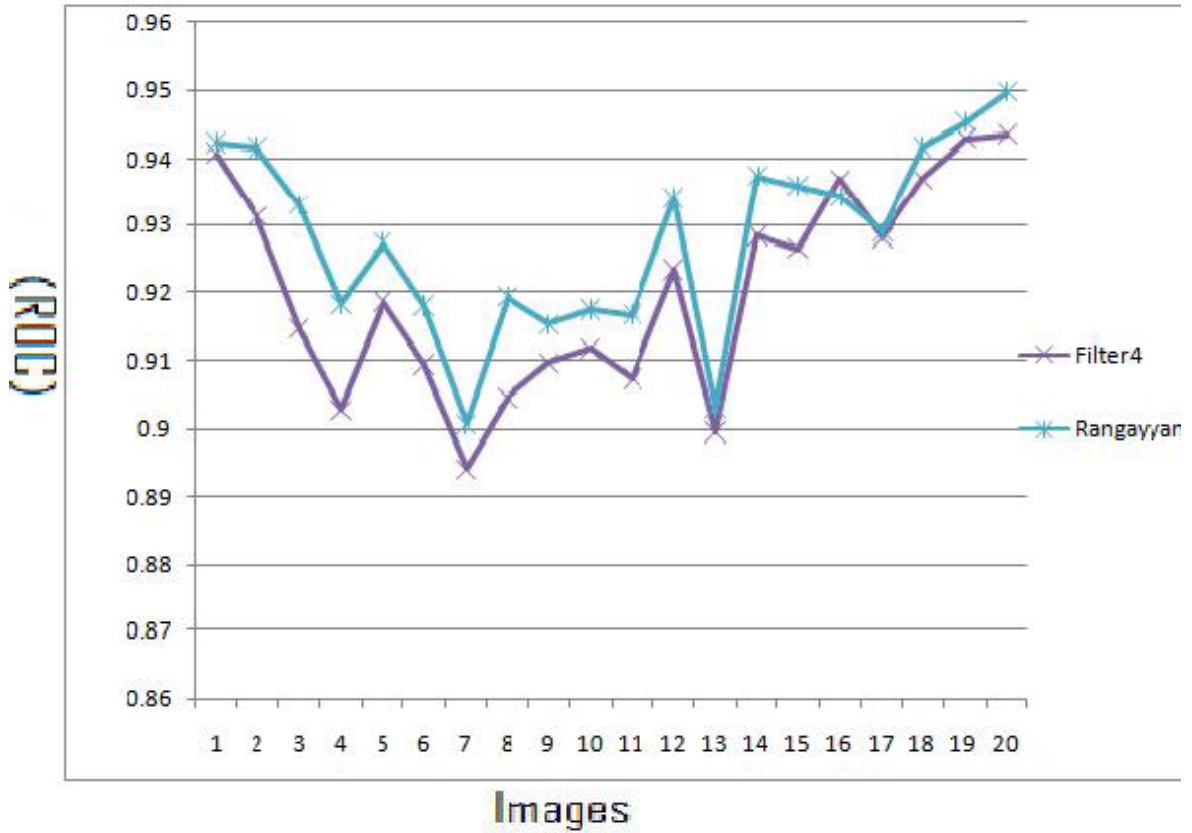

Figure 4.31: ROC Results of Filter4 Vs.(Rangayyan, et al., 2007).

Figure 4.32 shows the ROC curve for the first image of DRIVE using Filter4 vs. Gabor filter (Rangayyan, et al., 2007).

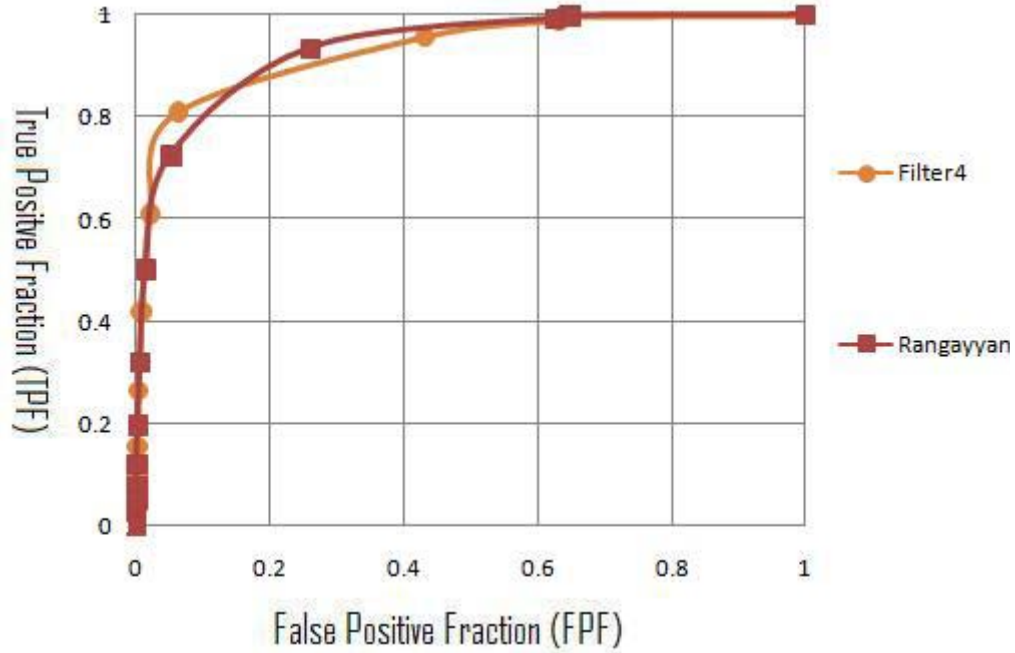**Figure 4.32: ROC Graph of Filter4 Vs. (Rangayyan et al. 2007).**

Table 4.28 shows the MA of DRIVE images compared with the results obtained by applying Gabor filter (Rangayyan, et al., 2007).

From the Table 4.28 it can be seen that the average MA for Filter4 = 0.94 and for Gabor filter it is 0.93862 (Rangayyan, et al., 2007), therefore it can be concluded that Filter4 improves (Rangayyan, et al., 2007) results.

Table 4.28: Results of MA Filter4 Vs. (Rangayyan et al. 2007).

Method	Filter4 t=9.902, l=.556	Rangayyan
Image1	0.9476	0.9435
Image2	0.9443	0.9433
Image3	0.9361	0.9379
Image4	0.941	0.9384
Image5	0.9388	0.9373
Image6	0.9322	0.9323
Image7	0.934	0.931
Image8	0.938	0.9384
Image9	0.934	0.9314
Image10	0.9428	0.9421
Image11	0.937	0.9352
Image12	0.9392	0.938
Image13	0.9279	0.9245
Image14	0.948	0.9471
Image15	0.953	0.9536
Image16	0.9337	0.9329
Image17	0.9377	0.9361
Image18	0.942	0.9392
Image19	0.9465	0.9445
Image20	0.9463	0.94
Average	**0.94**	**0.93862**

Figure 4.33 shows the results of MA of the 20 DRIVE images using Filter4 vs. Gabor filter (Rangayyan, et al., 2007).
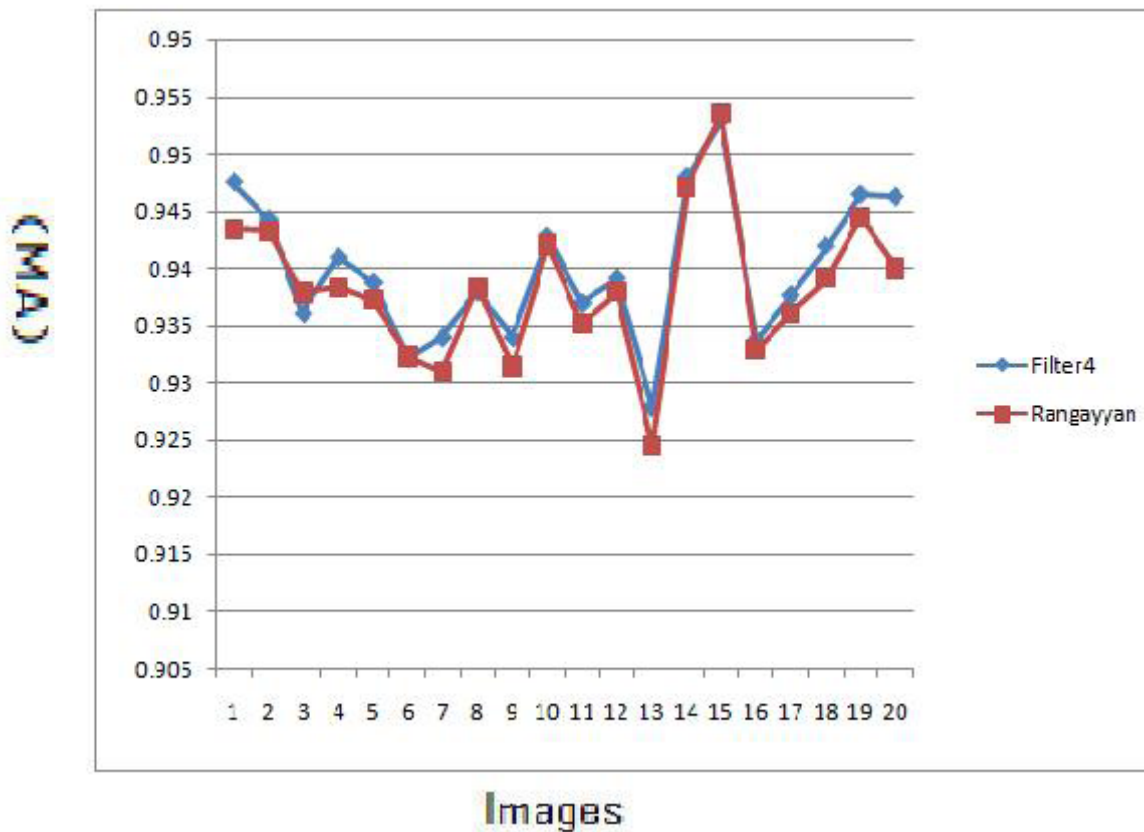

Figure 4.33: MA Results of Filter4 Vs. Rangayyan's Gabor Filter (Rangayyan et al. 2007).

Filter4 Vs. matched filter (Chaudhuri, et al., 1989)

Table 4.29 shows the area under ROC of DRIVE images compared with the results obtained by applying matched filter (Chaudhuri et al. 1989).

It can be noticed from the Table that the average area under ROC for Filter4 = 0.92056 and for the matched filter it is 0.8073, therefore it can be concluded that Filter4 improves matched filter results (Chaudhuri, et al., 1989).

Figure 4.34 shows the results of area under ROC for the 20 DRIVE images using Filter4 vs. matched filter (Chaudhuri et al. 1989).

Table 4.29: Results of Area Under ROC Filter4 Vs. Chaudhuri's matched filter(Chaudhuri, et al., 1989).

| Method	Filter4 t=9.902, l=.556	Chaudhuri
Image1	0.9408	0.8357
Image2	0.9312	0.822
Image3	0.9146	0.8145
Image4	0.9027	0.8025
Image5	0.9187	0.8299
Image6	0.9094	0.7692
Image7	0.8942	0.758
Image8	0.9046	0.7643
Image9	0.9096	0.8199
Image10	0.9117	0.8209
Image11	0.9074	0.7436
Image12	0.9234	0.822
Image13	0.8996	0.7835
Image14	0.9284	0.8281
Image15	0.9265	0.8084
Image16	0.937	0.8204
Image17	0.9281	0.7797
Image18	0.937	0.8295
Image19	0.9429	0.8522
Image20	0.9434	0.8409
Average	**0.92056**	**0.8073**
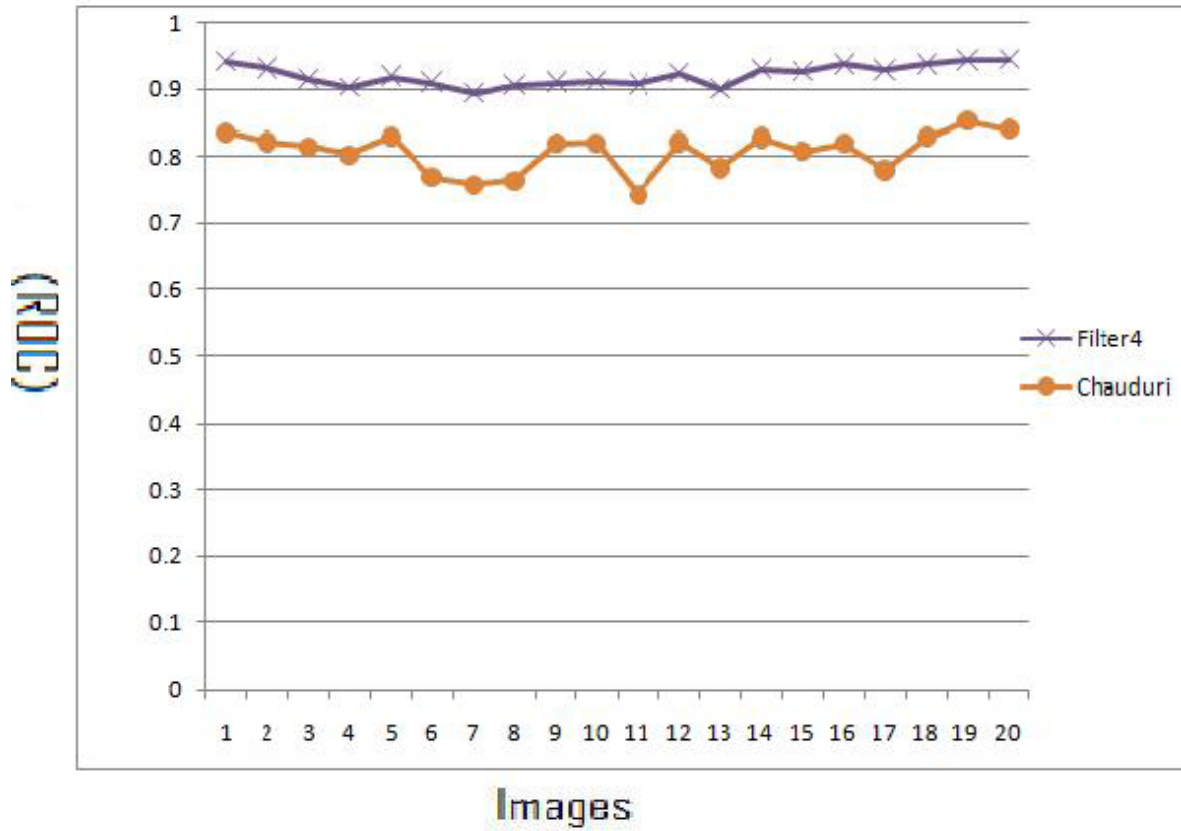
Figure 4.34: ROC Results of Filter4 Vs. Chauduri's matched filter (Chaudhuri et al. 1989).

Figure 4.35 shows the ROC curve for the first image of DRIVE using Filter4 vs. matched filter (Chaudhuri,et al., 1989) filter.
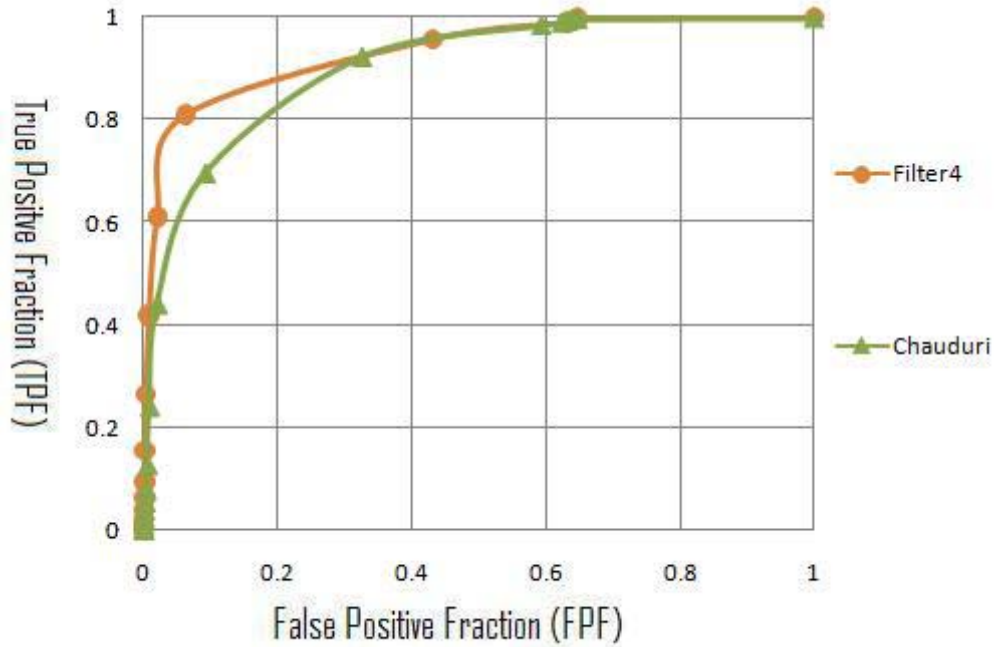
Figure 4.35: ROC Graph of Filter4 Vs. (Chaudhuri, et al., 1989).

Table 4.30 shows the MA for DRIVE images compared with the results obtained by

applying matched filter (Chaudhuri et al. 1989). From Table 4.30 it can be seen that the

average MA for Filter4 = 0.93901 and for the matched filter it is 0.8897 (Chaudhuri et al.

1989), therefore it can be concluded that Filter4 improves matched filter results (Chaudhuri

et al. 1989).

Figure 4.36 shows the results of MA of the 20 DRIVE images using Filter4 vs. matched

filter (Chaudhuri et al. 1989).

Table 4.30: Results of MA Filter4 Vs.(Chaudhuri et al. 1989).

| Method	Filter4 t=9.902, l=.556	Chaudhuri
Image1	0.9476	0.9012
Image2	0.9443	0.8917
Image3	0.9361	0.8946
Image4	0.941	0.8788
Image5	0.9388	0.8898
Image6	0.9322	0.8598
Image7	0.934	0.878
Image8	0.938	0.878
Image9	0.934	0.8906
Image10	0.9428	0.8982
Image11	0.937	0.8786
Image12	0.9392	0.8898
Image13	0.9279	0.8892
Image14	0.948	0.897
Image15	0.953	0.9003
Image16	0.9337	0.8936
Image17	0.9377	0.8795
Image18	0.942	0.8996
Image19	0.9465	0.9015
Image20	0.9463	0.9053
Average	**0.94**	**0.8897**
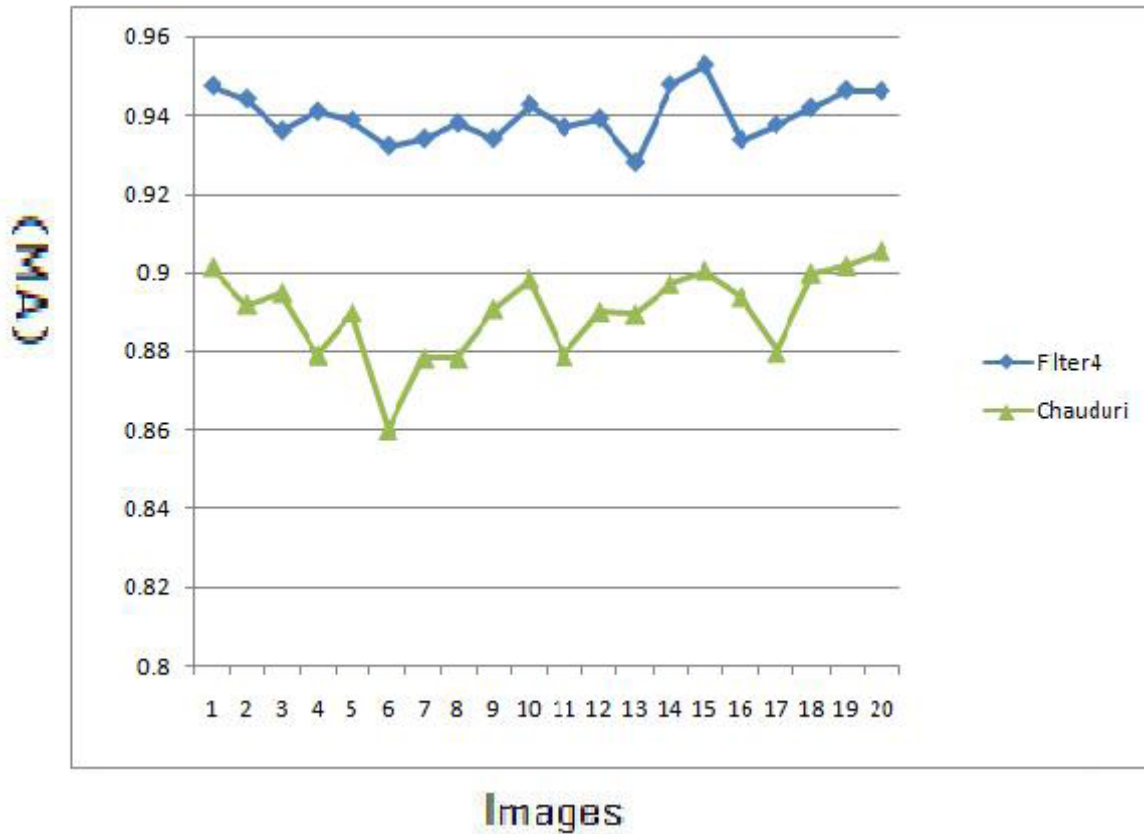
Figure 4.36: MA Results of Filter4 Vs.(Chaudhuri, et al., 1989).

Filter4 Vs. Traditional Edge Detection Techniques

Table 4.31 shows the area under ROC of DRIVE images compared with the results

obtained by applying Sobel and Prewitt filters described by (Gonzalez & Woods 2002).

From Table 4.31 it can be seen that the average area under ROC for Filter4 = 0.92056 and

for Sobel it is 0.7275, and for Prewitt it is 0.72636, therefore, it can be concluded that

Filter4's results are better than traditional edge techniques.

Table 4.31: Results of Area Under ROC for Filter4 Vs. Sobel and Prewitt.

Method	Filter4 t=9.902, l=.556	Sobel	Prewitt
Image1	0.9408	0.7325	0.7322
Image2	0.9312	0.7611	0.7591
Image3	0.9146	0.7088	0.7088
Image4	0.9027	0.767	0.7646
Image5	0.9187	0.7369	0.7362
Image6	0.9094	0.7232	0.7219
Image7	0.8942	0.7484	0.7478
Image8	0.9046	0.7169	0.7167
Image9	0.9096	0.7397	0.7383
Image10	0.9117	0.7306	0.7308
Image11	0.9074	0.7538	0.7531
Image12	0.9234	0.706	0.7045
Image13	0.8996	0.7428	0.7414
Image14	0.9284	0.7274	0.7251
Image15	0.9265	0.7476	0.7474
Image16	0.937	0.7202	0.718
Image17	0.9281	0.6974	0.6956
Image18	0.937	0.6797	0.6788
Image19	0.9429	0.7136	0.7129
Image20	0.9434	0.6962	0.6939
Average	**0.92056**	**0.7275**	**0.72636**

Table 4.32 shows the MA of DRIVE images compared with the results obtained by applying Sobel and Prewitt filters described by Gonzalez & Woods (Gonzalez and Woods, 2002). From the Table 4.32 it can be seen that the average MA for Filter4 = 0.94 and for Sobel it is 0.8714, and for Prewitt it is 0.8749 which indicate significant improvement for Filter4 over traditional edge techniques.

Table 4.32: Results MA for Filter4 Vs. Sobel and Prewitt.

Method	Filter4 t=9.902, l=.556	Sobel	Prewitt
Image1	0.9476	0.8699	0.8715
Image2	0.9443	0.8612	0.861
Image3	0.9361	0.8572	0.8572
Image4	.941	0.8728	0.8733
Image5	0.9388	0.867	0.8672
Image6	0.9322	0.8587	0.8598
Image7	0.934	0.8694	0.8696
Image8	0.938	0.87	0.876
Image9	0.934	0.8776	0.8832
Image10	0.9428	0.8777	0.8814
Image11	0.937	0.873	0.8732
Image12	0.9392	0.8681	0.8756
Image13	0.9279	0.8608	0.861
Image14	0.948	0.8786	0.8835
Image15	0.953	0.897	0.897
Image16	0.9337	0.861	0.8699
Image17	0.9377	0.8683	0.8784
Image18	0.942	0.8764	0.8858
Image19	0.9465	0.8745	0.8805
Image20	0.9463	0.8871	0.894
Average	**0.94**	**0.8714**	**0.8749**

4.5 Dividing The First DRIVE Image Into Four Regions

In this section another experiment is conducted which is dividing the image into 4 regions and finding the parameters for each region. The rational behind this is to find the best parameters for each region on its own, these parameters will be optimized for that regions and consequently are expected to perform better than the parameters that are calculated over the whole original image. One note though is dividing the image into 4 regions is just an experiment and further division is possible into any number of regions, the larger the number of regions, the greater the overhead and the needed time for filtering.

Pseudo Code

The pseudo code of the fitness function of the GA is described in Figure 4.37

```
Function DivideImage(image,l[4],tau[4])
1.Extract green-band form image.
2.Invert green-band.
3.Divide Image into four regions.
4.For i=1 to 4
5.ROC(region[i],l[i],tau[i])
6.end For
7.return the average ROC of the four regions.
```

Figure 4.37: Pseudo Code For Method 5.

Using this method, ROC is calculated for each region as shown in Figure 4.38 and listed in Table 4.33. The ROC for the original image is calculated by averaging ROC from each region and it is calculated as = 0.95035. This is higher than the ROC from matched filter which is 0.88 and from Gabor filter which is 0.937325.
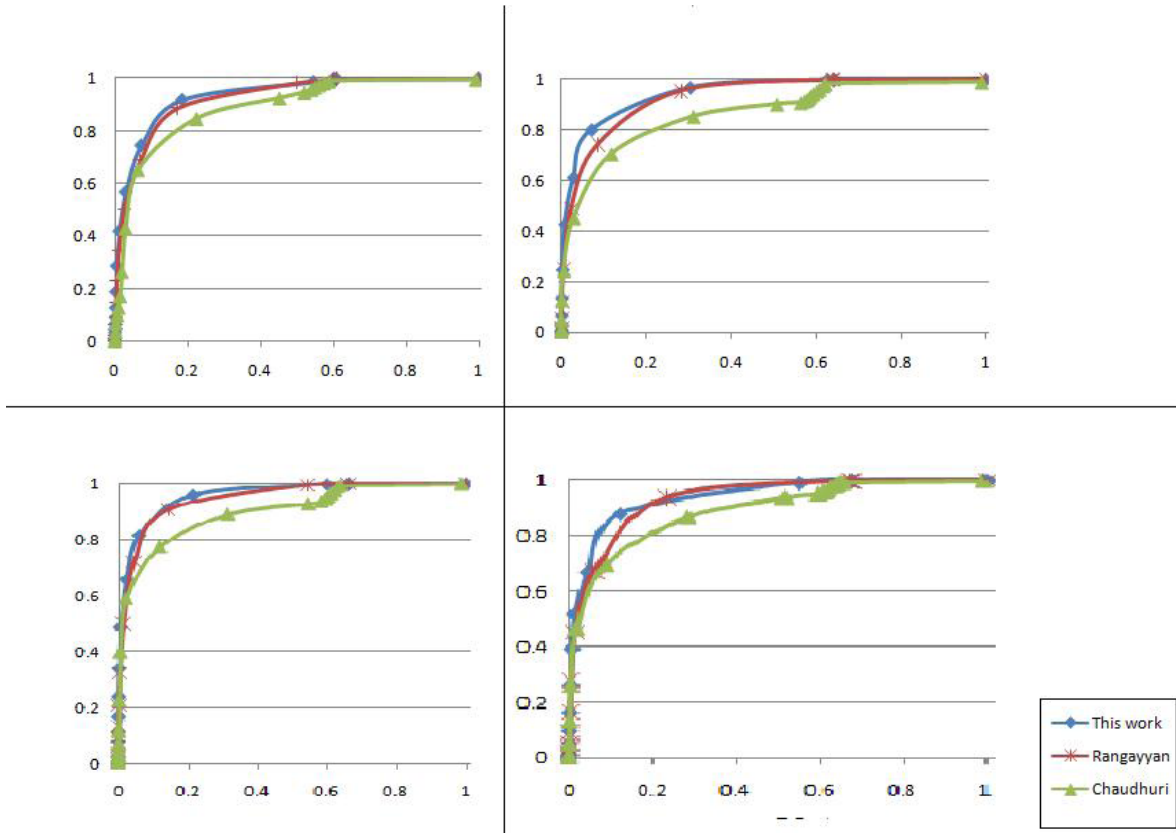
Figure 4.38: ROC for the first DRIVE image vs. (Rangayyan, et al., 2007) and (Chaudhuri, et al., 1989).

Table 4.33: Results of ROC for Filter5 Vs. Rangayyan and Chauduri.

Method	This Work	Rangayyan	Chauduri
ROC Region1	0.9455	0.9304	0.8839
ROC Region2	0.9507	0.9338	0.8598
ROC Region3	0.9613	0.9516	0.8935
ROC Region4	0.9439	0.9335	0.8828
Average ROC	**0.95035**	**0.937325**	**0.88**

After applying the GA , the parameters that gave the best results are:

for region one τ=9.33 and ℓ=1.564, for region two τ=8.379 and ℓ =1.145

for region three τ=9.714 and ℓ =1.221, and for region four τ=9.814 and ℓ =1.179.

4.6 Summary of Results

This section presents an overall summery of the implementation's results.

Table 4.34 shows the average area under ROC for the methods that are represented in this work compared with previous work.

Table 4.34: Summery of The Average of Area Under ROC.

Method	Filter1 t=10.188, l=1.26	Filter2 t=9.519, l=.403	Filter3 t=10.352, l=1.541	Filter4 t=9.902, l=.556	Gabor	Matched	Sobel	Prewitt
Average	0.93317	0.915435	0.934035	0.92056	0.92798	0.80726	0.7275	0.72636

As noticed from the Table the best average area under ROC for Filter3 is the best among all methods, it improve the result of Gabor filter (Rangayyan et al. 2007) filter by 0.01 and improves Matched filter (Chaudhuri et al. 1989) filter by 0.13 .

Table 4.35 shows the average MA for the methods that are represented in this work compared with previous work, as can be noticed that Filter4 has the best results among all methods as it improves Gabor filter by 0.0014 and improves matched filter by 0.06 .

Table 4.35: Summery of Average MA.

Method	Filter1 t=10.188, l=1.26	Filter2 t=9.519, l=.403	Filter3 t=10.352, l=1.541	Filter4 t=9.902, l=.556	Gabor	Matched	Sobel	Prewitt
Average	0.93901	0.939085	0.93901	0.94	0.9386	0.8897	0.8714	0.8749

Figure 4.39 shows the ROC curve of the first image in DRIVE for the proposed methods vs. previous methods. It can be realized clearly that the area under ROC for Filter1 is the largest among all methods.
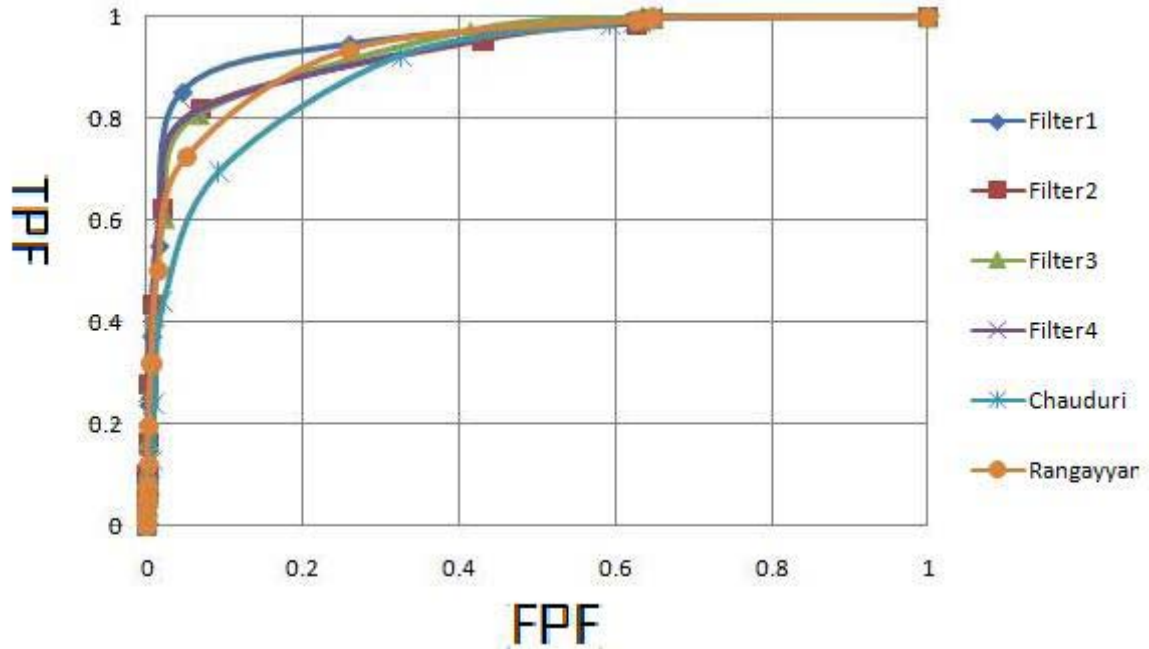
Figure 4.39: ROC Curve for The First Image of DRIVE for All Methods.

Table 4.36 show the average time of filtering the 20 images of DRIVE using the methods in presented in this work, compared with the previous methods.

**Table 4.36: The Average Time of Implementation.**

Method	Filter1 t=10.188, l=1.26	Filter2 t=9.519, l=.403	Filter3 t=10.352, l=1.541	Filter4 t=9.902, l=.556	Matched	Gabor	Sobel	Prewitt
Time	13.6883	13.4723	13.9067	13.0557	13.2380	11.3969	0.1672	0.1679

Figure 4.40 shows the the first DRIVE image with the filtered images using our methods and previous methods.

Figure 4.41 shows a house image with the filtered images using our methods and previous methods.
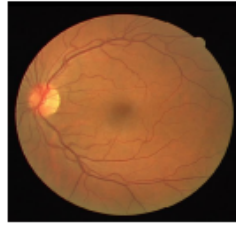
(a) Retina Test Image.
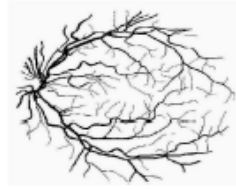
(b) Retinal Vessels Detected Manually.
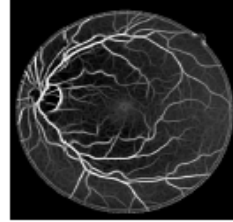
(c) The Result of Filter1

(d) The Binary Version of Filter1

(e) The Result of Filter2

(f) The Binary Version of Filter2

(g) The Result of Filter3
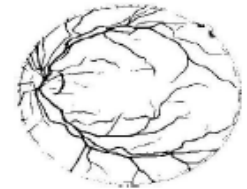
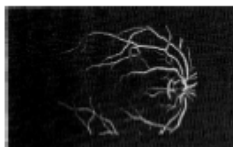(h) The Binary Version of Filter3

(i) The Result of Filter4

(j) The Binary Version of Filter4

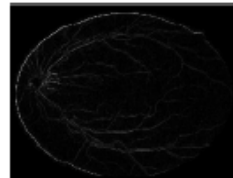(k) The Result of Rangayyan et al. Filter

(l) The Binary Version of Rangayyan et al. Filter
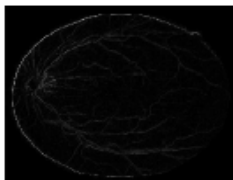
(m) The Result of Chaudhuri Filter

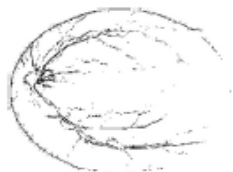(n) The Binary Version of Chaudhuri Filter

(o) The Result of Sobel Filter

(p) The Binary Version of Sobel Filter

(q) The Result of Prewitt Filter

(r) The Binary Version of Prewitt Filter

Figure 4.40: The Filtered Images.

Figure 4.41: An Image of a House Filtered With All Methods.

CHAPTER 5

CONCLUSIONS AND FUTUREWORK

5.1 Conclusions

Retinal blood vessels are used by ophthalmologists to diagnose many diseases such as diabetes. Therefore, automating the extraction and detection of retinal vessels gives many advantages over manual detection, and facilitate the diagnoses process.

Many researchers worked in the field of vessels' detection due to its medical importance, the main approaches that are examined in this thesis are the traditional edge detection including Sobel and Prewitt, and modeled edge detection including Rangayyan's et al. Gabor filter (Rangayyan, et al., 2007) and Chaudhuri's et al. matched filter (Chaudhuri, et al., 1989). In this these Gabor filter is optimized using Genetic Algorithms (GA), to maximize the response of Gabor filter in detecting retinal blood vessels. For the purpose of optimization five methods have been introduced, each method aims to optimize Gabor filter depending on a different measuring factor. After comparing our results with previous methods, this work improves all the previous methods in terms of average area under Receiver Operator Characteristics (ROC) and average Maximum Accuracy (MA) for the 20 DRIVE image, except methods 2 and 4 which do not improve Gabor (Rangayyan et al. 2007) in average area under ROC because in these methods the optimization emphasis on MA only.

The average area under ROC for Filter3 is the best among all methods, it improves the result of Gabor (Rangayyan et al. 2007) filter by 0.01 and improves (Chaudhuri et al. 1989) filter by 0.13.

By comparing the average MA for the methods that are represented in this work vs. previous work, it can be noticed that Filter4 has the best results among all methods as it improves Gabor (Rangayyan et al. 2007) filter by 0.01 and it improves matched filter

by 0.06.

By dividing the fist image of DRIVE into four regions, comparing the average area under ROC for the four regions for this work improves Gabor (Rangayyan, et al., 2007) by 0.02 and improves matched (Chaudhuri et al. 1989) by 0.07.

This thesis differs from previous work in mnay aspects which are:

- Using GA to improve Gabor filter in blood vessels' detection.

- Using a multi-scale thresholding of gray-levels to find all the possible blood vessels.

- Using the ROC as the fitness function for GAs.

- Dividing the first DRIVE image into 4 regions, and calculate different Gabor parameters for each region.

5.2 Future Work

There are many domains that are still open for research in the field of using Gabor filter in vessels' detection, few papers investigate and study the performance of Gabor filter as a model-based vessels' detection technique. The following are some possible suggestions to research for:

- Optimizing Gabor filter in vessel detection using other optimization methods such as successive approximation and Exhaustive Search.

- Optimizing the time taken by Gabor for the filtering process

- Using another images' database as benchmark such as STARE (?).

- Implementation of a multi-stage Gabor filter approach.

- Investigation of a hybrid approach that gains the advantages of two or more vessel detection techniques

- Use the proposed methods on other problems than vessel detection.

REFERENCES

Al-Akhras, M. (2007), Quality of Media Traffic Over Lossy Internet Protocol Networks: Measurment and improvement, **De Montfort University**.

Al-Rawi, M. & Karajeh, H. (2007), 'Genetic algorithm matched filter optimization for automated detection of blood vessels from digital retinal images', **computer methods and programs in biomedicine** 87, 248–253.

Al-Rawi, M., Qutaishat, M. & Arrar, M. (2007), 'An improved matched filter for blood vessel detection of digital retinal images', **Computers in Biology and Medicine** 37, 262–267.

Chaudhuri, S., Chatterjee, S., Katz, N. & Goldbaum, M. (1989), 'Dettection of blood vessels in retinal images using two - dimensional matched filter', **Medical Imaging, IEEE Transactions** on 8(3), 263–269.

David, J., Krishnan, R. & Kumar. A, S. (2008), 'Neural Network Based Retinal Image Analysis', **Congress on Image and Signal Processing 1**, 49–53.

Gonzalez, R. & Woods, R. (2002), Digital **Image Processing**, Prentice - Hall,Inc. Upper Saddle River, New Jersey 07458.

Hoover, A., Kouznetsova, V. & Goldbaum, M. (2000), 'Locating blood vessels in retinal images by piecewise threshold probing of a matched filter response', **Medical Imaging, IEEE Transactions on 19(3),** 203–210.

Jiang, X. & Mojon, D. (2003), 'Adaptive local thresholding by verification-based multithreshold probing with application to vessel detection in retinal images', **Ieee transactions on pattern analysis and machine intelligence 25(1)**, 131–137.

Jin, J. S. & Gao, Y. (2002), 'Recursive Implementation of LoG Filtering'.

Jung, E. & Hong, K. (2006), 'Automatic Retinal Vasculature Structure Tracing and Vascular Landmark Extraction from Human Eye Image', **International Conference on Hybrid Information Technology IEEE 1**, **1–7**.

Patton, N., Aslam, T., MacGillivray, T., Deary, I., Dhillon, B., Eikelboom, R., Yogesan, K. & Constable, I. (2006), 'Retinal image analysis: Concepts,applications and potential', **Progress in Retinal and Eye Research 25, 99127**.

Rangayyan, R. M., Ayres, F. J., Oloumi, F., Oloumi, F. & Eshghzadeh-Zanjani, P. P. (2007), 'Detection of Blood Vessels in the Retina Using Gabor Filters'**, Electrical and Computer Engineering,Canadian Conference on pp. 717 – 720.**

Sezgin, M. & Sankur, B. (2004), 'Survey over image thresholding techniques and quantitative performance evaluation'**, Journal of Electronic Imaging 13, 146–168.**

Soares, J., Leandro, J., Cesar, R.M., J., Jelinek, H. & Cree, M. (2006), 'Retinal vessel segmentation using the 2-D Gabor wavelet and supervised classification', **Medical Imaging, IEEE Transactions on 25(9),** 1214–1222.

Staal, J., Abrmoff, M. D., Niemeijer, M., Viergever, M. A. & B.V., G. (2004), 'Ridge-Based Vessel Segmentation in Color Images of the Retina', IEEE **transactions On medical imaging 23(4),** 501–509.

Thede, S. (2004), 'An Introduction to Genetic Algorithms', **DePauw University Greencastle, IN 46135** .

Ziou, D. & Tabbone, S. (1997), 'Edge detection techniques - an overview

استخدام الخوارزمية الجينية لتطوير أداء فلتر غابور في تحديد الأوعية الدموية من الصور الرقمية لشبكية العين

إعداد

هيام محمد زهير بدر

المشرف

الدكتور عبد اللطيف ابو دلهوم

مساعد المشرف

الدكتور موسى الأخرس

ملخص

تحديد الأوعية الدموية من شبكية العين له أهمية كبيرة في تشخيص الكثير من الأمراض. بسبب أهمية هذا المجال ظهرت عدة طرق تهدف لاستنباط الاوعية الدموية من الشبكية. في البداية كانت عملية استنباط الاوعية الدموية تتم بواسطة الطرق التقليدية للكشف عن الحواف , و لكن الطرق التقليدية كانت غير دقيقة في تحديد الأوعية الدموية مما دعا الباحثين إلى ابتكار طرق مختصة في عملية تحديد الأوعية الدموية. من أهم الطرق المستخدمة في عملية استنباط الأوعية الدموية من شبكية العين هي طريقة فلتر غابور.

هذه الرسالة تقترح طرق جديدة تهدف إلى تحسين أداء فلتر غابور عن طريق استخدام الخوارزميات الجينية.

تقوم الخوارزميات الجينية بإيجاد أفضل العوامل التي تؤدي إلى أفضل أداء لغابور فلتر في تحديد الأوعية الدموية.

المعايير المستخدمة لمقارنة النتائج في هذه الرسالة مع النتائج السابقة تتضمن : المساحة تحت منحنى ROC ، و الدقة القصوى للصورة الناتجة(MA).

استخدمت خمس تجارب من اجل عملية التحسين، و هذه التجارب تشمل:

1. إيجاد القيمة القصوى للمساحة تحت منحنى ROC للصورة الأولى في DRIVE.

2. إيجاد القيمة القصوى للدقة القصوى للصورة الأولى في DRIVE.

3. إيجاد القيمة القصوى لمعدل المساحات تحت منحنى ROC لجميع الصور في DRIVE.

4. إيجاد القيمة القصوى لمعدل الدقة القصوى لجميع الصور في DRIVE.

5. تقسيم الصورة الأولى في DRIVE إلى أربع أجزاء، و إيجاد المساحة القصوى تحت منحنى ROC لكل جزء.

بعد مقارنة النتائج التي تم الحصول عليها من هذه التجارب مع الطرق السابقة ، تمت ملاحظة التالي:

تحسنت المساحة تحت ROC بمقدار 1% تقريباً مقارنة ب "فلتر غابور" و 13% مقارنة ب فلتر التطابق المقترح من قبل تشودوري.

أما بالنسبة للدقة القصوى فقد تحسنت بنسبة 0.14 % مقارنة ب "فلتر غابور" و بنسبة 6% مقارنة بفلتر التطابق